

AD-A093 375

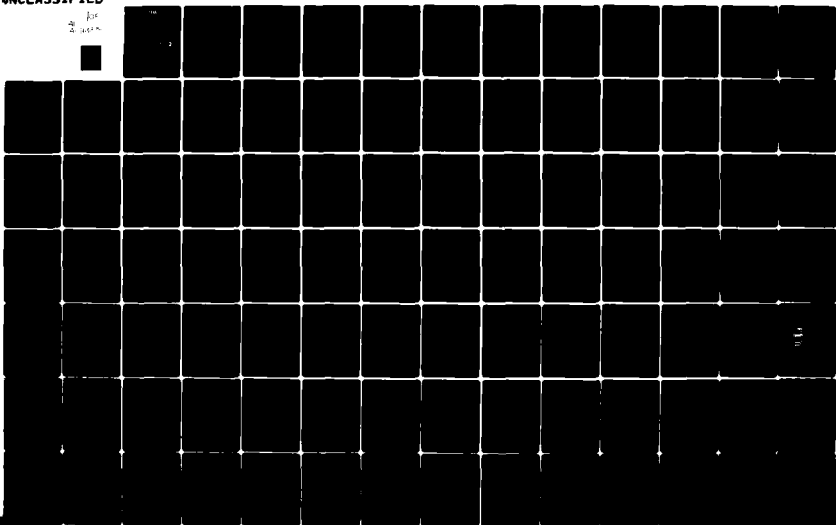
MASSACHUSETTS INST OF TECH CAMBRIDGE GAS TURBINE AND--ETC F/G 20/4
CURRENT PROBLEMS IN TURBOMACHINERY FLUID DYNAMICS.(U)
NOV 80 E M GREITZER, W T THOMPkins F49620-78-C-0084

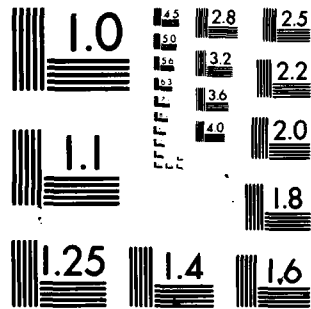
UNCLASSIFIED

AFOSR-TR-80-1355

NL

10
24
1980





MICROCOPY RESOLUTION TEST CHART
NATIONAL BUREAU OF STANDARDS-1963-A

SECURITY CLASS ~~UNCLASSIFIED~~

REPORT DOCUMENTATION

READ INSTRUCTIONS
BEFORE COMPLETING FORM

1. REPORT NUMBER

AFOSR-TR- 80 - 1355

GOVT ACCESSION NO

RECIPIENT'S CATALOG NUMBER

4. TITLE (and Subtitle)

CURRENT PROBLEMS IN TURBOMACHINERY FLUID DYNAMICS

5. TYPE OF REPORT & PERIOD COVERED
Interim

6. PERFORMING ORG. REPORT NUMBER

7. AUTHOR(s)

E. M. Greitzer, W. T. Thompkins, J. E. McCune,
A. H. Epstein, C. S. Tan, W. R. Hawthorne

8. CONTRACT OR GRANT NUMBER(s)

F49620-78-C-0084

9. PERFORMING ORGANIZATION NAME AND ADDRESS

Gas Turbine & Plasma Dynamics Laboratory
Department of Aeronautics & Astronautics
Massachusetts Institute of Technology10. PROGRAM ELEMENT, PROJECT, TASK
AREA & WORK UNIT NUMBERS61102F
2307/A1

11. CONTROLLING OFFICE NAME AND ADDRESS

Cambridge, MA 02139
Air Force Office of Scientific Research
Directorate of Aerospace Sciences AFOSR (AFSC)
Bolling AFB, DC 20332

12. REPORT DATE

November 26, 1980

13. NUMBER OF PAGES

180

14. MONITORING AGENCY NAME & ADDRESS (if different from Controlling Office)

15. SECURITY CLASS. (of this report)

Unclassified

15a. DECLASSIFICATION/DOWNGRADING
SCHEDULE

16. DISTRIBUTION STATEMENT (of this Report)

Approved for Public Release; Distribution Unlimited

DTIC
ELECTE
JANO 2 1981

17. DISTRIBUTION STATEMENT (of the abstract entered in Block 20, if different from Report)

18. SUPPLEMENTARY NOTES

19. KEY WORDS (Continue on reverse side if necessary and identify by block number)

casing treatment

axial flow turbomachinery

axial flow compressors

computational fluid dynamics

compressor stall

three-dimensional flow

flow measurements in transonic fans

transonic flow

vortex flows

inlet distortion

20. ABSTRACT (Continue on reverse side if necessary and identify by block number)

A multi-investigator effort on problems of current interest in turbomachinery fluid dynamics is being carried out in the Gas Turbine and Plasma Dynamics Laboratory of MIT. Within the overall program four different tasks having to do with a wide range of design and off-design flow fields have been identified. These are: 1) Investigation of fan and compressor design point fluid dynamics (including formulation of design procedures using current three-dimensional transonic codes and development of techniques for instantaneous measurements

DD FORM
1 JAN 73 1473

unclassified

SECURITY CLASSIFICATION OF THIS PAGE (When Data Entered)

AD A093375

DDC FILE COPY

UNCLASSIFIED

SECURITY CLASSIFICATION OF THIS PAGE(When Data Entered)

2. Abstract (continued)

in transonic fans); 2) Studies of compressor stability enhancement (including basic investigations of the fluid dynamics of rotor casing treatment); 3) Fluid mechanics of gas turbine engine operation in inlet flow distortion (including inlet vortex distortion); and 4) Investigations of three-dimensional flows in highly loaded turbomachines (including actuator duct theory and blade-to-blade flow analysis) and linearized analysis of swirling three-dimensional flows in turbomachines. This interim report summarizes progress made to date as well as indicates the direction of future efforts on the various tasks.

Accession For	
NTIS GRA&I	<input type="checkbox"/>
DTIC TAB	<input checked="" type="checkbox"/>
Unannounced	<input type="checkbox"/>
Justification	
By	
Distribution/	
Availability Codes	
Dist	Avail and/or Special
A	

UNCLASSIFIED

SECURITY CLASSIFICATION OF THIS PAGE(When Data Entered)

18
19
AFOSR TR-80-1355

GAS TURBINE & PLASMA DYNAMICS LABORATORY
DEPARTMENT OF AERONAUTICS & ASTRONAUTICS
MASSACHUSETTS INSTITUTE OF TECHNOLOGY
CAMBRIDGE, MASSACHUSETTS 02139

AN INTERIM REPORT

on

CONTRACT NO. F49620-78-C-0084

15
entitled

6 CURRENT PROBLEMS IN TURBOMACHINERY FLUID DYNAMICS.

for the period

1/20/79 to Sept. 1 June 1979 to Sep 1980

submitted to

AIR FORCE OFFICE OF SCIENTIFIC RESEARCH

Attention of:

Dr. James D. Wilson, Program Manager,
Directorate of Aerospace Sciences, AFOSR (AFSC)
Bolling Air Force Base, DC 20332

Principal
Investigators:

11 Edward M. Greitzer
William T. Thompson, Jr.
James E. McCune

Co-Investigators:

Alan H. Epstein
Choon S. Tan

Collaborating
Investigators:

Jack L. Kerrebrock
Sir William R. Hawthorne

November 26, 1980

Approved for public release:
distribution unlimited

410554 80 12 29 055 MT

TABLE OF CONTENTS

<u>SECTION</u>	<u>PAGE NO.</u>
1. INTRODUCTION AND RESEARCH OBJECTIVES	1
2. STATUS OF THE RESEARCH PROGRAM	3
Summary	3
Task I: Investigation of Fan and Compressor Design Point Fluid Dynamics.	5
A: Inverse (Design) Calculation Procedure	5
B: Further Measurements of AFAPL High Through-Flow Compressor Stage	24
Task II: Investigation of Basic Mechanisms for Compressor Stability Enhancement Using Casing Treatment.	30
Task III: Investigation of the Response of Gas Turbine Engines to Inlet Distortion.	38
A: Basic Studies of the Inlet Vortex Flow Field	38
B: Combined Radial/Circumferential Inlet Total Pressure Distortion.	67
Task IV: Investigation of Three-Dimensional Flow in Highly Loaded Turbomachines.	73
3. PUBLICATIONS	88
4. PROGRAM PERSONNEL	90
5. INTERACTIONS	91
6. DISCOVERIES, INVENTIONS, AND SCIENTIFIC APPLICATIONS	94
7. CONCLUDING REMARKS	95
REFERENCES	96

AIR FORCE OFFICE OF SCIENTIFIC RESEARCH (AFSC)
NOTICE OF TRANSMITTAL TO DDC
This technical report has been reviewed and is
approved for public release IAW AFR 190-18 (7b).
Distribution is unlimited.
A. D. BLOSE
Technical Information Officer

1. INTRODUCTION AND RESEARCH OBJECTIVES

The work described in this report is part of a multi-investigator effort in turbomachinery fluid dynamics which is being carried out at the Gas Turbine and Plasma Dynamics Laboratory at MIT. Support for this program is provided by the Air Force Office of Scientific Research under Contract. The aim of the program, which was started on 1 June 1979 is to focus on several topics in the above mentioned area which are of significant import for improvement of gas turbine engine technology. The program is thus problem oriented and cuts across different disciplines.

Within the overall goal, there are four different tasks that have been specifically defined. These are:

I. Investigation of fan and compressor design point fluid dynamics (including the formulation of design procedures using current three-dimensional transonic codes and development of techniques for, and analysis of, instantaneous time resolved measurements in transonic fans.)

II. Studies of compressor stability enhancement (including basic investigations of the fluid dynamics of compressor stall margin increase due to casing and hub treatments.)

III. Fluid mechanics of gas turbine engine operation in inlet flow distortion (including inlet vortex distortions as well as combined radial/circumferential total pressure distortion);

IV. Investigations of three-dimensional flows in highly loaded turbomachines (including actuator duct theory and blade-to-blade flow analysis and linearized analysis of swirling three-dimensional flows in

turbomachines). The overall thrust of these tasks is a numerical-experimental/analytical attack on those areas which are seen as being of high technological import as well as of fundamental interest.

This report summarizes progress on the four tasks during the period 1 June 1979 to 30 September 1980. A summary of significant accomplishments is first given and then the work accomplished in each task is described in greater detail.

2. STATUS OF THE RESEARCH PROGRAM

Summary

Task I: Investigation of Fan and Compressor Design Point Fluid Dynamics

A) Inverse (Design) Calculation Procedure: A method for inverse design of transonic compressor blades has been developed. A computer code has been written and run for the two-dimensional case. The method is inviscid but can include strong shocks, i.e., is not limited to potential flows. The results for the two-dimensional case, which will be reported in a forthcoming paper, are quite encouraging, and the basic approach appears to be able to be extended to include effects of viscosity and three-dimensionality.

B) Further Measurements of AFAPL HTF Compressor Stage: A mechanical diaphragm cutter has been installed in the MIT Blowdown Facility. The AFAPL Stage has been mounted in the facility and is being readied for testing.

Task II: Investigation of Basic Mechanisms for Compressor Stability Enhancement Using Casing Treatment

Groove geometries have been designed and fabricated for both the (rotor) tip and the (stator) hub. The latter is a rotating section that moves relative to the cantilevered stator. The aerodynamic design of the experiment has been carried out for both a rotor tip and a stator hub stall configuration. The low speed compressor has been instrumented and the basic data acquisition interfacing completed. Tests of the baseline (smoothwall) hub stall configuration are currently in progress.

Task III: Investigation of the Response of Gas Turbine Engines to Inlet Distortion

A) Basic Studies of the Inlet Vortex Flow Field: A model has been developed of the vorticity field associated with the inlet vortex. The model is based on a secondary flow approach, in which the vortex filaments are assumed to be convected by a primary irrotational flow. A three-dimensional potential flow code is used to calculate this primary flow field for an inlet in ground effect. Amplification of ambient vorticity can be found by tracking the deformations of the vortex filaments as they are convected by this primary flow. The complementary experimental effort on this task has been, up to now, mainly focussed on development of flow visualization techniques and experiments with profile generators to produce a suitable 'ambient' shear. These have been concluded and are now conducting flow visualization studies on a model inlet in the MIT Ocean Engineering Water Tunnel Facility.

B) Combined Radial/Circumferential Inlet Total Pressure Distortion: The analysis has been completed for the case where the total pressure distortion has a zero radial gradient at the hub and tip. Calculations have been carried out to show the differences that can exist between the three-dimensional and the quasi-two-dimensional strip theory approach. Conceptual formulation of the case with non-zero gradient at the boundaries has also been accomplished.

Task IV: Investigation of Three-Dimensional Flow in Highly Loaded Turbomachines

A formulation of the blade-to-blade problem for three-dimensional flow in highly loaded turbomachines, including especially finite chord effects, has been completed. A new form of "actuator duct" theory which is useful for examining both the axisymmetric and blade-to-blade features of turbomachinery flows has also been developed. Theoretical results of previously developed three-dimensional flow calculation procedure have been shown to compare favorably with experimental measurements on a low speed highly loaded compressor rotor. A three-dimensional analysis of unsteady flow in a turbomachinery blade row has been completed.

TASK I: INVESTIGATION OF FAN AND COMPRESSOR DESIGN POINT FLUID DYNAMICS

A) Inverse (Design) Calculation Procedure

Design or inverse techniques for turbomachinery blade rows exist for the special cases of two-dimensional shock-free flow, Bauer¹, or two-dimensional potential flows with weak shock waves, Ives². These schemes appear satisfactory for stator design problems, Stephens³, but are not satisfactory for high approach Mach number rotor designs or for three-dimensional designs. In addition, geometric constraints such as closed trailing edge conditions are difficult to enforce. Considerable progress for inlet diffuser or duct flow problems has been made by Zannetti⁴ in which some geometric constraints are satisfied directly.

Direct or analysis techniques (for which the geometry is always specified) now exist which consider, at least in an approximate manner, all of the characteristic features of high Mach number turbomachinery flows: mixed subsonic and supersonic zones, approach Mach numbers of 1.5 and above, strong shock waves, and a high degree of geometric complexity. Such computer codes are nearly always shock-capturing, time marching schemes, see Thompkins⁵ or Steger⁶ as examples, and it is natural to ask if these solvers can be used as the basis of an inverse calculations scheme without the need for numerical optimization techniques or a "cut and try" approach. This review proposes a framework in which various time-marching direct solvers may be used as inverse solvers, solves some two-dimensional, inviscid transonic cascade problems, and discusses the extension of these techniques to three-dimensional designs.

Flow Equations for Two-Dimensional Inviscid Example

The inverse technique presented under development uses the strong conservation law form of the Euler or Navier-Stokes expressed in a form suitable for use with time dependent, body-fitted coordinate systems, see Vivian⁷ or Steger⁸. For two-dimensional, inviscid flow, these equations when written in vector form for Cartesian coordinates are:

$$\partial_t \bar{q} + \partial_x \bar{F} + \partial_y \bar{G} = 0 \quad (1)$$

where

$$\bar{q} = \begin{bmatrix} \rho \\ \rho u \\ \rho v \end{bmatrix} \quad \bar{F} = \begin{bmatrix} \rho u \\ \rho u^2 + P \\ \rho uv \end{bmatrix} \quad \bar{G} = \begin{bmatrix} \rho v \\ \rho uv \\ \rho v^2 + P \end{bmatrix}$$

These equations express conservation of mass and momentum. In inverse code applications where only steady state solutions are required, the energy equation may be replaced with the assumption of iso-energetic flow, or the assumption that the stagnation enthalpy is constant everywhere. This assumption provides a simple algebraic relation between the pressure, density and velocity components.

$$P = \rho \frac{(\gamma - 1)}{\gamma} \left[h_{\text{Stag}} - \frac{(u^2 + v^2)}{2} \right] \quad (2)$$

These equations can seldom be solved for realistic geometries without transforming from a Cartesian system (t, x, y as independent variables) to a more general computational system (t, ζ, η as independent variables). The transformed equations are most useful when the new coordinate system is at least a body-fitted system. In a body-fitted coordinate system, flow boundary surfaces, such as blade profile shapes, become coordinate lines in the computational space. A simple body-fitted coordinate mapping is illustrated in Fig. 1 and a more complex one is illustrated in Fig. 2.

Following Viviani⁷, a coordinate mapping may be defined as

$$\zeta = \zeta(x, y, t) \quad \eta = \eta(x, y, t) \quad t = t \quad (3)$$

where ζ and z are general mapping functions that may depend on time.

Subject to such a mapping, the flow equations may be written as

$$\partial_t \hat{q} + \partial_\xi \hat{F} + \partial_\eta \hat{G} = 0 \quad (4)$$

where

$$\hat{q} = \bar{q}/J \quad \hat{F} = \left[(\partial_t \xi) \bar{q} + (\partial_x \xi) \bar{F} + (\partial_y \xi) \bar{G} \right] / J \quad (5a)$$

$$\hat{G} = \left[(\partial_t \eta) \bar{q} + (\partial_x \eta) \bar{F} + (\partial_y \eta) \bar{G} \right] / J \quad (5b)$$

Here J is the transformation Jacobian

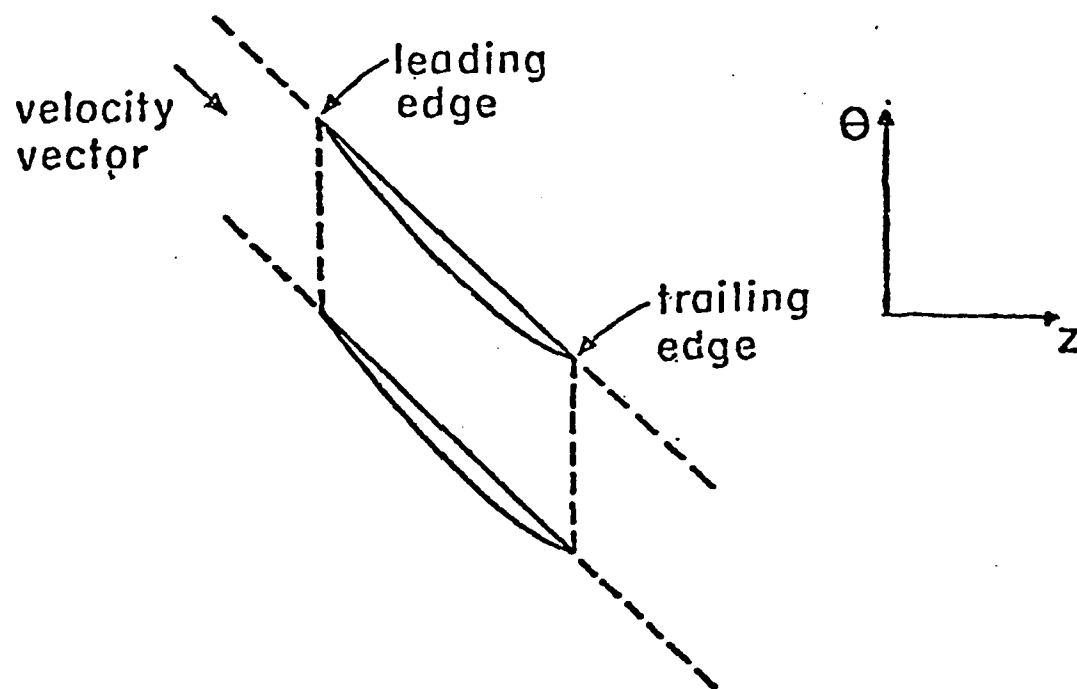
$$J = (\partial_x \xi)(\partial_y \eta) - (\partial_y \xi)(\partial_x \eta) \quad (6)$$

These equations have a particularly instructive form when the contravariant velocities along coordinate lines are introduced:

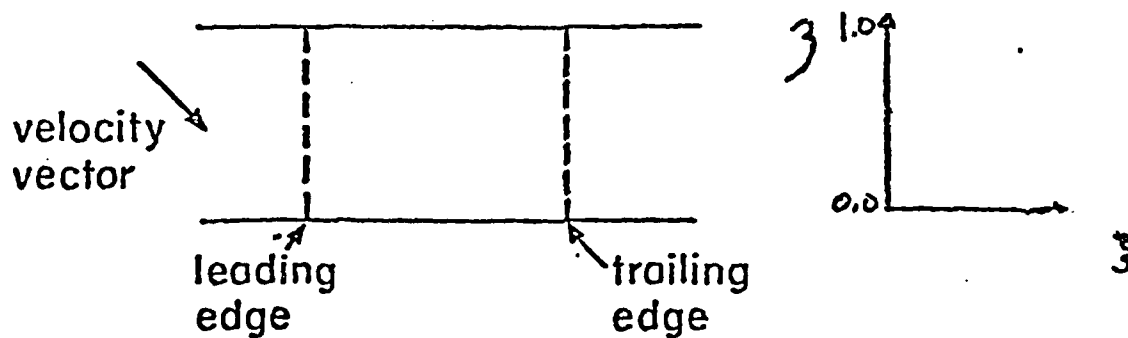
Normal to the ξ coordinate line

$$U = \partial_t \xi + (\partial_x \xi)u + (\partial_y \xi)v \quad (7a)$$

TYPICAL BLADE TO BLADE VIEW, PHYSICAL SPACE



BLADE TO BLADE VIEW, COMPUTATIONAL SPACE



Mapping Function

$$\zeta = \frac{\theta - \theta_{ps}}{\theta_{ss} - \theta_{ps}}$$

Figure 1

PHYSICAL SPACE VIEW OF COMPRESSOR CASCADE GRID

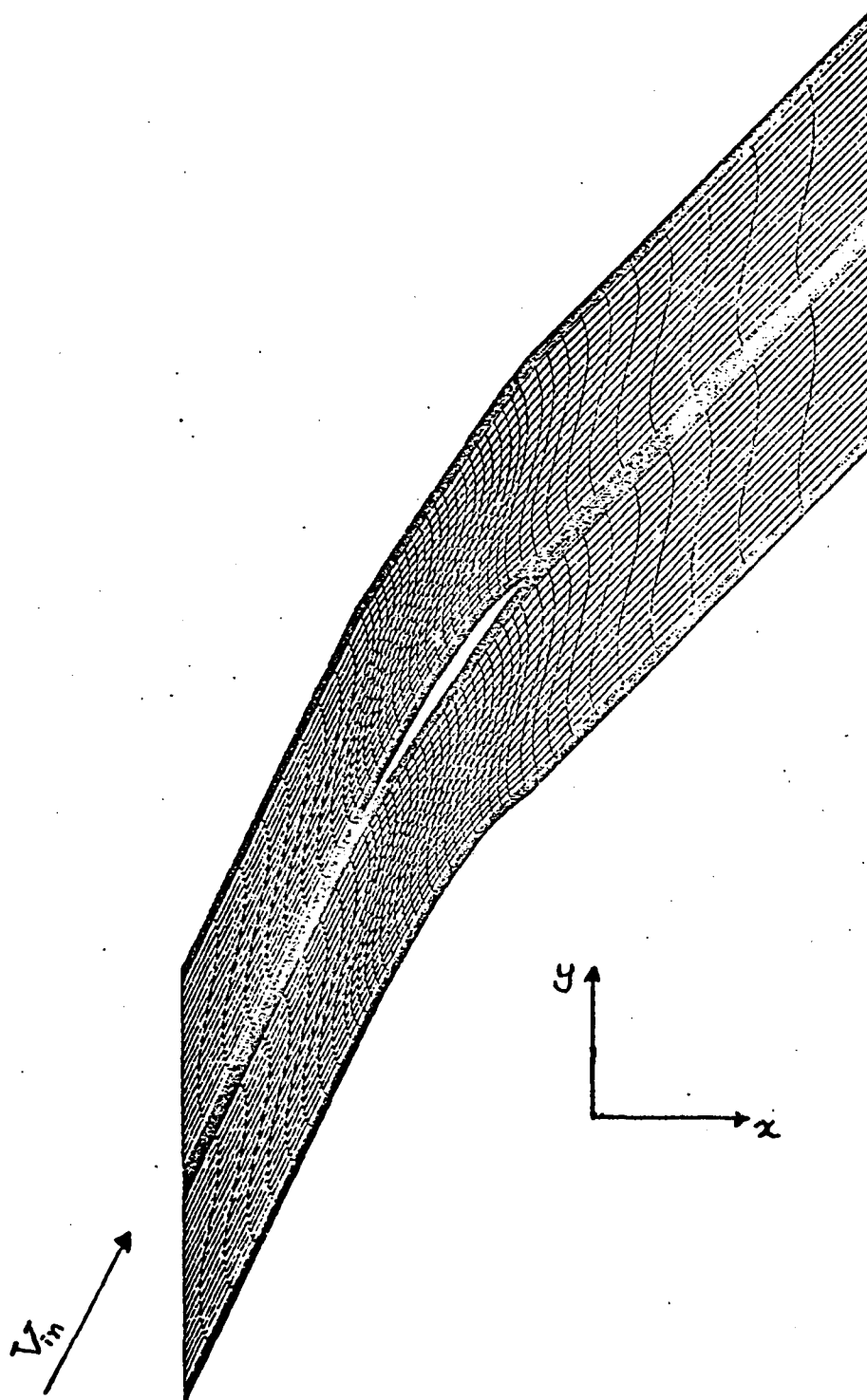


Figure 2

and normal to the η coordinate line:

$$V = \partial_t \eta + (\partial_x \eta)u + (\partial_y \eta)v \quad (7b)$$

With these definitions, the flux vectors \hat{F} and \hat{G} may be rewritten as:

$$J\hat{F} = \begin{bmatrix} \rho U \\ \rho u U + (\partial_x \xi)P \\ \rho v U + (\partial_y \xi)P \end{bmatrix}, \quad J\hat{G} = \begin{bmatrix} \rho V \\ \rho u V + (\partial_x \eta)P \\ \rho v V + (\partial_y \eta)P \end{bmatrix} \quad (8)$$

Along the body surface, $\eta = 0$ and $\eta = 1$ in figure 1, the flow tangency boundary condition is simply expressed as $V = 0$. The wall pressure is usually found from a compatibility condition derived from the momentum equation such as:

$$\partial_n P = \frac{\rho U^2}{R_s} \quad (9)$$

where

n indicates the direction normal to the surface

U_p is the velocity parallel to the surface

R_s is the radius of curvature of the surface.

Inverse Technique

An inverse calculation procedure which is fundamentally a sequence of direct calculations for a time-dependent geometry can be constructed using the observation that the flow equation (4) may be integrated at all interim points using only a specified wall pressure. To illustrate this point consider the simplest time-marching scheme (forward time, centered space

differencing) applied at grid node points near a solid wall, see figure 3 for grid illustration. This differencing applied to equation (4) yields:

$$\frac{\hat{q}_{i,1}^{n+1} - \hat{q}_{i,1}^n}{\Delta t} = - \left[\frac{\hat{F}_{i+1,1}^n - \hat{F}_{i-1,1}^n}{\Delta \xi} \right] - \left[\frac{\hat{G}_{1,2}^n - \hat{G}_{1,0}^n}{\Delta \eta} \right] \quad (10)$$

The flux vectors $\hat{F}_{i+1,1}^n$, $\hat{F}_{i-1,1}^n$ and $\hat{G}_{1,2}^n$ pose no difficulties, but the flux vector $\hat{G}_{1,0}^n$ must incorporate the solid wall boundary conditions. This flux vector may be written in a form containing only the wall pressure since $\bar{v}_{1,0}$ is always zero. This form is

$$\bar{G}_{1,0}^n = \begin{bmatrix} \rho V \\ \rho u V + (\partial_x \eta) P \\ \rho v V + (\partial_y \eta) P \end{bmatrix}_{1,0}^n = \begin{bmatrix} 0 \\ (\partial_x \eta) P \\ (\partial_x \eta) P \end{bmatrix}_{1,0}^n \quad (11)$$

The present inverse technique proceeds by first assuming a trial geometry, coordinate system and Jacobian members. The flow equations are then integrated at all interior points using a pressure derived from the compatibility equation (9). A new wall pressure consistent with the current flow field is computed and the difference between the design pressure and the computed pressure is used to predict a corrected wall shape. When a new wall shape has been predicted, a new coordinate system is computed and the flow solution is updated at each interior node point. For convenience during the present exploratory phase, the direct solver used has been an explicit method by MacCormack⁸. Nearly any other explicit scheme could have been used as well as implicit schemes like that of Beam and Warming⁹.

Two key elements in this procedure are the frequency with which the blade shape is updated and the scheme by which the wall shape corrections are derived from the wall pressure error. It has been found by experimentation

COMPUTATIONAL SPACE GRID DEFINITION

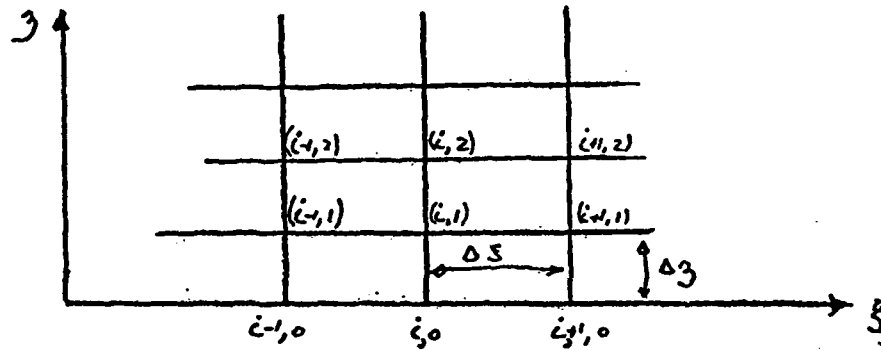


Figure 3

that updating the blade shape at every time step in the time marching scheme is not efficient in total CPU time, but rather, the blade shapes are updated every 4 time steps. The local blade shape correction is determined by setting the difference between the design wall flux vector and transient wall flux vector to zero. This difference is defined as:

$$\hat{G}_{1,0}^t - \hat{G}_{1,0}^d = \begin{bmatrix} 0 \\ \rho u V^s + (\partial_x \eta) P \\ \rho v V^s + (\partial_y \eta) P \end{bmatrix}_{1,0}^n - \begin{bmatrix} 0 \\ (\partial_x \eta) P \\ (\partial_y \eta) P \end{bmatrix}_{1,0}^d = 0 \quad (12)$$

where

$$V^s = (\partial_x \eta) u + (\partial_y \eta) v$$

For a steady state solution, $V_{1,0}^s$ would be zero, and $\hat{G}_{1,0}^t$ would equal to $\hat{G}_{1,0}^d$. This flux vector error term yields two equations for $u_{1,0}$ and $v_{1,0}$ which are:

$$\left[(\rho u) [(\partial_x \eta) u + (\partial_y \eta) v] \right]_{1,0} = (\partial_x \eta) (P_{1,0}^d - P_{1,0}^n) \quad (13)$$

$$\left[(\rho v) [(\partial_x \eta) u + (\partial_y \eta) v] \right]_{1,0} = (\partial_y \eta) (P_{1,0}^d - P_{1,0}^n) \quad (14)$$

where

$P_{1,0}^n$ is the pressure found from the wall compatibility equation, and the wall density is found by extrapolation.

However, the true value of $V_{1,0}^n$ is always zero, and this may now be used to find the time derivative of $\eta(x, y, t)$.

$$(\partial_t \eta)_{1,0}^n = -V_{1,0}^s \quad (15)$$

The wall velocity is proportional to $(\partial_t \eta)_{1,0}^n$ and the new wall positions are found by time integration of the wall velocities. It was found to be computationally efficient to under-relax the wall movement calculation with an under-relaxation factor of 0.025.

Constraints

In an axial compressor design, the blade profile shapes are nearly the last design element to be specified. The blade shapes must then satisfy several geometric and non-geometric constraints. Typically the blade chord, the number of blades, the blade row inflow angle and the desired static pressure rise will be specified before blade shapes are decided. In addition geometric constraints like trailing edge closure, maximum or minimum blade thickness or prescribed leading edge radius or wedge angle must also be satisfied.

The proposed inverse technique allows these types of constraints to be satisfied with little difficulty. Most non-geometric constraints are satisfied through selection of far-field boundary conditions or control of the grid generation process. Specific geometric constraints are satisfied by using the wall compatibility pressure rather than a design pressure when either a section of the blade shape is to be specified or the computed blade shape would violate the constraint. For example, the blade trailing edge is always specified to be closed and thus the pressure at this point may not be specified.

Special Boundary Conditions

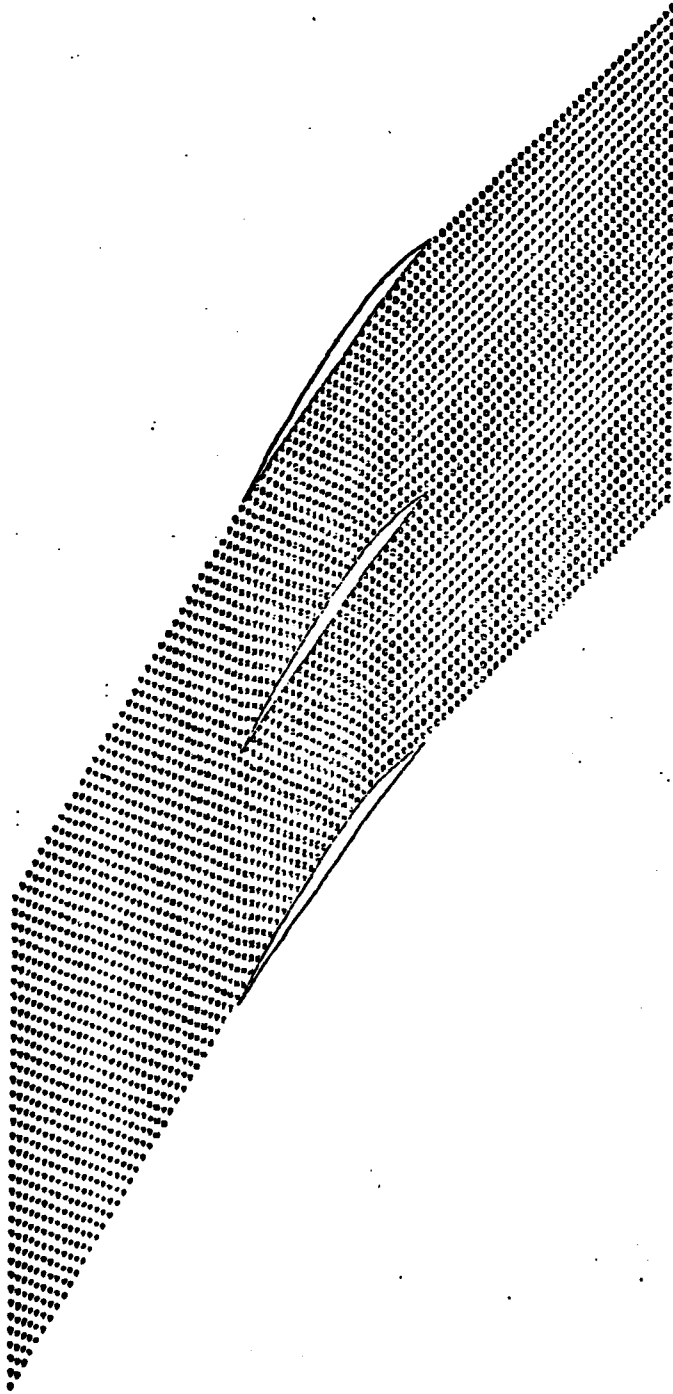
The two-dimensional cascade problem requires far-field boundary conditions, flow periodicity conditions and a Kutta condition as well as the hard wall boundary conditions. The far-field inflow condition maintains a specified value of stagnation pressure, stagnation temperature and inlet flow angle. The inlet velocity is calculated using a method of characteristics analysis similar to that of Gopalakrishnan¹⁰. The far-field exit velocity is calculated using a similar model but with the exit static pressure specified. A Kutta condition is imposed by requiring that the static pressure at the last grid point on the blades be equal on the suction and pressure surfaces. Periodic flow conditions are implemented directly in either the grid system or the numerical solution scheme.

Direct Solver Test Case

The inverse technique requires an accurate direct solver to be available and the scheme chosen for development calculations is that of MacCormack⁸. This scheme is an explicit, second order accurate, time-marching scheme of shock capturing type. The problems chosen for development testing were typical sharp leading blade sections for moderately supersonic inflow, M_{in} approximately 1.55. A typical flow field calculated for a row static pressure ratio of 2.5 is shown in Fig. 4 in terms of Mach number contour levels. Of special note in this figure is the upstream extent of the bow wave shock system and the strong passage shock. The flow is subsonic behind the passage shock. Static pressure profiles on the suction surface and pressure surface are shown in Fig. 5. The passage shock on the suction surface is resolved over 5 to 6 mesh points.

TYPICAL COMPRESSOR CASCADE
MACH NUMBER DISTRIBUTION

INLET ANGLE FIXED



DT=0.030

ITERATION=3000.

INLET FLOW ANGLE=64.13
T.E. FLOW ANGLE=50.74

A	0.200
B	0.264
C	0.328
D	0.392
E	0.456
F	0.520
G	0.584
H	0.648
I	0.712
J	0.776
K	0.840
L	0.904
M	0.968
N	1.032
O	1.096
P	1.160
Q	1.224
R	1.288
S	1.352
T	1.416
U	1.480
V	1.544
W	1.608
X	1.672
Y	1.736
Z	1.800

letters indicate value of
Mach Number at Node Point

Figure 4

TYPICAL BLADE PRESSURE DISTRIBUTION
FOR INLET MACH NUMBER OF 1.55

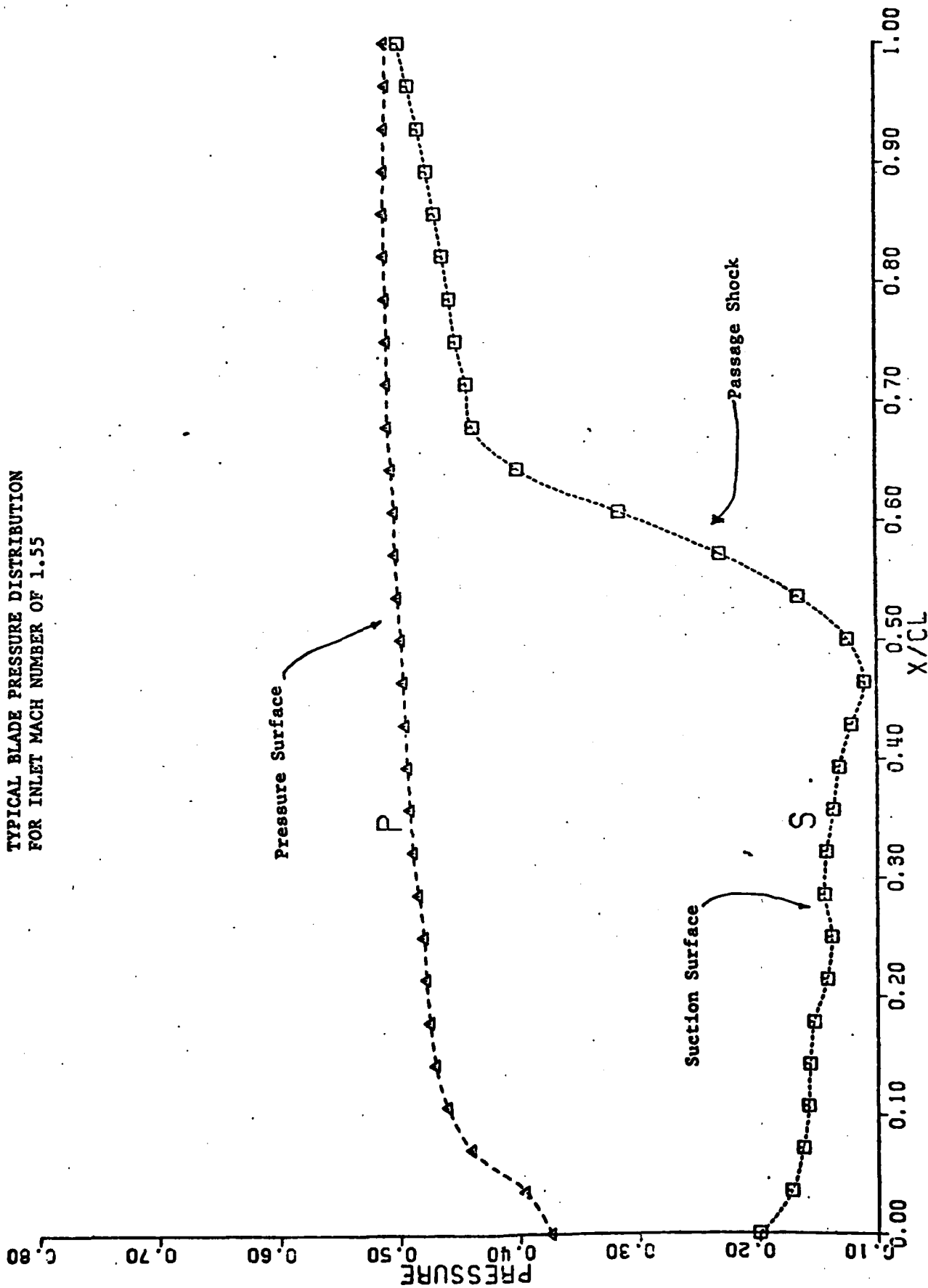


Figure 5

Inverse Technique Test Case

Figure 5 illustrates a typical problem in blade turbomachinery blade row design which is that the suction surface Mach number in front of the passage shock is well above the upstream Mach number, nearly 1.8 for an inlet value of 1.55. A pressure profile like that of figure 6 reduces this suction surface expansion and would be more desirable. This pressure distribution was used as input to the inverse technique and the blade shapes illustrated in Fig. 7 calculated. The constraints were that the value of chord length, inlet flow angle, exit static pressure and leading edge wedge angle were to be the same as the direct solver test case. As a check on this solution, the direct solver solution was repeated for the blade shapes calculated by the inverse technique. Figure 8 shows a comparison between the input pressure distribution and the direct solver results. Quite satisfactory agreement is found.

Conclusions

These results demonstrate that an inverse technique for non-potential flow in turbomachinery blade passages is possible. The present technique is in an early state of development but already is able to solve some important problems in blade shape optimization. Much work remains to be done before a practical design procedure exists, and it is not expected that the present shape correction procedures or even time-marching direct solvers will prove to be the most efficient schemes.

An important feature of this inverse formulation is the extension to three-dimensional flow fields. This extension is the ultimate goal of the present research effort since a two-dimensional technique is felt to

IMPROVED BLADE PRESSURE DISTRIBUTION TO REDUCE
SUCTION SURFACE MACH NUMBER

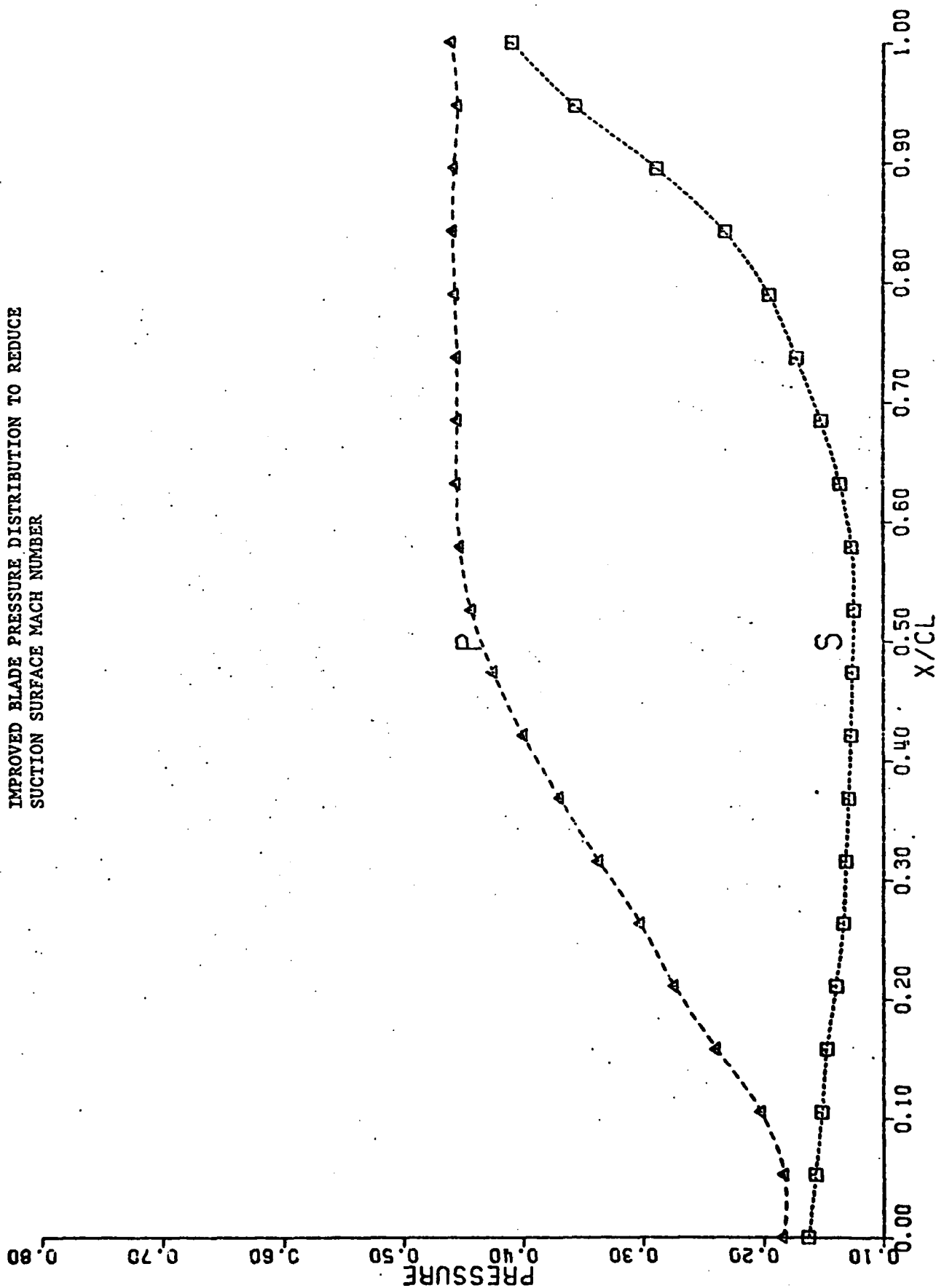
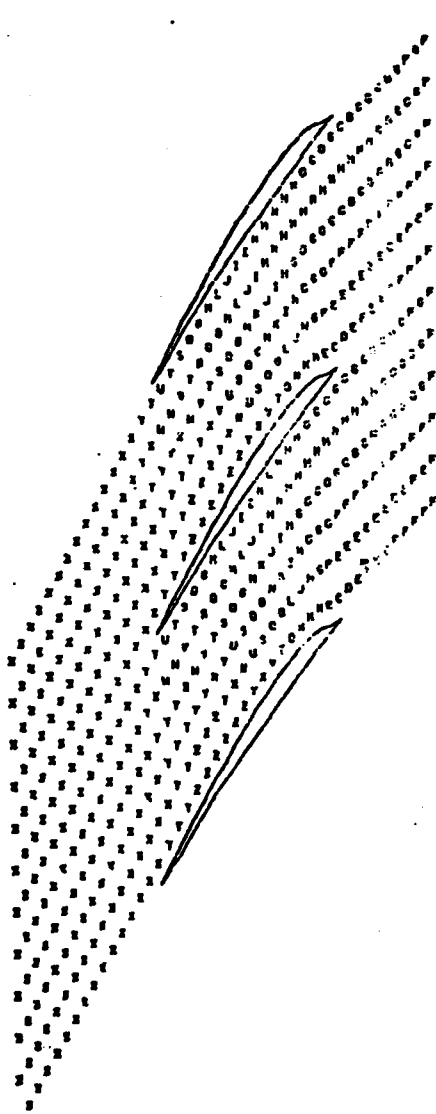


Figure 6

MACH NUMBER DISTRIBUTION AND BLADE SHAPE AS
PREDICTED BY INVERSE TECHNIQUE



DT=0.030
ITERATION=4000
ISHBC=0 PDOWN=0.4500
INLET FLOW ANGLE=64.13
T.E. FLOW ANGLE=50.00
A 0.200
B 0.264
C 0.328
D 0.392
E 0.456
F 0.520
G 0.584
H 0.648
I 0.712
J 0.776
K 0.840
L 0.904
M 0.968
N 1.032
O 1.096
P 1.160
Q 1.224
R 1.288
S 1.352
T 1.416
U 1.480
V 1.544
W 1.608
X 1.672
Y 1.736
Z 1.800

letters indicate value of
Mach Number at Node Point

Figure 7

BLADE PRESSURE DISTRIBUTION USING PREDICTED
BLADE SHAPE AS INPUT TO DIRECT SOLVER

21

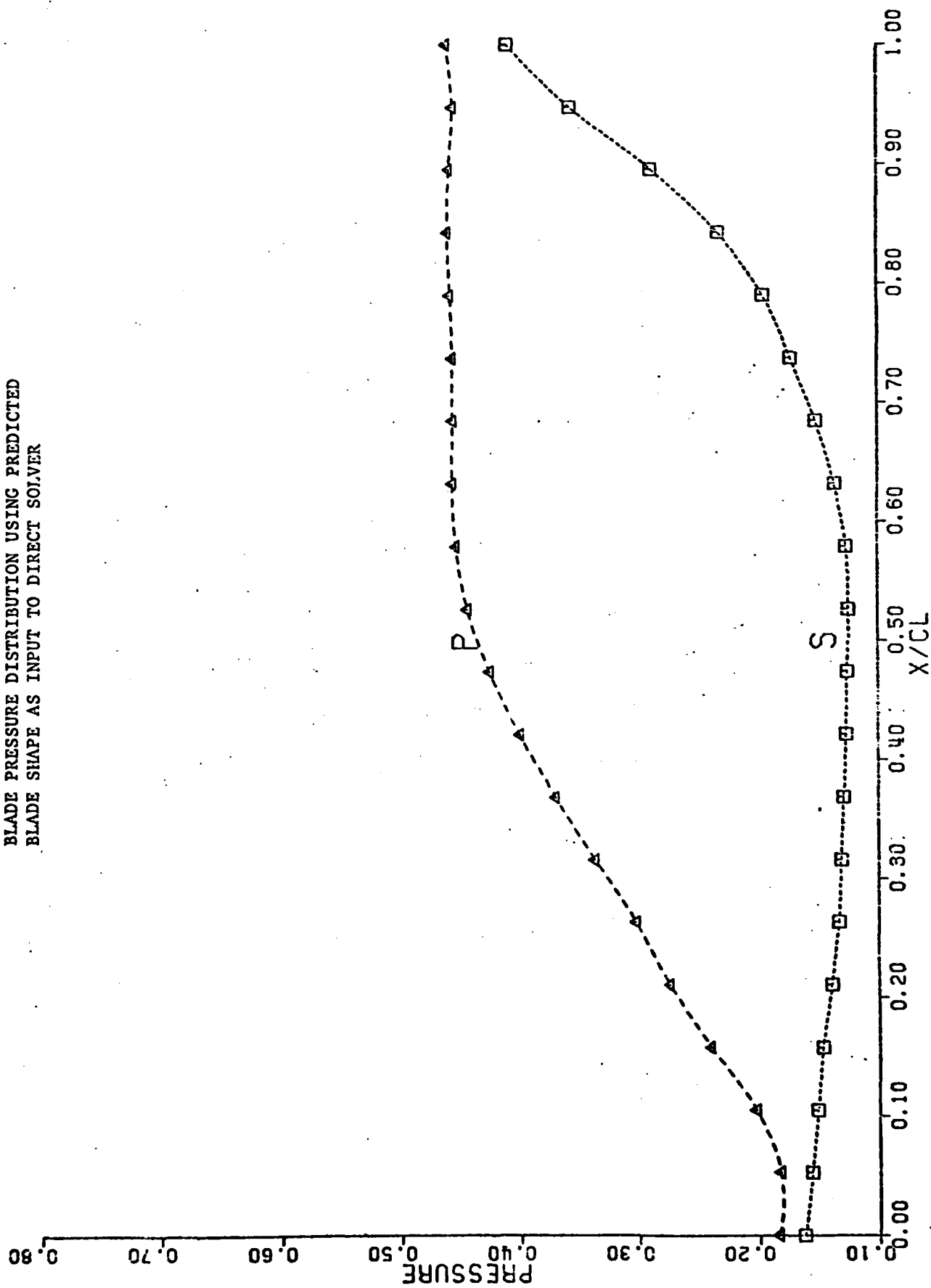


Figure 8

be of marginal utility. The extension is based on the fact that the form of the three-dimensional Navier-Stokes or Euler equations is identical to the two-dimensional forms. These forms are:

$$\partial_t \bar{q} + \partial_{\xi} \hat{\bar{F}} + \partial_{\eta} \hat{\bar{G}} + \partial_{\zeta} \hat{\bar{H}} = 0 \quad (16)$$

where

$$\hat{\bar{q}} = \bar{q}/J, \quad \hat{\bar{F}} = [(\partial_t \xi) \bar{q} + (\partial_x \xi) \bar{F} + (\partial_y \xi) \bar{G} + (\partial_z \xi) \bar{H}] / J$$

$$\hat{\bar{G}} = [(\partial_t \eta) \bar{q} + (\partial_x \eta) \bar{F} + (\partial_y \eta) \bar{G} + (\partial_z \eta) \bar{H}] / J$$

$$\hat{\bar{H}} = [(\partial_t \zeta) \bar{q} + (\partial_x \zeta) \bar{F} + (\partial_y \zeta) \bar{G} + (\partial_z \zeta) \bar{H}] / J$$

J is the Jacobian of the transformation

$$\xi = \xi(x,y,z,t), \quad \eta = \eta(x,y,z,t), \quad \zeta = \zeta(x,y,z,t), \quad t = t \quad (17)$$

The flux vectors retain the same general form:

$$\bar{G} = \begin{bmatrix} \rho V \\ \rho u V + (\partial_x \eta) P \\ \rho v V + (\partial_y \eta) P \\ \rho w V + (\partial_z \eta) P \end{bmatrix} \quad (18)$$

where

$$V = (\partial_t \eta) + (\partial_x \eta) u + (\partial_y \eta) v + (\partial_z \eta) w$$

The flow tangency condition is still $V = 0$ and the same general analysis of the interior node calculation problem will apply.

A three-dimensional inverse technique would be expected to require the same type of wall pressure information and follow closely the development

of the two-dimensional version. General experience with three-dimensional solvers suggests that the practical extension to a three-dimensional inverse solver will not be a simple process.

B) Further Measurements of AFAPL High Through-Flow Compressor Stage

Introduction

The primary goal of this research effort is to elucidate the fluid physics of the Air Force Aero Propulsion Laboratory's (AFAPL) High Through Flow (HTF) Compressor Stage. This stage is characterized by its unusually high performance in terms of both mass flow and efficiency. The approach taken is to measure the time and spatially resolved flow field in the machine in an attempt to further understand its performance. These measurements are made in the MIT Blowdown Compressor Tunnel¹¹ using unique high frequency pressure instrumentation in development at MIT over the last ten years.

Since flow measurement at frequencies capable of resolving transonic compressor blade passing is at the edge of the state of the art, instrumentation development is a part of this program.

Data Reduction

The first effort in this period was to attempt the data reduction and analysis of a set of measurements made on the HTF rotor under a previous AFAPL sponsored project. This consisted primarily of data taken with an MIT developed miniature (4.6 mm diameter) high frequency sphere probe¹². Detailed analysis showed that the early version of the probe used on the HTF stage suffered from excessive thermal drift. After considerable effort, reduction of that data set was abandoned.

Instrumentation Development

A new version of the probe was developed, this one incorporating integral water cooling to stabilize the probe temperature. This probe consists of five silicon wafer diaphragms compactly arranged on the surface of a sphere. The probe can simultaneously measure total and static pressure and two flow angles.

The modified probe gave satisfactory results. By the time the new probe was constructed and tested, however, the HTF stage lost its scheduled tunnel time and had to vacate the Blowdown Tunnel.

The new sphere probe was then proven on a companion NASA sponsored effort¹³. The probe proved to give reliable results. However, its 4.6 mm diameter limited the measurement resolution, especially in the blade wakes. Since the smallest stable silicon wafer transducers manufactured are approximately 1.5 mm in diameter, the 4.6 mm diameter sphere is a realistic lower limit upon which to arrange five transducers. Therefore, a new geometry was adapted. This consists of four transducers mounted on a 2.8 mm diameter cylinder (Fig. 9). Three of the transducers are arranged around the circumference of the cylinder at 0° and at ±45°. Measurements from these three establish total and static pressure and one flow angle. The fourth transducer is angled at 45° off the end of the cylinder and measures the second flow angle. This probe is also water cooled.

In addition to increased spatial resolution, the new geometry offers the advantage of utilizing the newly developed "third generation" silicon wafer transducers. These have four times less thermal drift than do the second generation transducers but demand a larger, oblong mounting area. By orienting the long axis of the oblong along the cylinder axis, the new transducer could be used while the geometry is kept compact.

A pneumatic full scale model of the cylinder probe was constructed and extensively tested in a 0.15 m diameter free jet. (The silicon transducers are too fragile to permit their use unprotected in an air jet for the many hours necessary to calibrate a new probe geometry.) The new geometry has been calibrated in terms of pressure, Mach number, Reynolds number, and flow angles. This calibration yields a set of parametric curves which are used

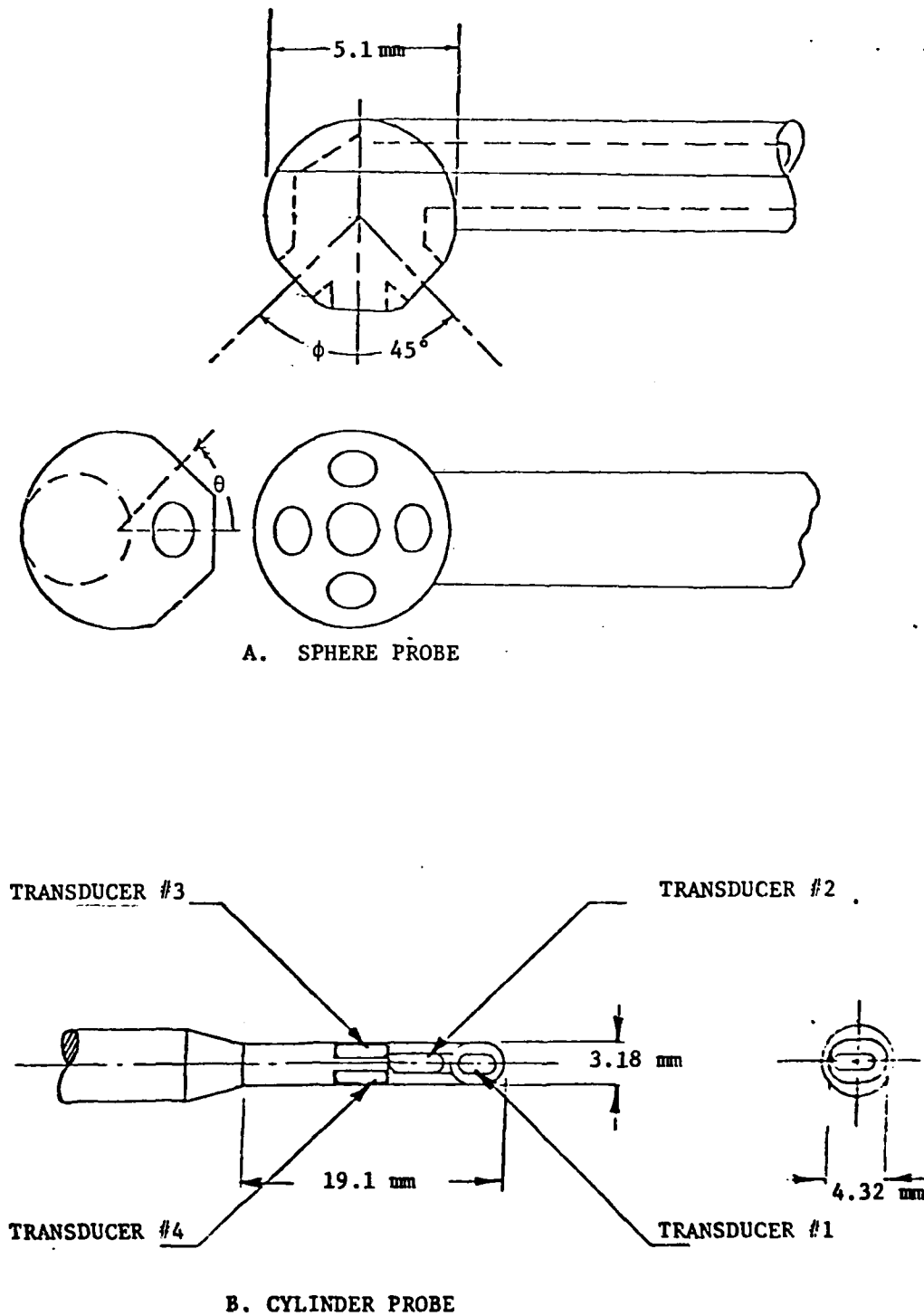


FIGURE 9 - PROBE GEOMETRY AND TRANSDUCER LAYOUT

to reduce the pressure output from the transducers.

The actual probe body itself has been fabricated from Invar and the transducers mounted. Only final wiring is required.

Diaphragm Cutter

The MIT Blowdown Tunnel is a transient facility which consists of a supply tank initially separated by a diaphragm from a test section followed by a dump tank. The compressor stage to be tested is in the test section. The entire facility is pumped to vacuum and then the supply tank filled to 10 psia with the test gas. The compressor rotor is spun up by an auxiliary drive while in vacuum and the diaphragm then ruptured to start the test.

The requirements on the diaphragm opening in the Blowdown Tunnel are quite rigorous - not at all similar to those for a shock tube. The diaphragm must hold a relatively small pressure difference over a large area and be vacuum tight. It must open and its petals completely fold out of the flow within 10 ms. After extensive development, a method involving thin strips of plastic explosive arranged in pie segments on the diaphragm was perfected. Although demanding in terms of explosive quality and handling, this has served well for the last ten years. Recently, the sole manufacturer of the explosives ceased production. Rather than try to manufacture the explosive at MIT, we elected to build a mechanical diaphragm cutter¹⁴.

The construction of the diaphragm cutter was initially funded by NASA. It has proven to be more complicated and costly than the initial construction of the tunnel itself. Since the cutter is needed for complete testing of the AFAPL stage, final assembly and testing of the cutter has been included in this effort. The cutter consists of a moving diaphragm which impacts on stationary knives (Fig. 10). To date, the cutter has been assembled and tested approximately 8 times. The mechanical operation is satisfactory, however,

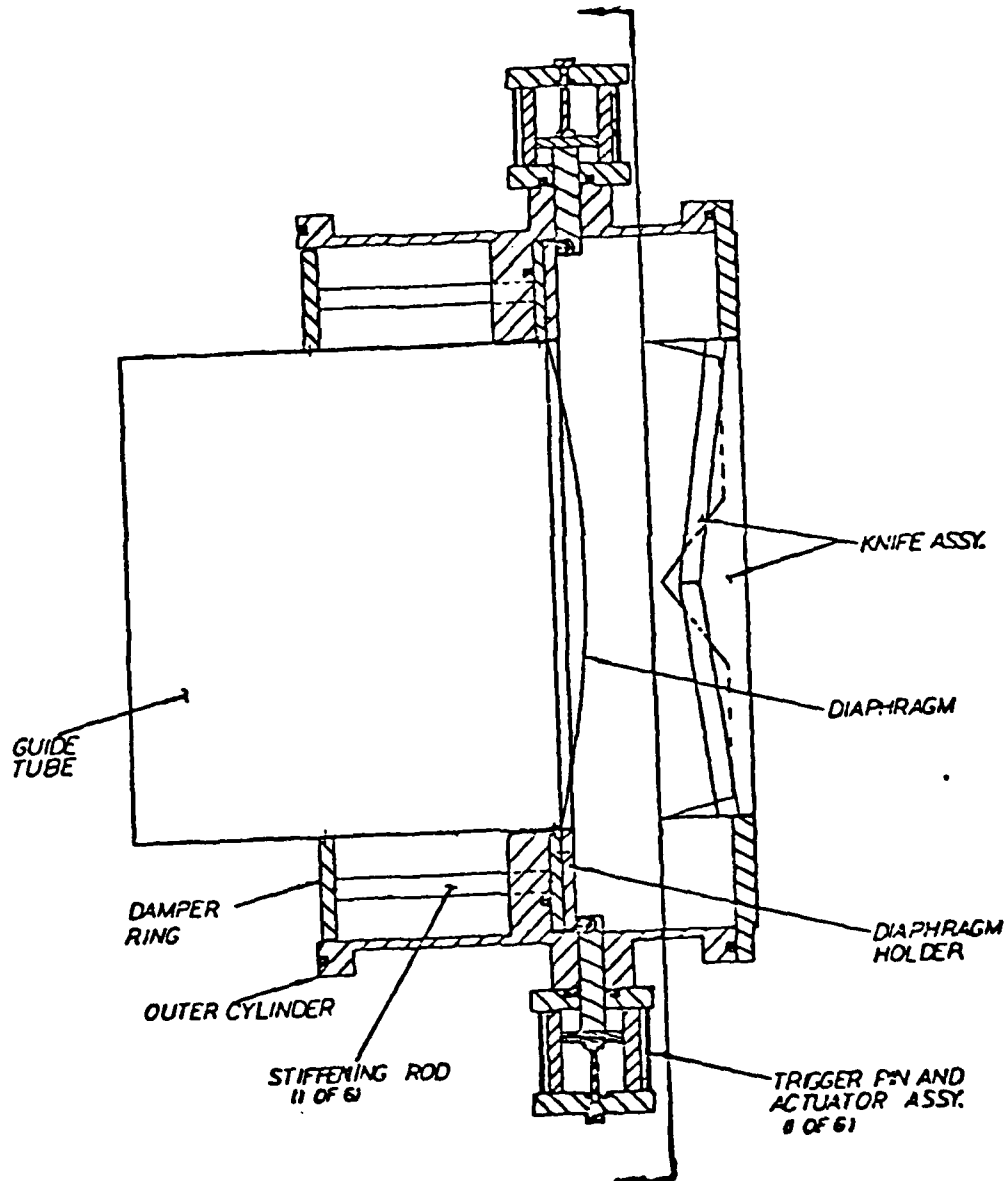


FIGURE 10. DIAPHRAGM CUTTER

The Diaphragm holder slide forward into the stationary knives propelled by the gas loading on the diaphragm.

the cut diaphragm segments do not fold out of the flow as completely as desired. The knife configuration is presently being modified to alleviate this problem.

Further Testing

Previous tests at MIT have consisted of tests of the AFAPL rotor operating without the stators. This was both to allow flow field measurements directly behind the stator as well as due to AFAPL operational constraints. In particular, the stators were needed at AFAPL for another program. The tests for this period were to be with the stators. AFAPL was not, however, able to furnish the stators until the eleventh month of the twelve month period. The stators are now at MIT and the HTF stage is in the tunnel.

Preliminary tests have been conducted using the new instrumentation. Testing of the HTF stage is expected to continue through late Fall 1980.

There is also a further aspect to the planned work on this topic. In transonic compressor stages conventionally measured tip efficiencies are much lower than can be explained on the basis of boundary layer and steady shock losses. The trend is true for both the NASA stage and the Air Force High Through-Flow stage. Latest measurements made in the NASA stage indicate that these losses may be due to unsteady passage shock motion. In order to investigate the existence and importance of this new loss mechanism, it now becomes critically important to measure local rotor outflow total temperature at least in the rotor core flow.

It now appears that available frequency response from hot film anemometer gauges is adequate to measure local core flow total temperature in combination with local total pressure measurements. It is thus planned that part of the this year's work on this task be devoted to designing and calibrating such an "efficiency" probe to measure local streamtube efficiency for the Air Force rotor.

TASK II: INVESTIGATION OF BASIC MECHANISMS FOR COMPRESSOR STABILITY
ENHANCEMENT USING CASING TREATMENT

This task is directed towards obtaining a basic understanding of the fluid mechanics of compressor casing treatment. It has been known for over a decade that the presence of a grooved or perforated casing over the tips of an axial compressor rotor can provide a substantial increase in the stable flow range of the machine. Numerous experiments that have been carried out with such configurations to demonstrate their effectiveness in compressor blading ranging from high hub/tip radius ratio and large camber, to low hub/tip ratio with small camber, and from low Mach numbers (0.15) to high Mach numbers (~ 0.15)¹⁵⁻²⁵. Casing treatments have even been used successfully in centrifugal compressors to increase the stall margin²⁶.

Of the various trends that have emerged from these experiments, one that has been of particular concern is that generally those treatments which are most useful in extending flow range have some performance penalty. Thus an important problem is the "optimization" of the grooves, or, in other words, the obtaining of a configuration with combination of good stall margin with low efficiency penalty.

In spite of the extensive number of tests that have been carried out with casing treatment, even a qualitative understanding of the mechanisms of operation of the grooves is lacking at present, and essentially all of the information has been obtained on a cut and try basis. Such understanding, which would be useful in optimizing the treatments and attempting to formulate rational rules for its design and use, is the main objective of the work being carried out under this task.

Work to date on this task has centered on carrying out the mechanical and aerodynamic design of the grooves and of the compressor geometry to be used, as well as readying the compressor rig for testing. We can discuss each of these in turn.

Axial skewed grooves extending over approximately the central 60% of the blades are the configuration to be used. These have been fabricated by first machining a circumferential trench or slot in the casing and then inserting plexiglass strips, which form the walls of the grooves. These are then bonded to the casing with epoxy. In addition to the casing treatment, we will also be examining treatment on the hub of a cantilevered stator. Thus there are two locations at which the treatment can be used, and these are shown in Fig. 11. Note that the use of the hub treatment involves the design of an additional rotating section which extends rearward from the compressor rotor disk under the stator hub. In fact two of these rotating sections were designed and fabricated, one with a constant area outer diameter and one with a slot machined on the outside so that the grooved configuration can be built up in the same manner as with the casing treatment. Both of these rotating pieces are completed, and, as will be described below, we have currently started to run the compressor using the smooth hub (i.e., the baseline case).

The design of the compressor configuration to be used was also an item to which we devoted some attention. The predominant consideration here is that if one is using a casing treatment it should be the region of the (rotor tip) endwall that is responsible for the origination of the stall. Similarly if one is using a hub treatment the stall should be associated with the stator hub. Thus it was necessary to examine different design

CASING/HUB TREATMENT EXPERIMENT
CROSS SECTIONAL VIEW

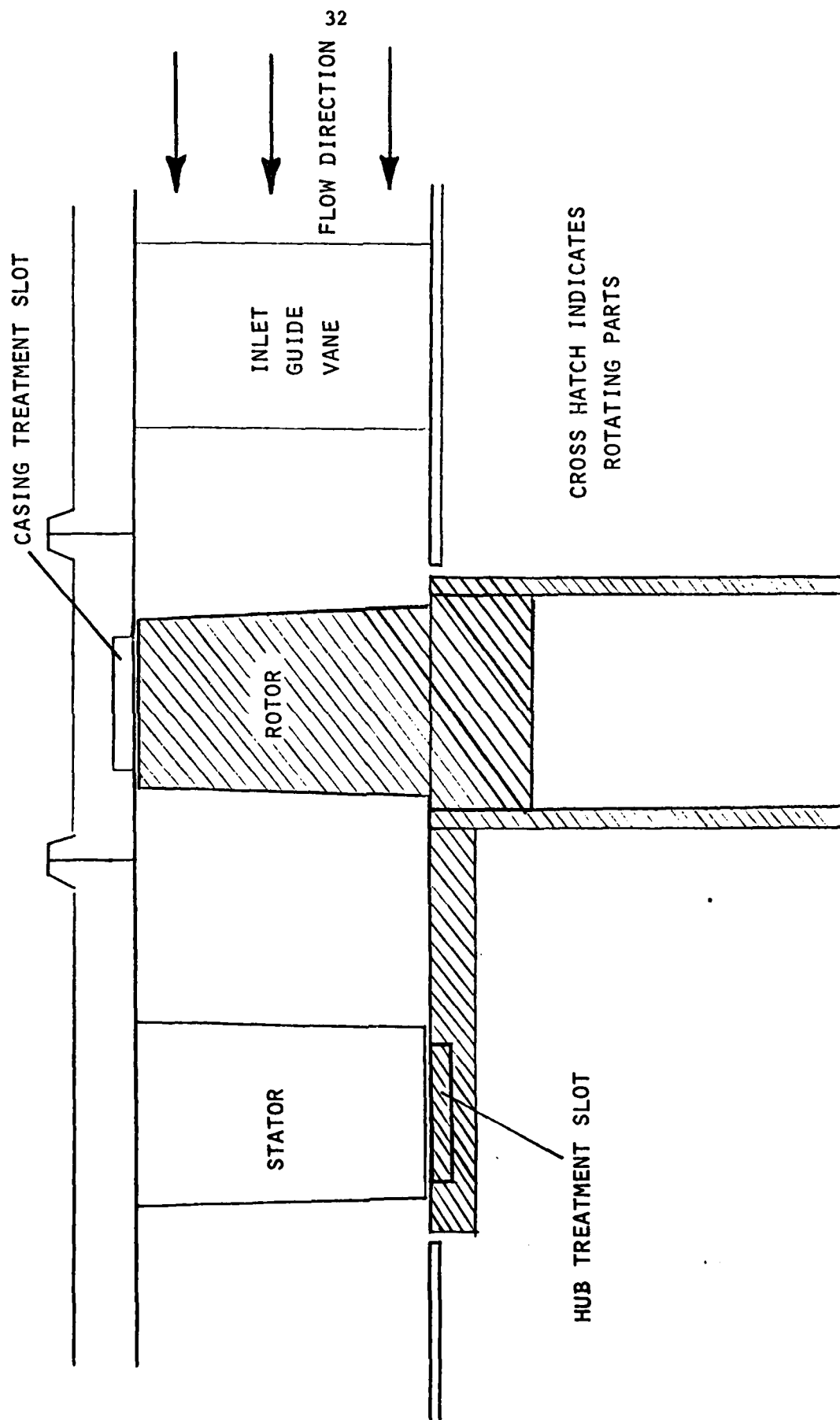


FIGURE 11

configurations to ensure that these two requirements are achieved.

In carrying out this study, we also had, for obvious reasons, a strong motivation to use existing blading, so that our idea was to see whether the above criteria could be achieved through changes in blade stagger angle only.

To accomplish these objectives, it is really necessary to design two compressor configurations, one where the rotor tip stalls and one where the stator hub stalls. For the rotor tip stall situation we can make use of the rotor alone (which is the "clearest" configuration). However to ensure that the tip is the section that is setting the stall we must run it with a radially non-uniform inlet. This procedure has been used in the past in other investigations (see Ref. 25 for a notable example), however the additional pressure drop associated with the radial profile generator, which will be a screen or combination of screens, is high enough so that we will use the auxiliary fan, which was brought under AFOSR funding, in combination with the compressor. The radial profiles of D-factor and static pressure rise divided by inlet dynamic pressure, $\Delta P/Q$ for this case are shown in Fig. 12. The flow rate is that for a highly loaded condition. It can be seen that using either of these criteria the tip section is heavily loaded.

For the stator hub stall configuration the situation is somewhat different. Although one is really interested in the stator performance only, one must create a swirling flow at inlet to the stator. There are several possible means of doing this, however, one of the most straight forward (as well as perhaps the most realistic) is to use the rotor and IGV of our existing stage as the "flow generator". In doing this there

AERODYNAMIC DESIGN OF ROTOR TIP STALL CONFIGURATION
(ROTOR ALONE WITH TIP DISTORTION)

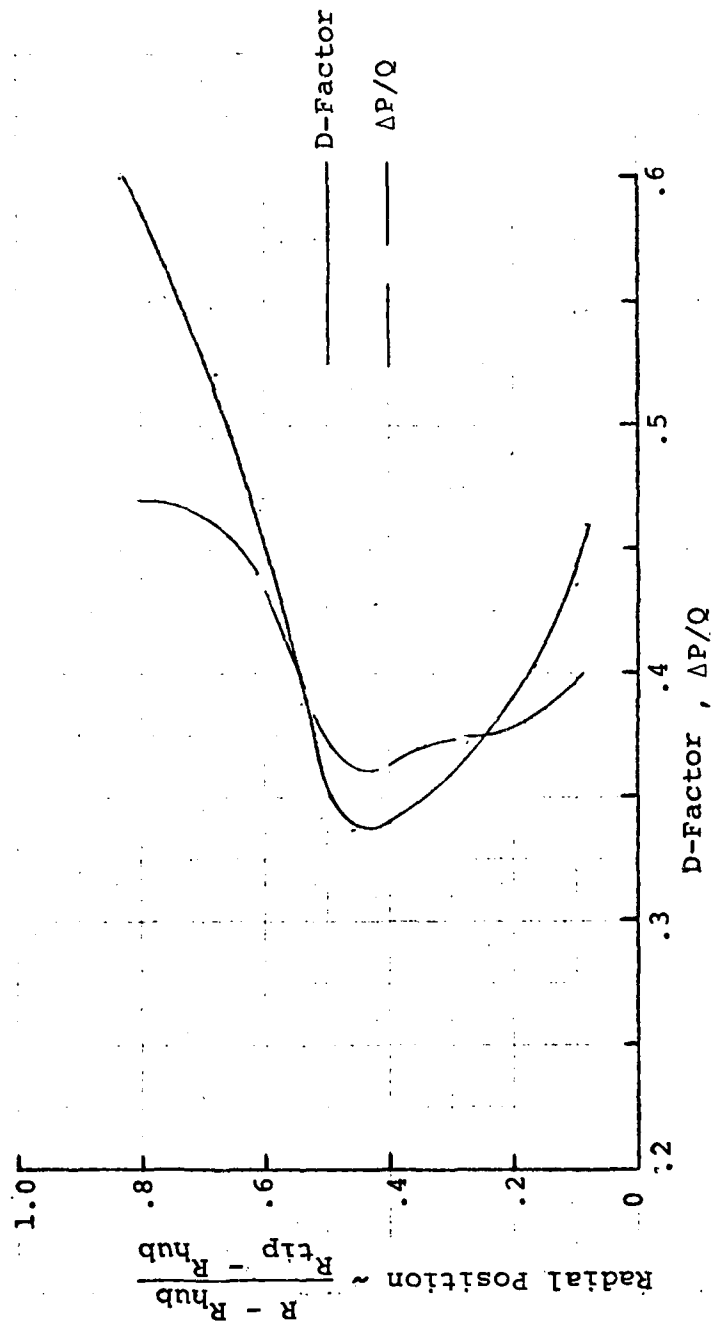


FIGURE 12

appear to be several criteria which drive the design of the stage. First, as previously, one needs to match the rotor such that it is far away from stall so that the stall initiation is due to the stator hub region. Second one would like to space the rotor and stator a bit apart so that the two are somewhat decoupled. Third it seems reasonable to try to obtain as much pressure rise in the stator as possible relative to that in the rotor, i.e., to have as low reaction as possible. To achieve this a parametric study was carried out using an axisymmetric streamline curvature program. In this the stagger angles of the existing rotor stator and IGV were varied in order to determine the appropriate settings for each of these. The configuration eventually chosen yielded radial profiles of aerodynamic loadings that are shown in Fig. 13 . This gives rotor and stator D-factor and $\Delta P/Q$ and it can be seen that the stator hub is much more highly loaded than the tip as well as that rotor levels of these quantities are quite low.

Current status is that the re-instrumentation of the compressor with the total and static pressure taps that are necessary for adequate performance monitoring during the experiments has been completed. In addition the interfacing between the scani-value and the mini-computer used for data acquisition has also been done. Tests are now being run with the smooth wall stator hub configuration, using both the steady state instrumentation and the hot wire. These results should appear in the M.S. Thesis of Mr. Mark Prell, which is expected in early 1981. The plan for the next few months is to attempt to answer the question "Does hub treatment work?", in other words testing back to back configurations with smooth wall and hub treatment.

AERODYNAMIC DESIGN OF STATOR HUB STALL CONFIGURATION

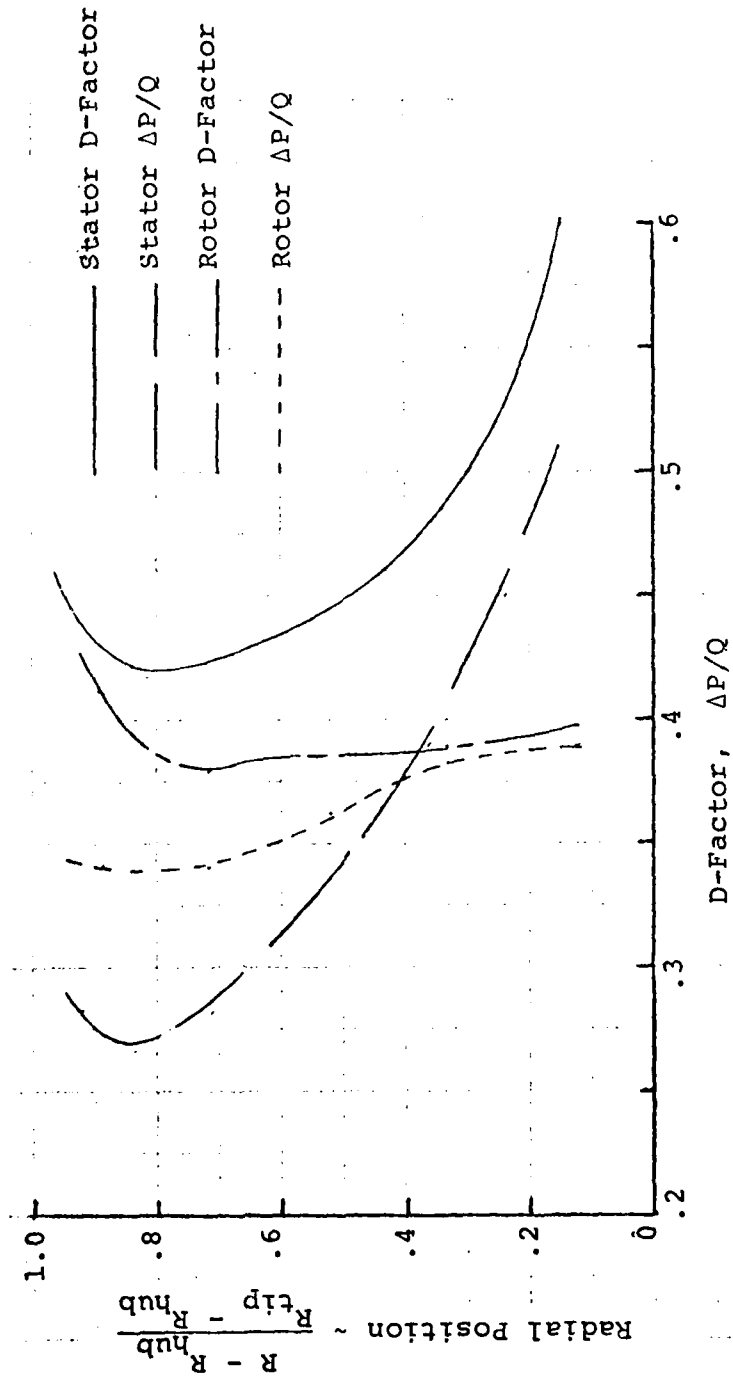


FIGURE 13

Further, if the hub treatment is successful a detailed mapping of the stator pressure endwall flow field will be carried out with both the baseline and the grooved treatment. Based on our previous studies of the problem we feel, at present, that one of the crucial points concerns the flow blockage.²⁵ It is the generation and growth of this blockage that is associated with the onset of rotating stall, which is the event that limits the stable flow range of a compressor. It has been shown that casing treatment can have a substantial effect on the flow blockage in a compressor rotor. The work during the next year period will concentrate on the interaction between the flow in and out of the grooves and that in the passage endwall region, in order to clarify this strong impact on endwall region flow blockage.

TASK III: INVESTIGATION OF THE RESPONSE OF GAS TURBINE ENGINES TO INLET
VORTEX DISTORTION

A) Inlet Vortex Flow Field Study

This task is directed at the quantitative prediction of the engine inlet flow field distortion which results from the presence of an inlet vortex (or ground vortex). Such flows can have only small total pressure defects, but very large non-uniformities in angle. Hence even though they can lead to substantial reductions in engine stall margin²⁷, they cannot be predicted by present distortion analysis. Although there have been some previous investigations of this problem these have been either qualitative in nature^(e.g. 28) or have only described the effects of the vortex²⁹.

The problem can usefully be broken into two phases. The first addresses the question of the conditions under which an inlet vortex forms and the quantitative connection between the strength of such vortices and the geometrical and physical parameters which describe the engine inlet, ambient wind, etc. This part is essentially independent of the turbomachinery components since it is the net inflow that is responsible for the formation of the vortex. The second phase addresses the interaction between a vortex (of known strength) and the turbomachinery, with emphasis on the details of the conditions both ahead of and inside the compressor.

The work to date on this task has been concentrated on the first phase, which we regard as a necessary first step before attacking the second, and is both theoretical and experimental. The theoretical work has been based on the use of a small shear, large disturbance approach, (i.e., a secondary flow approximation), to computing the three-dimensional vorticity

field associated with the inlet vortex. In this approach the vorticity is regarded as a small amplitude shear perturbation which is superposed on an irrotational mean flow.³⁰ The vortex filaments associated with the perturbation are then convected by the mean flow. It is this process which gives rise to the generation and amplification of the streamwise vorticity that is inherent in the inlet vortex phenomenon. While it is realized that some aspects, such as the self induced (non-linear) interaction between vortex filaments cannot be described, by this technique, it is nevertheless felt that the approach can, in fact, account for the many of the salient features of the phenomenon.

The key components of the method used are thus: a potential flow analysis of the three-dimensional flow around an inlet in ground effect, a computational procedure for tracking fluid particle along the streamlines associated with this flow, and the concept that vortex lines, which are material lines, move with the fluid.

The initial model used for the potential flow was a very simple one with two sinks. This was useful in obtaining some qualitative understanding of the global flow pattern including the occurrence of stagnation points, the 'drift times' of the fluid particles³¹ (i.e., the times taken for specified fluid particles to travel from a given initial location to a given final location), the streamline configuration near stagnation points, etc. A typical result of the calculation is presented in Fig. 14 which shows the projection of the streamlines in the plane of symmetry through the two sinks. As can be seen there are three stagnation points in the flow for this particular sink strength (this is analogous to the ratio of inlet velocity to ambient velocity), which is representative of that actually encountered.

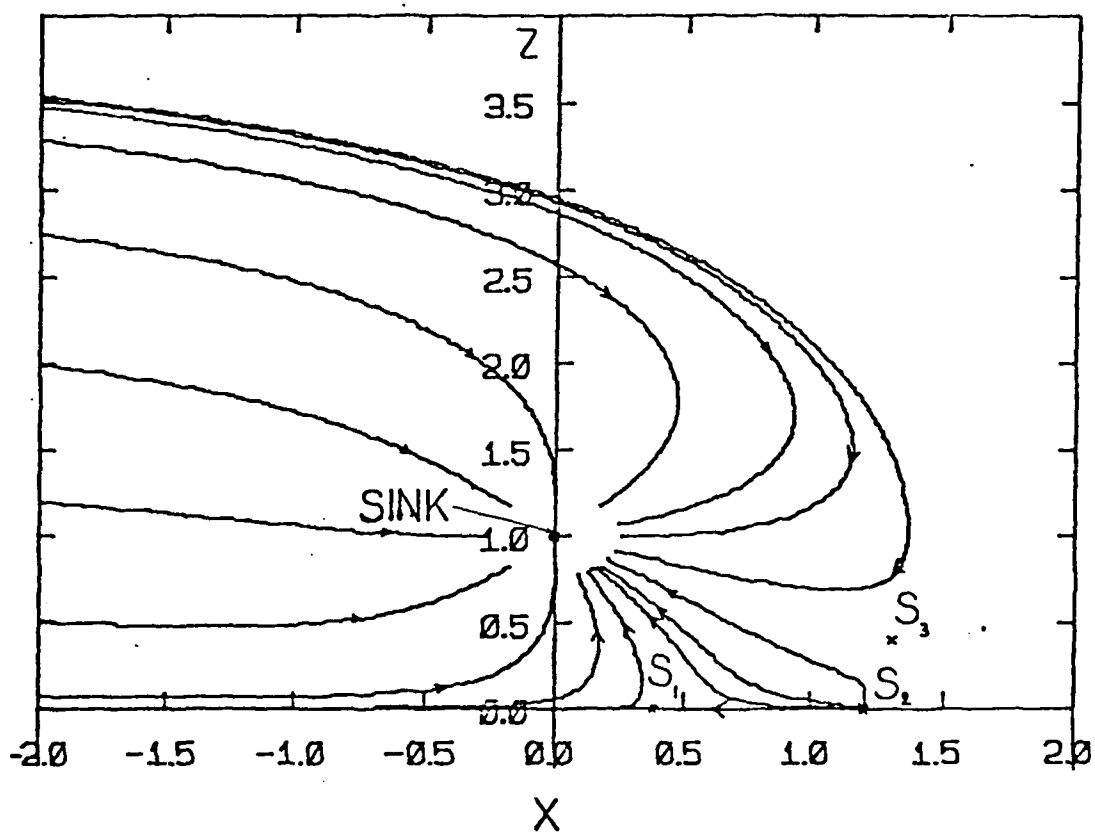


FIGURE 14 Streamlines in the x, z Plane

In addition the streamline configuration is totally different than in a two-dimensional flow, and, in fact, this streamline pattern cannot exist in a purely two-dimensional flow.

It was evident, however, that one also needs more local information, in other words, information on the length scale of the inlet height above the ground (which is the relevant length scale in the problem) or less. To obtain this we have adopted a recently developed three-dimensional potential flow code which can be used to calculate the flow around a representative inlet geometry. The code is based on a three-dimensional panel method and the actual inlet configuration used is shown in Figure 15a and 15b which gives the details of the division into panels.

The second component of the method is the particle tracking procedure. This is based on a numerical integration to find the mean flow streamlines. The velocity components needed in this integration are found directly from the above mentioned potential flow calculations. This procedure was first implemented using the two sink mean flow (where the velocity components at any point could be readily checked by hand calculation) and then applied to the panel method. The details of this calculation, as well as more discussion of the panel method used, can be found in (32) and we will therefore concentrate on some of the results of the calculations that have been carried out so far.

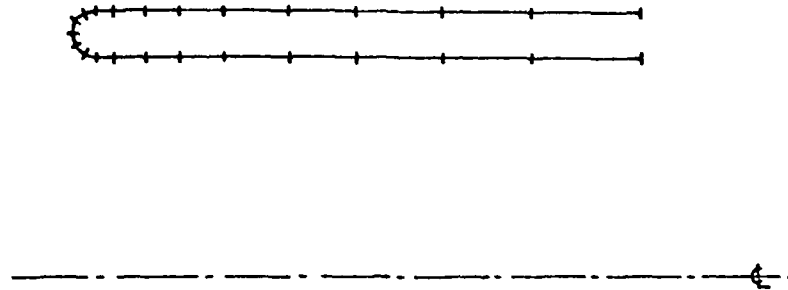


FIGURE 15A N-line and Panel Vertices

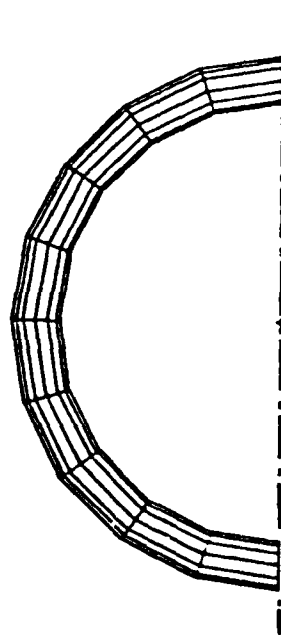


FIGURE 15B Front View (because of Symmetry, only Half the Inlet is Shown)

FIGURE 15 Inlet Panel Representation

Two specific inlet geometries have been examined. The first (Case 1) is a cylindrical inlet with a height to diameter ratio of 1.25 at zero yaw and zero angle of attack. The ratio of inlet velocity to far upstream velocity is thirty, i.e., the inlet is running at near static conditions (which are typical of those associated with inlet vortex formation). The second case (Case 2) has the same inlet and height to diameter ratio, but at forty-five degrees of yaw, i.e., with crosswind. The ratio of inlet velocity to far upstream velocity for this latter case is forty-five.

The results of the calculations are of several types. First we have examined the mean flow streamlines to obtain some insight into the details of the mean flow. In addition we have also tracked material lines (or vortex lines) from a far upstream location to the location at which the engine face would be in order to see the distortion of these filaments as they enter the engine. Third, we are attempting to quantify the vortex stretching by examining the behavior of two particles which are close together far upstream. We will describe the different types of results separately.

The basic inlet geometry used is shown in Fig. 16, where we see the inlet and the "image" inlet, the latter being put in to simulate the effect of ground plane. Results of the streamline calculation are shown in Fig. 17 and 18, where several of the important features of the flow can be determined. These figures show the streamlines for the zero yaw case, and represents the streamlines on the planes of symmetry of the inlet. Perhaps first in import in this figure is the evidence of a stagnation point on the "ground" with a so-called stagnation streamline going into the inlet. This is shown in Fig. 17. The existence of a stagnation point

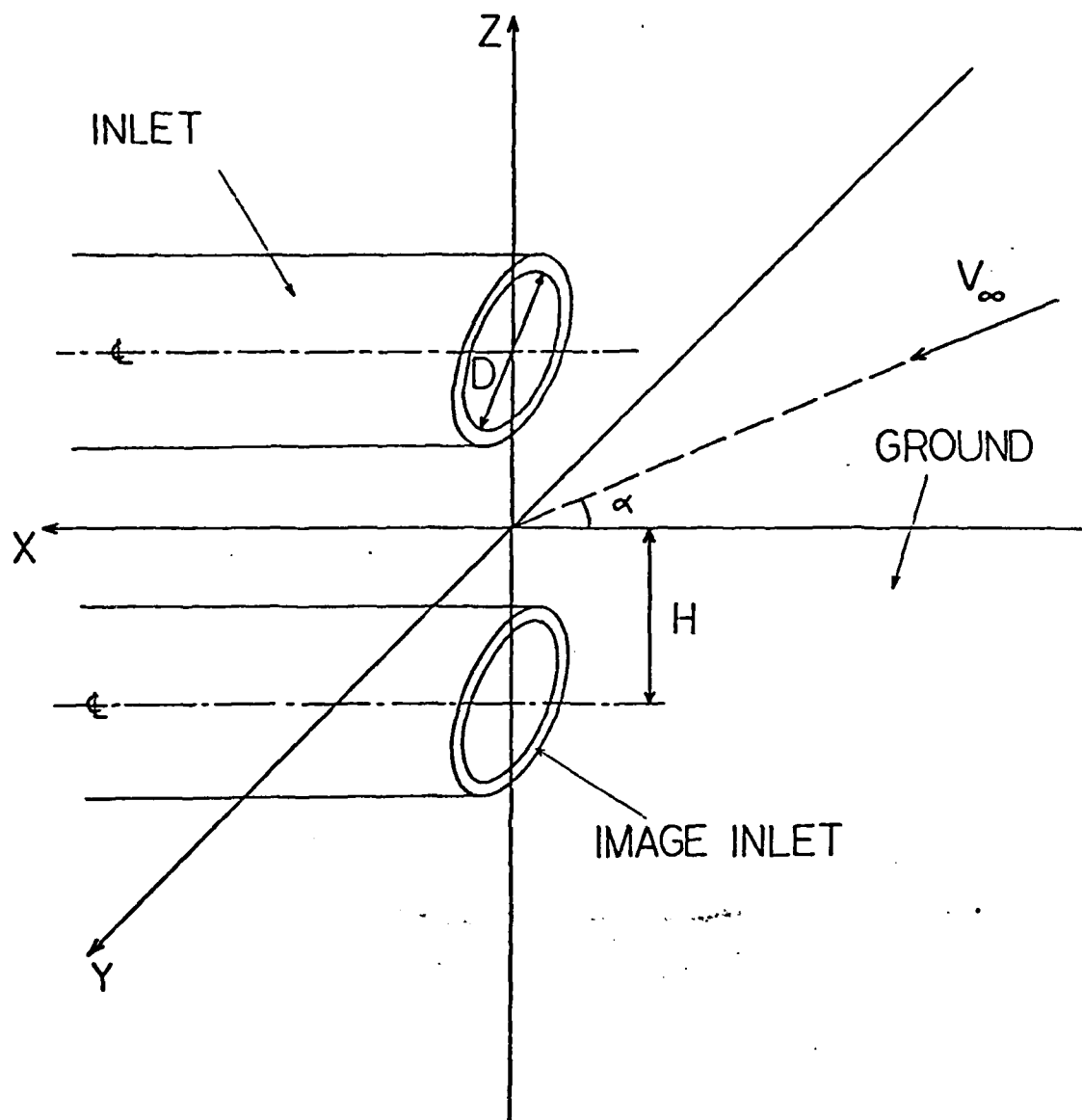


FIGURE. 16 Flow Geometry

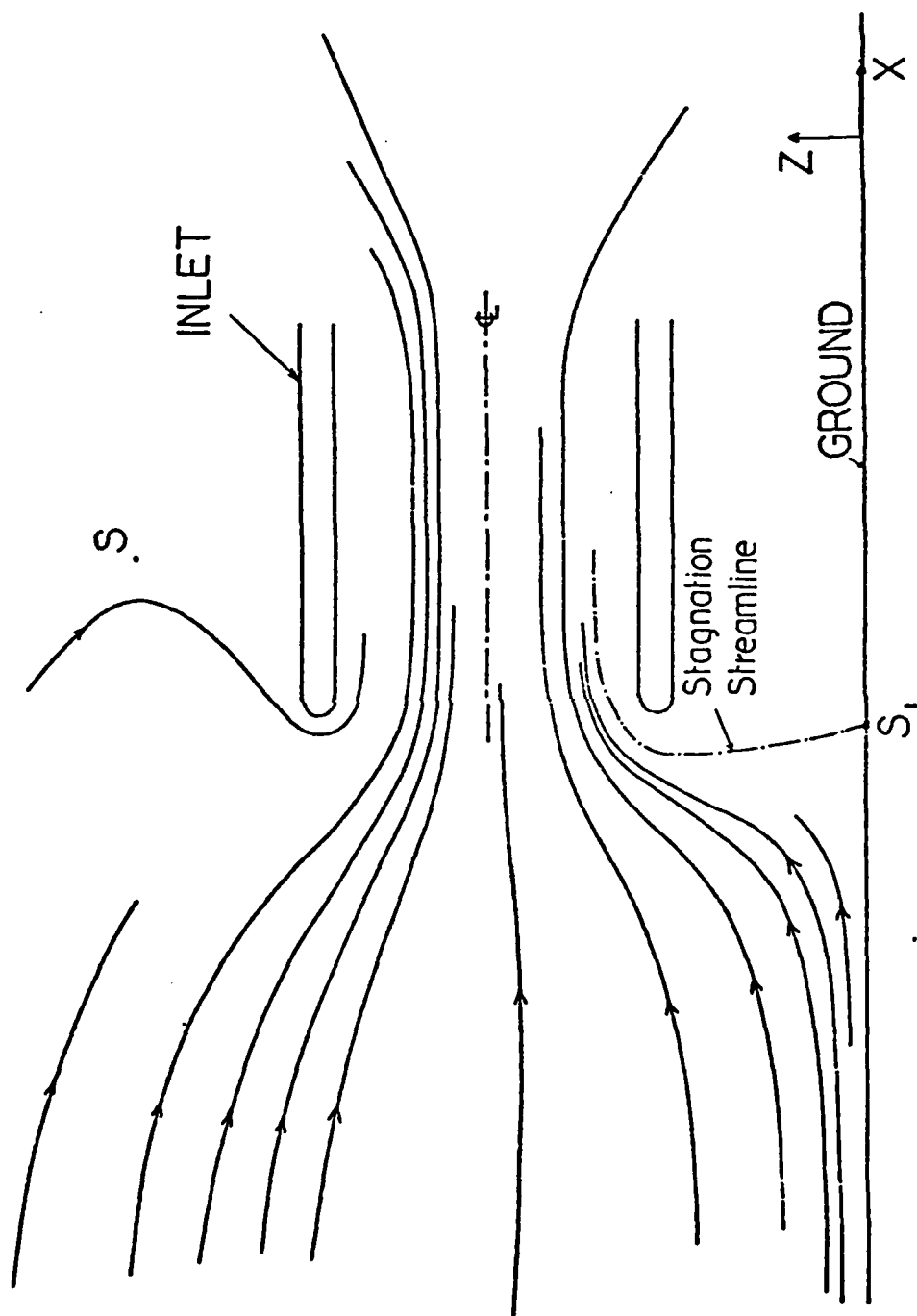


FIGURE 17 Streamlines in the x, z Plane, Case 1

has been mentioned by several investigators as having a strong connection with the existence of the inlet vortex. The second feature is the bounding streamline of the capture surface (the surface that separates fluid that enters the inlet and that which bypasses it) as indicated in Fig. 18a and 18b. It can be seen that if one moves more than a few inlet heights upstream of the inlet face the capture streamline has attained essentially its final height and the streamlines are basically parallel. This again emphasizes that much of the vorticity amplification occurs in the local neighborhood of the inlet face and it is thus important to have a good description of the flow in this region. Other stream line patterns are given in Ref. (33).

Two types of material lines (vortex lines) were studied, namely those which were vertical and normal to the mean flow direction far upstream and those that were parallel to the ground and normal to the mean flow direction far upstream. The latter, for example, would be the type of vorticity that would be associated with a ground boundary layer. (For the zero yaw case only the former is necessary since within the context of the model the latter can only give rise to two symmetrically placed counter rotating vortices).

Figures 19 and 20 show two different views of a vortex line which is vertical far upstream and 0.60 inlet heights (0.75 inlet diameters) from the x, z plane. Figure 19 shows the projections on the x, z plane with the numbers corresponding to different times.

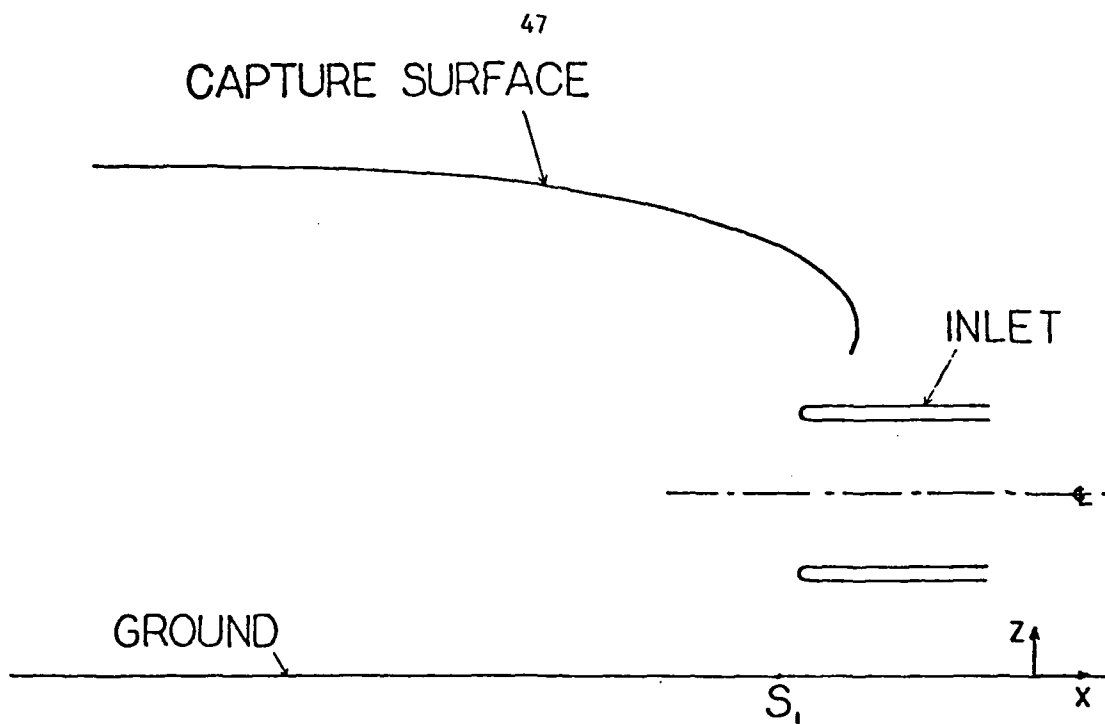


FIGURE 18A: Trace on the x, z Plane

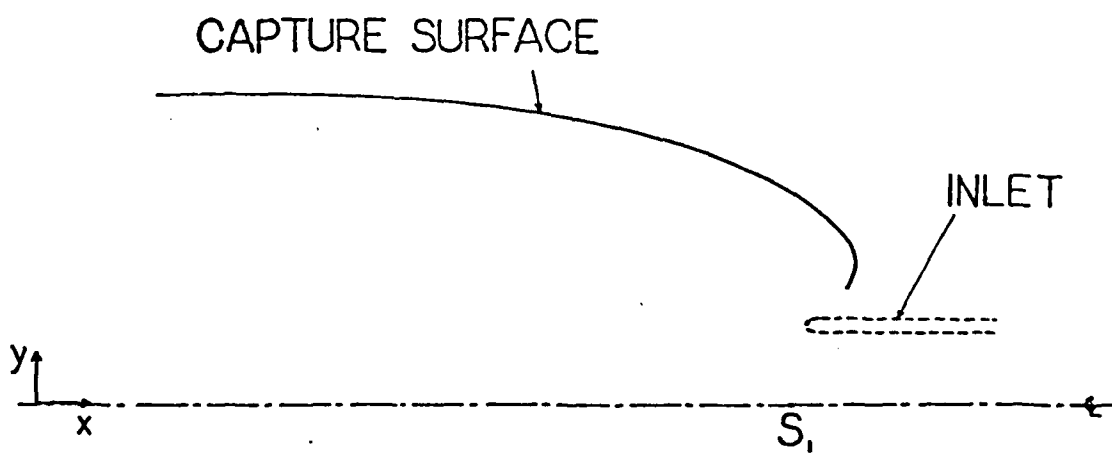


FIGURE 18B Trace on the x, y Plane

FIGURE 18 Capture Surface, Case 1

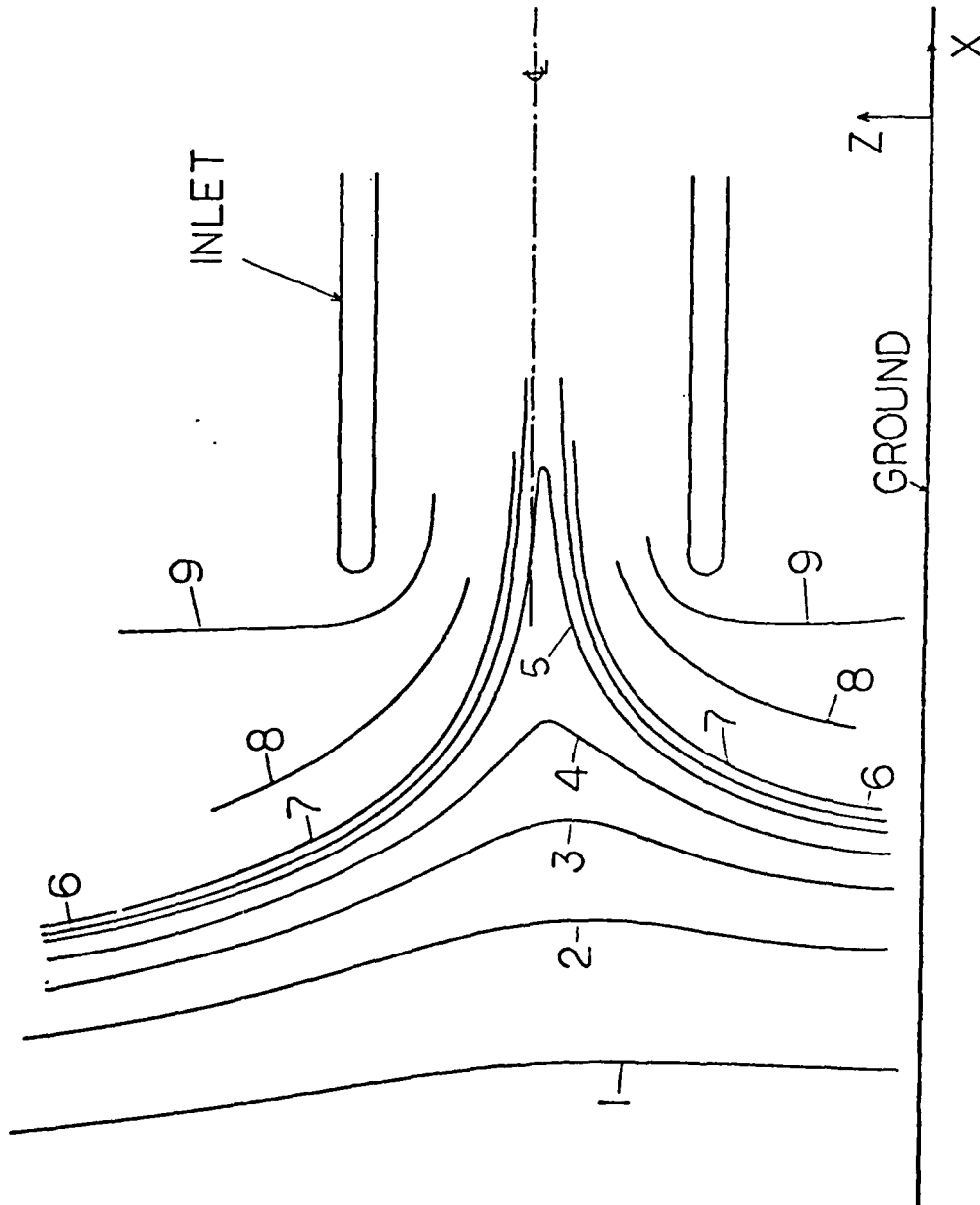


FIGURE 19 Deformations of a Fluid Line which is Vertical and 0.6 Inlet Heights from the x, z Plane at a Location Four Inlet Heights Upstream of the Inlet, Projections on the x, z Plane, Case 1

Figure 20 shows the projections on a plane normal to the inlet axis (the y, z plane). Figure 21 shows the projections, on the same plane, of the positions of a vortex line that is initially 1.6 inlet heights (2.0 inlet diameters) from the x, z plane, i.e., near the capture surface. Note that since vortex lines cannot end in the flow the lines tracked must extend to infinity. However those portions of the material lines outside the capture surface, which do not enter the inlet, are not shown. Note also that both the head (top) and the foot (bottom) of the parts of the material lines that are shown will lag behind the middle part since particles which are on the ground plane will stay there, while particles on the capture surface will approach the stagnation line as described in the previous section. The velocity differential means that the particles near the center of the fluid line will exit the engine while those at the foot and head remain near the stagnation regions*. Once a vortex line enters the inlet, we can no longer track it entirely and only parts of the legs extending from the stagnation regions to the inlet can be traced. These legs are both strongly stretched and, consequently, have high vorticity levels, although a quantitative appreciation for their stretching is difficult from just the tracking of material lines since the deformation increases rapidly for fluid particles close to the ground plane or the capture surface.

*By the definition of a stagnation point, the closer to such a point the streamline followed by a fluid particle is, the longer time it takes to this particle to reach a position "downstream" of the stagnation point.

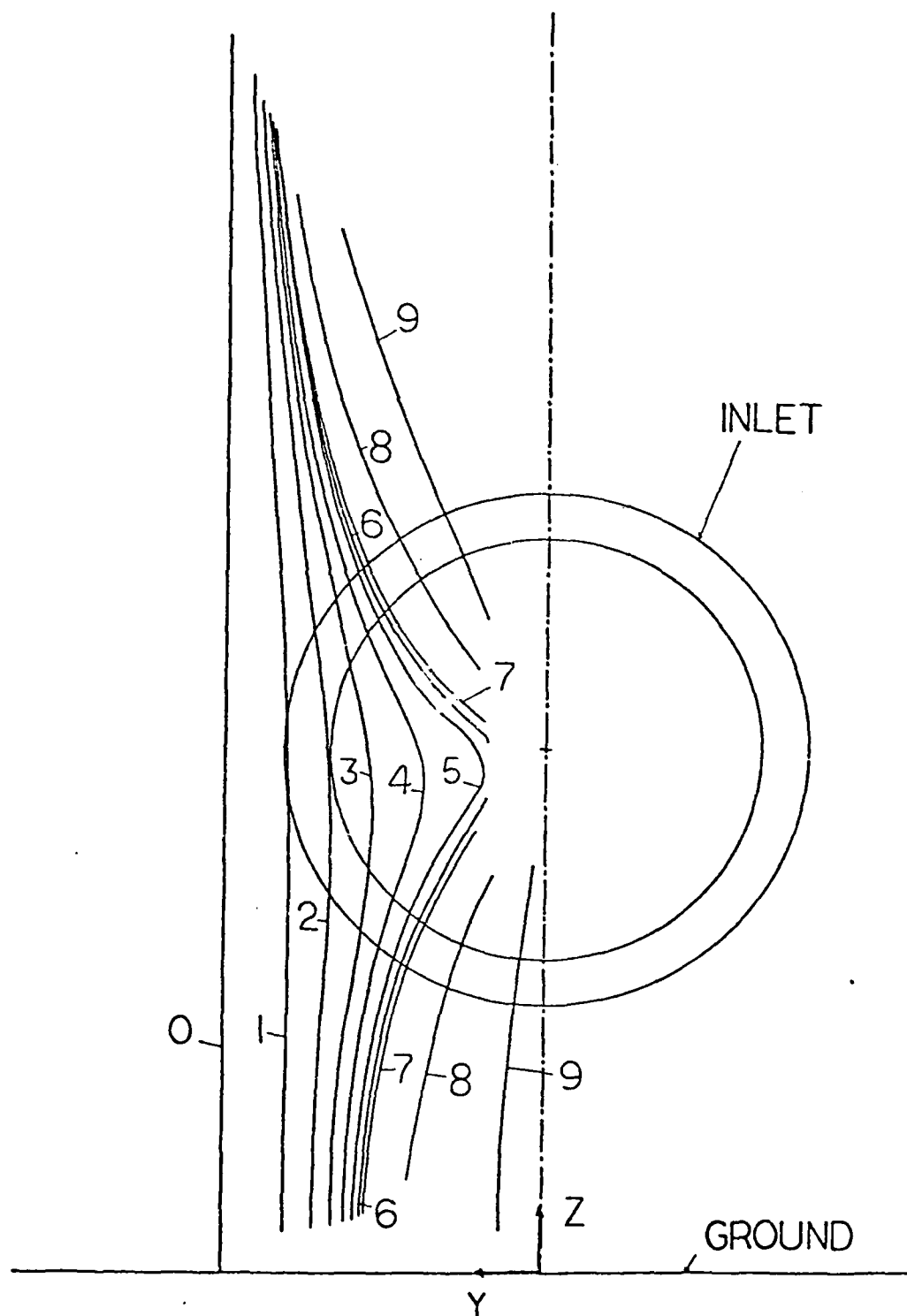


FIGURE 20 Projections of the Material Lines Shown in Figure 19 on the y, z Plane

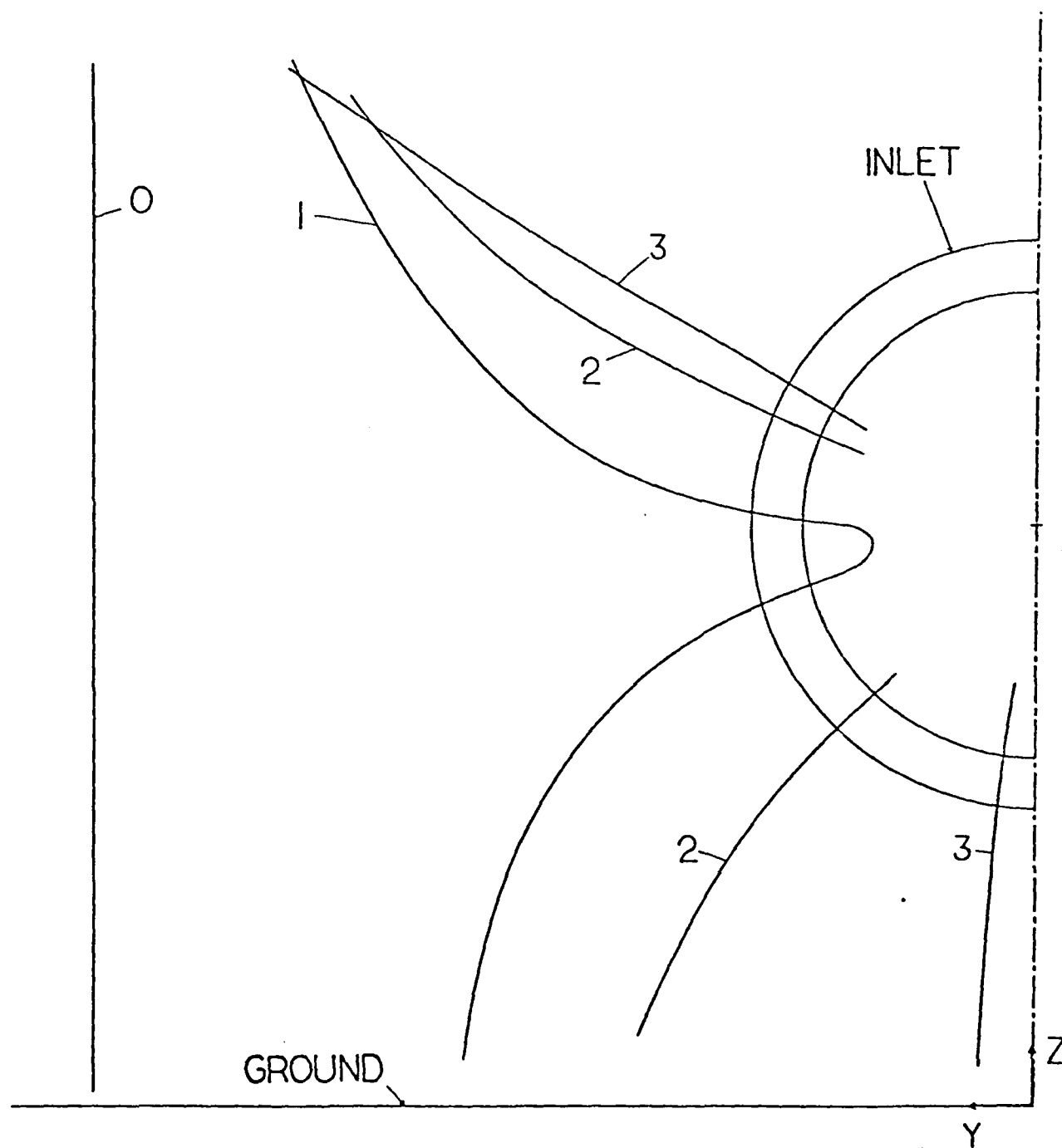


FIGURE 21 Deformations of a Fluid Line which is Vertical and 1.6 Inlet Heights from the x, z Plane at a Location Four Inlet Heights Upstream of the Inlet, Projections on the y, z Plane, Case 1

The study of the deformations of material lines initially off the x, z plane gives a clue to a possible inlet vortex formation mechanism. The existence of two stretched legs and the observation of a single vortex seem difficult to reconcile. However the locations of these legs must also be examined. While the foot of any vortex line approaches the stagnation point S_1 and the associated leg nears the corresponding stagnation streamline, the location reached by the upper leg which extends from the inlet up to the vortex line head (defined as the top of that part of the vortex line which is on the "inside" of the capture surface) depends on the vortex line initial position. Knowing the location of the vortex line head far upstream is sufficient to determine the location reached by the latter after an infinitely long time. To a close approximation the streamline followed by the fluid particle which coincides with the vortex line head lies in a plane containing the inlet centerline. Further since it is on the capture surface this particle cannot ever pass the arch-shaped stagnation line. Eventually, using these two pieces of information, it is possible to determine the ultimate position of the vortex line head. Figure 22 thus shows the suggested deformations of vertical material lines. A far upstream uniform distribution of vertical vortex lines evolves into a configuration in which the upper legs of the lines are "fanned out" over the upper part of the inlet while the lower legs are squeezed around the stagnation streamline associated with S_1 . (Although the stagnation regions are never reached in an actual flow, these trends remain valid). The predicted squeezing goes with an increase of the associated circulation per unit area, and the problem remains to compare this rise with that due to vorticity

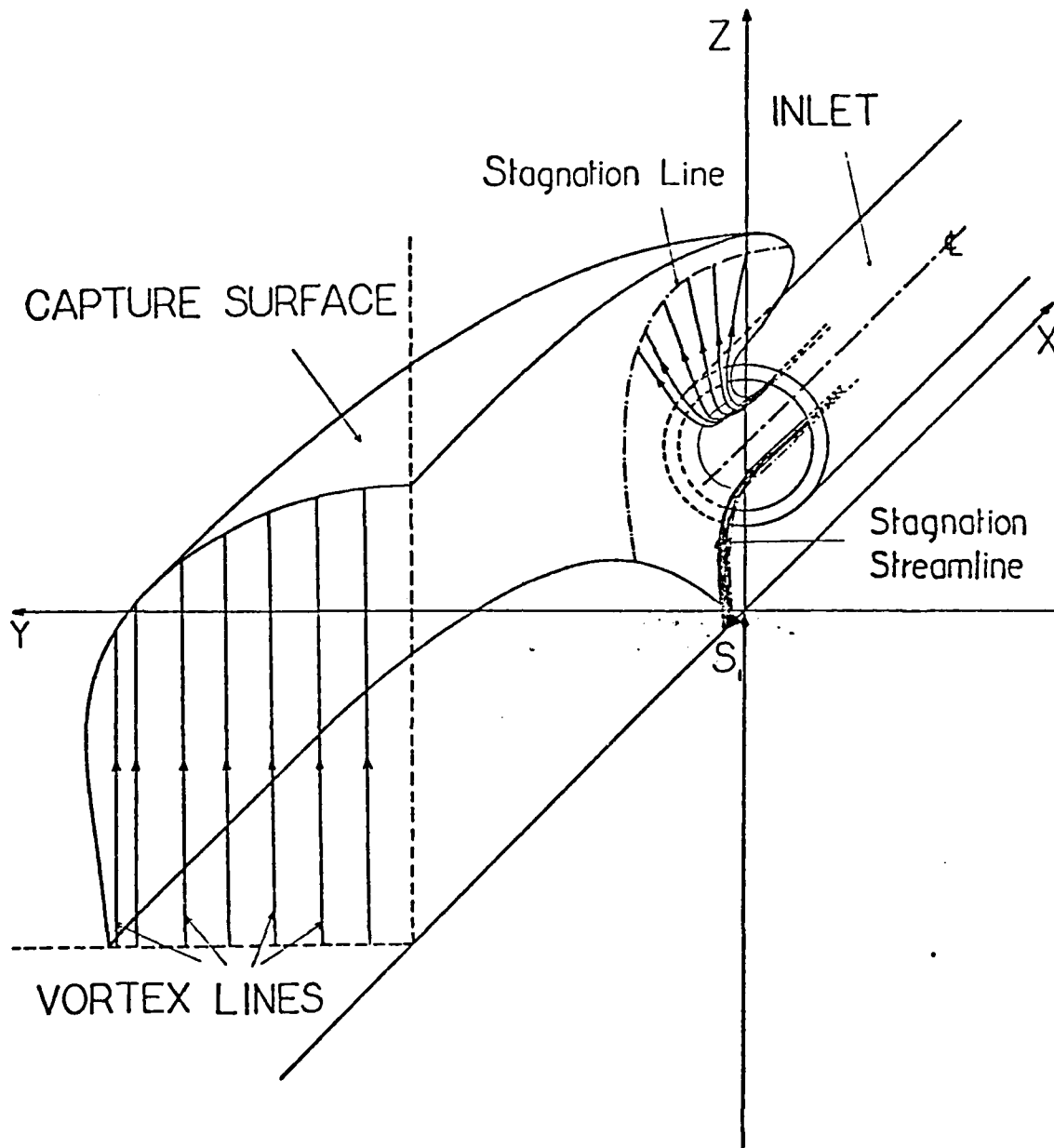


FIGURE 22 Suggested Deformation of a Far Upstream Uniform Distribution of Vertical Vortex Lines, Case 1

amplification in the upper legs. Note that if the existence of a mean flow stagnation point is admitted (i.e., separation effects are neglected) as in the current model, the stretching of both legs is infinite. The difference lies in the spatial distribution of the associated vorticity amplification as can be seen in Fig. 21 where fluid particles close to the foot and head of the vortex line are tracked.

For the inlet with yaw, one must also look at the horizontal vortex filaments as well. A typical result of doing this is shown in Fig. 23 where it can be seen that the central portion of the line is sucked into the inlet giving rise to large local stretching. Again for more details of the behavior of these material lines as well as for streamline calculations one can refer to Ref. (33).

The last type of result is the calculation of the differential drift of two particles which are a small distance apart in the far upstream flow field. The basic idea is to follow the two particles, and to compute the distance between them at the engine face location as is indicated schematically in Fig. 24. This would then give a quantitative measure of the vorticity amplification for an element of a vortex line which was initially at the far upstream position between the two particles. If one does this for two small line elements which are normal to the mean stream velocity and are horizontal and vertical, one can then get the three component of vorticity since the streamwise component (or Beltrami vorticity) is amplified directly as the ratio of streamwise velocity and can be calculated immediately once one knows the ratio of inlet to far upstream velocity.

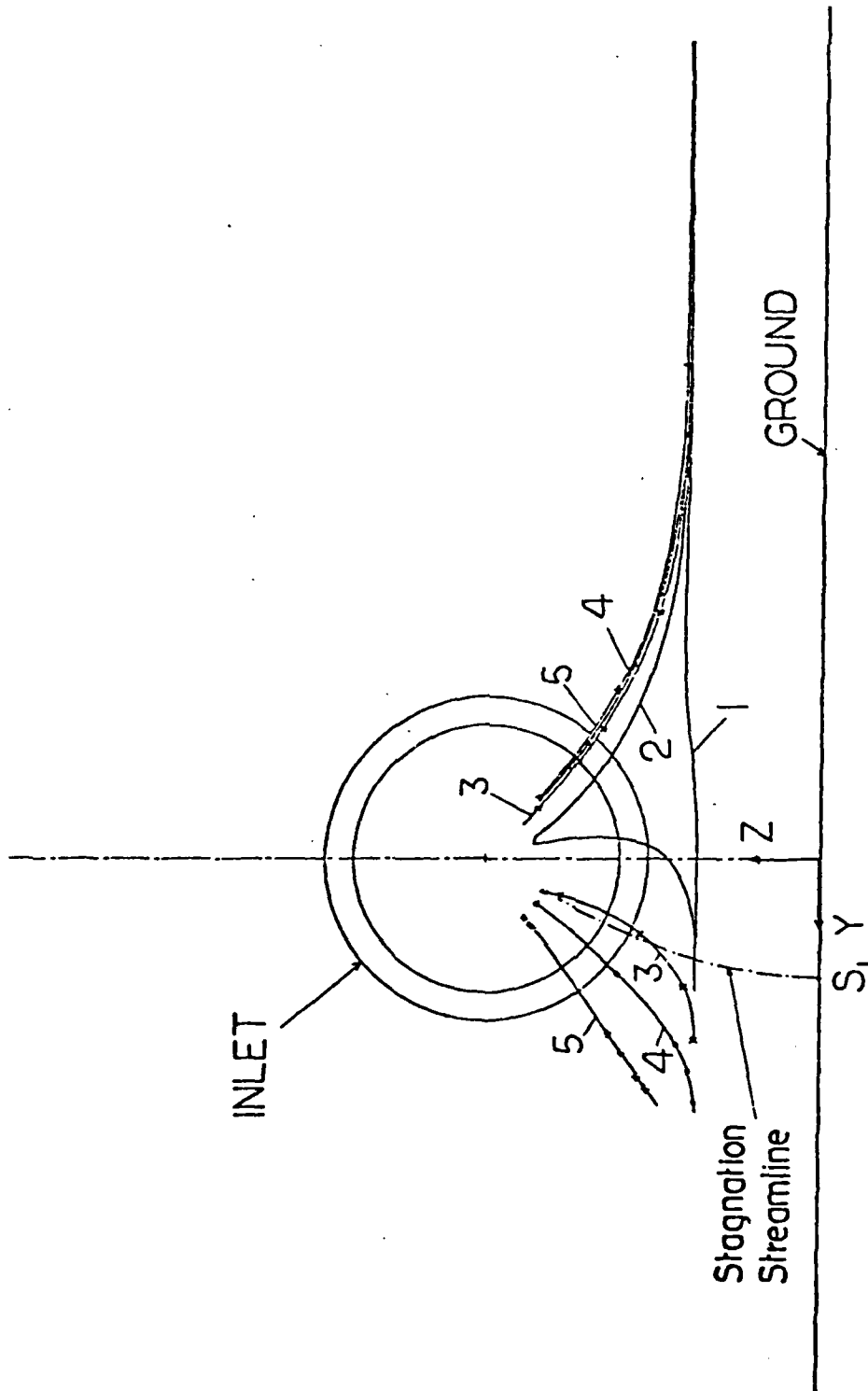


FIGURE 23 Projections of the Material Lines Shown in Figure 30 on the y, z Plane

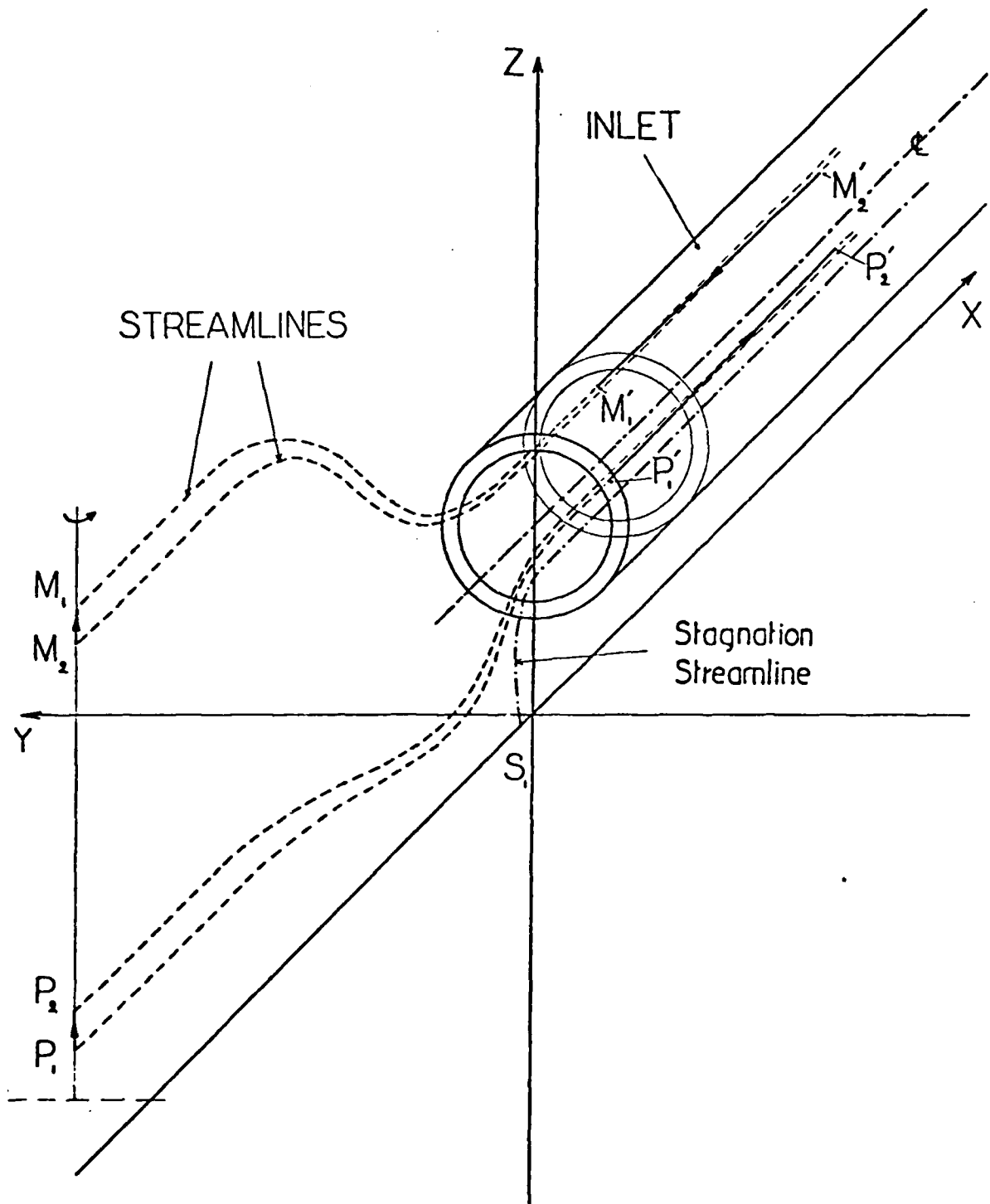


FIGURE 24 Behavior of Fluid Lines Connecting Neighbouring Particles

The procedure is being carried out using a far upstream grid as shown in Fig. 25. It can be seen that the grid is substantially finer near the stagnation streamline--this has been found to be necessary to resolve the details of the high rates of change in this region. This calculation will be carried out for the two cases described above.

The results with the calculation procedure appear encouraging. Plans for the next year are first to complete the vorticity amplification calculations using the present fluid dynamic model. In addition to this however there are some modifications that should be made to the model. In particular we wish to obtain an improved description of the flow field in the neighborhood of the stagnation streamline. This is necessary to fully resolve, in a quantitative way, the vortex stretching. In addition there are several other aspects that should be examined. One of these concerns the approximate description of the effects of viscosity on the phenomenon.

The inviscid calculation leads to an infinite value of vorticity amplification on certain streamlines. (Basically one section of the streamline remains at a stagnation point, whereas other parts are sucked in through the engine and flow downstream). In reality this is precluded by viscous effects. Thus it is of interest to examine these bounds on the vorticity amplification. It should be emphasized however that the interest here is still in the overall, i.e., integrated effects of the vorticity. Since viscosity will only tend to diffuse the existing vorticity, rather than creating it, phenomena that are characterized by length scales greater than that of the (viscous) core are not likely to be greatly influenced by the details of the vorticity distribution within the core. To summarize it seems that the approach to modelling viscous

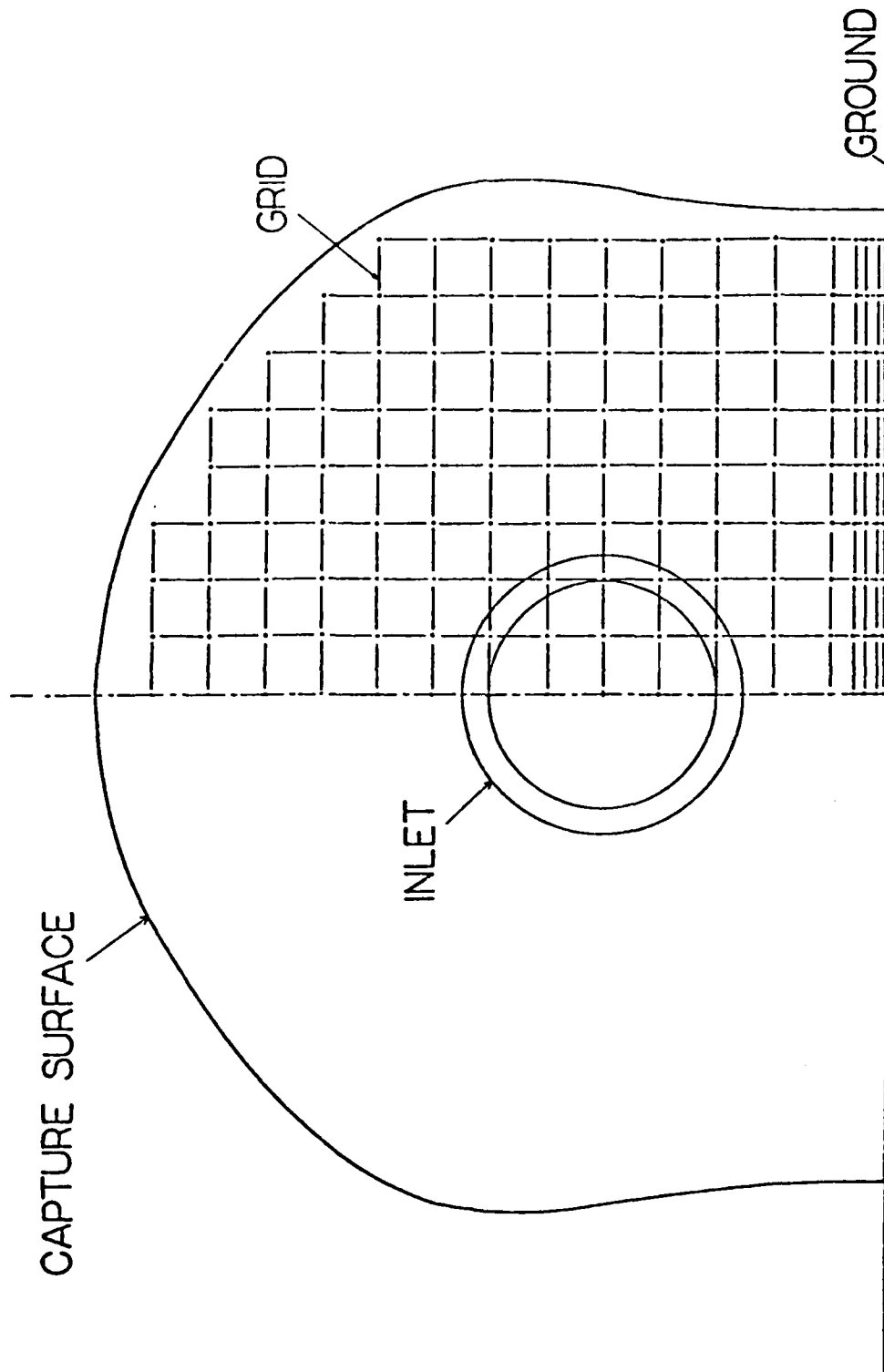


FIGURE 25 Front View of Grid Tracked at a "Far Upstream" Location, Case 1

effects can be done in an approximate manner and we intend to pursue this.

The experimental work on this topic is being conducted at two different levels. The initial efforts are directed at using flow visualization to obtain a basic understanding of the three-dimensional inlet velocity field including the kinematics of the vortex lines. This will then be followed by a quantitative investigation, which will be started during the present contract period.

The flow visualization studies are currently being carried out in the MIT Ocean Engineering .51 x .51 m x 20" Water Tunnel. However, because this facility is in high use, preliminary studies were carried out in a small water channel that we constructed. A schematic of this is shown in Figure 26 . Although the channel design is somewhat unorthodox (to expedite its completion) it produces a low turbulence flow suitable for flow visualization, with hydrogen bubbles or dye, at the velocities of interest. We have also constructed a hydrogen bubble generator and used this to develop the necessary optical system as well as to determine the most convenient method of creating the inlet shear profiles that are needed for the large tunnel experiments. After much investigation of devices such as porous foam, screens, soda straws, etc. it was found that a honeycomb of non-uniform length gave the most suitable results. We then employed the calculation procedure developed in Ref. 34 to design the honeycomb to be used in the actual experiments.

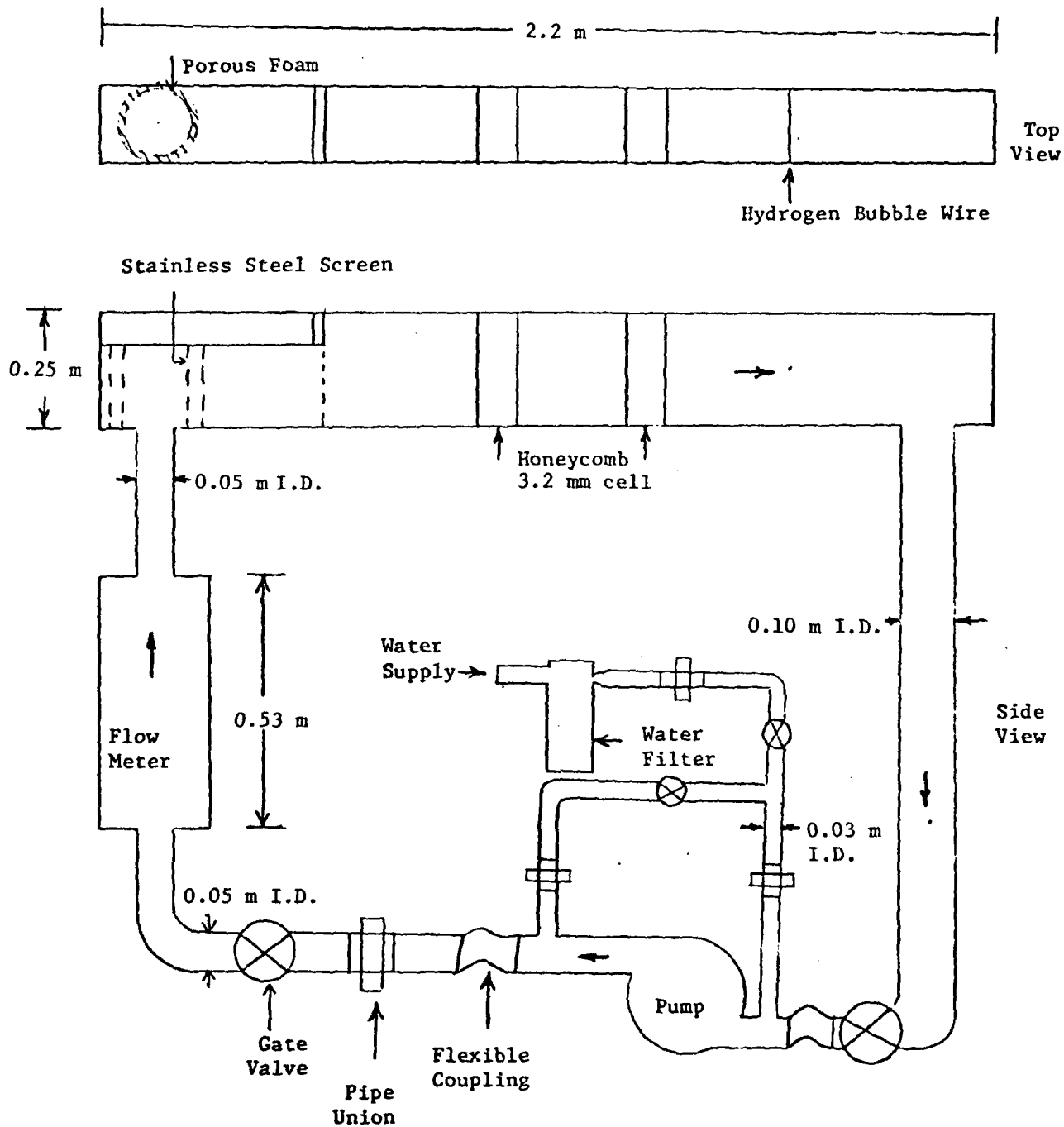


FIG. 26 Sketch of Small Water Tunnel

The present status is that the inlets, associated pipework , optical system, and electronics are all completed and we are now carrying out our studies in the Ocean Engineering Water Tunnel. A sketch of this facility is shown in Fig. 27. It can be seen that there is a large settling tank, a contraction and then the .51 x .51 m test section. In the configuration that we use it, the tunnel is run with a free surface. A typical configuration is shown in Fig. 28 which gives a rough indication of the relation between inlet height and shear layer thickness for one of the inlets that we have looked at. A photograph of the actual profile used is shown in Fig. 29. The maximum velocity is .11 m/s. Although there is a small "notch" of approximately 10% of free stream velocity (coming from a joining of two pieces of honeycomb) the overall profile is reasonably satisfactory. (It should be noted that this notch, which is seen at a location somewhat upstream of the inlet, includes vorticity of opposite sign and nearly equal magnitude in close proximity and hence should only have a very local effect. It should not be of import as far as the overall vortex formation is concerned).

Although we have only started the flow visualizations we can show, in Fig. 30, one of the interesting feature which has emerged. This concerns the ingestion of a vortex filament, which is initially horizontal, parallel to the ground and perpendicular to the mean flow direction, by an inlet which is at ninety degrees to the far upstream flow. The figure shows a plan view (a) as well as a view looking into the inlet and is a sketch of the actual phenomena as indicated by a hydrogen bubble marked material line.

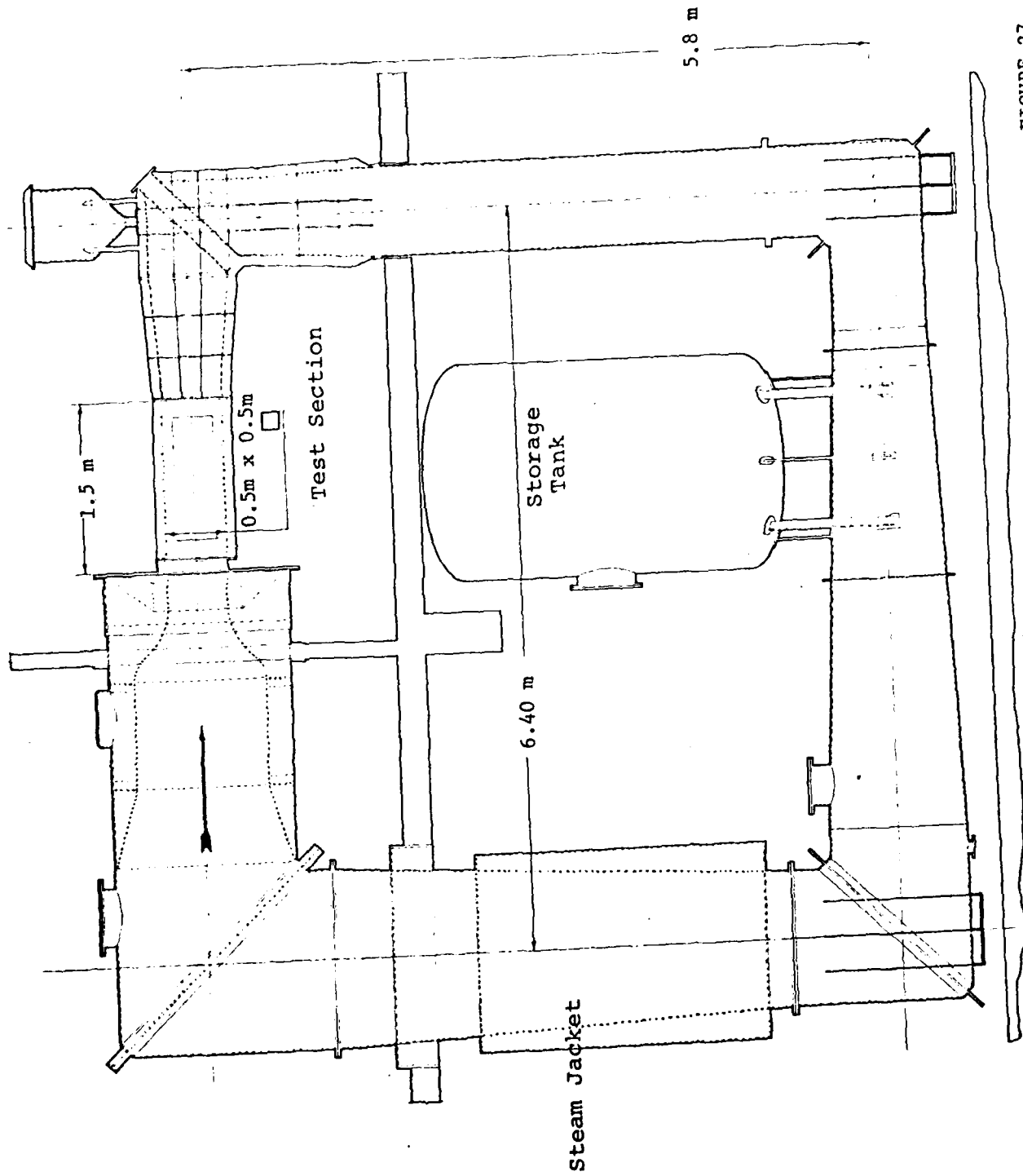


FIGURE 27

Ocean Engineering Water Tunnel

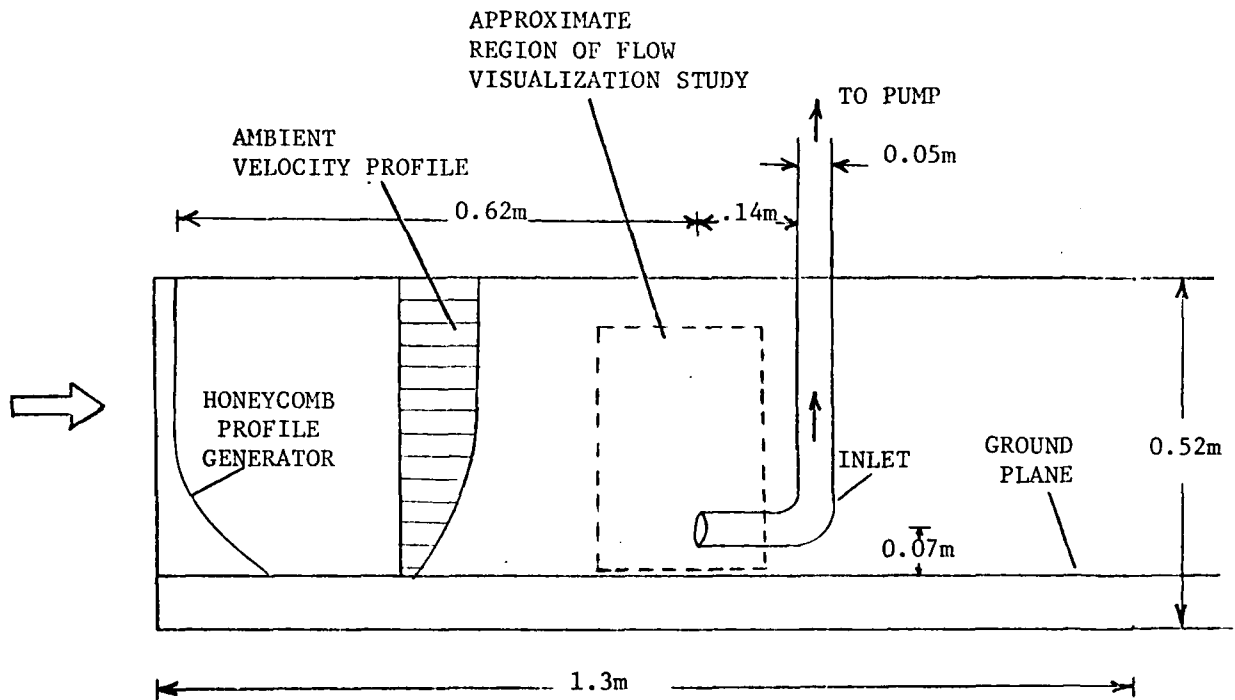
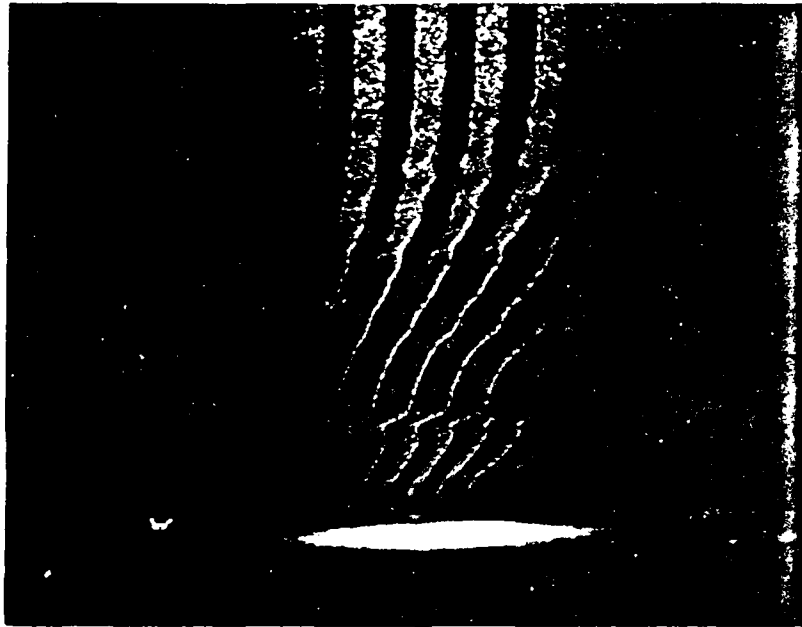


FIGURE 28 SKETCH OF WATER TUNNEL TEST SECTION



Hydrogen Bubble Flow Visualization of
Honeycomb Generated Velocity Profile

FIGURE 29

It can be seen that a central portion of the line is ingested into the inlet first with the two "ends" entering at a later time. The circulation around this two vortex lines is of equal and opposite sign (although the vorticity may not be) and, as indicated, evidence of rotation of opposite sign can be seen in the actual phenomenon.

As stated, this work has really just been started and we have to complete it over the next several months. In addition we are starting the design of the quantitative experiment to be carried out in the Wright Brothers Wind Tunnel and thus will be the main experimental effort of this year.

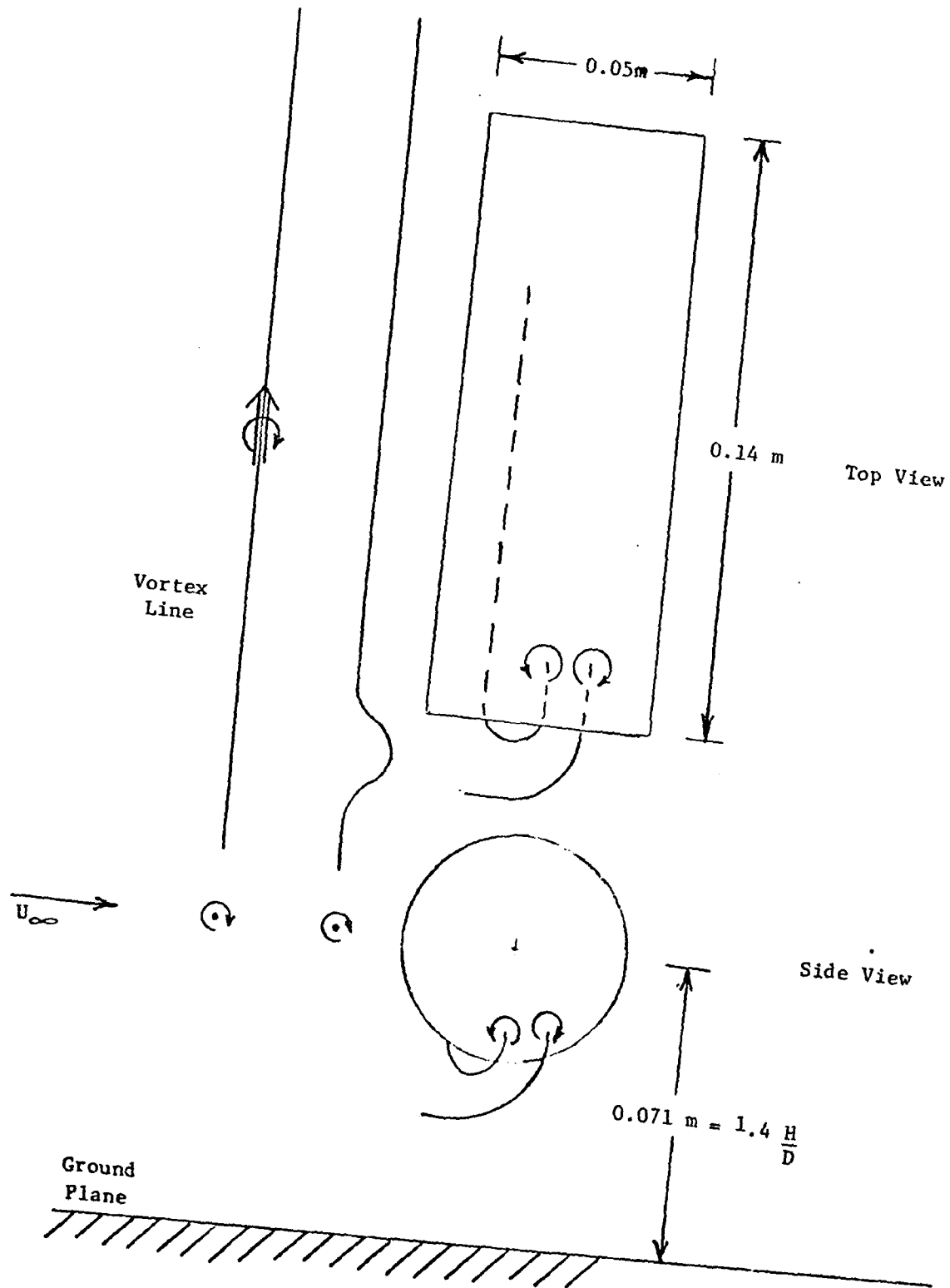


FIGURE 30

Ingestion of Horizontal Vortex Lines into a 90° Inlet
 (Drawn from Hydrogen Bubble Flow Visualization)

B) Inlet Distortion

Introduction

The performance of axial compressors when operating with non-uniform inlet flows has been widely studied because of the effect of inlet flow distortion on compressor performance and stall margin. Most of the analyses on this topic have been implemented with the assumption that the mean flow is uniform. In a two-dimensional analysis of this type (e.g., Refs. 35,36,37), it is shown that the resulting disturbances are basically of two types: those that are convected along the mean streamlines and potential disturbances which have an exponential decaying behavior. This is also the case for the analysis for rectilinear three-dimensional cascades (Refs. 38 & 39).

Under the sponsorship of AFOSR over the past several years, the Gas Turbine and Plasma Dynamics Laboratory has developed a non-axisymmetric actuator disk theory to treat three-dimensional flow through an annular blade row with circumferentially non-uniform inlet total pressure and a strongly swirling mean flow. The blade-row considered could be rotating (a rotor) or stationary (a stator). A computer program has also been developed and numerical results obtained. In contrast to two-dimensional theories and three-dimensional analyses for rectilinear cascades, these analyses showed the presence of essentially three type of disturbances in the flow field: (i) potential disturbances, (ii) convected disturbances and (iii) a new type which is absent in a situation with no mean swirl. These non-convected disturbances arise due to the interaction of

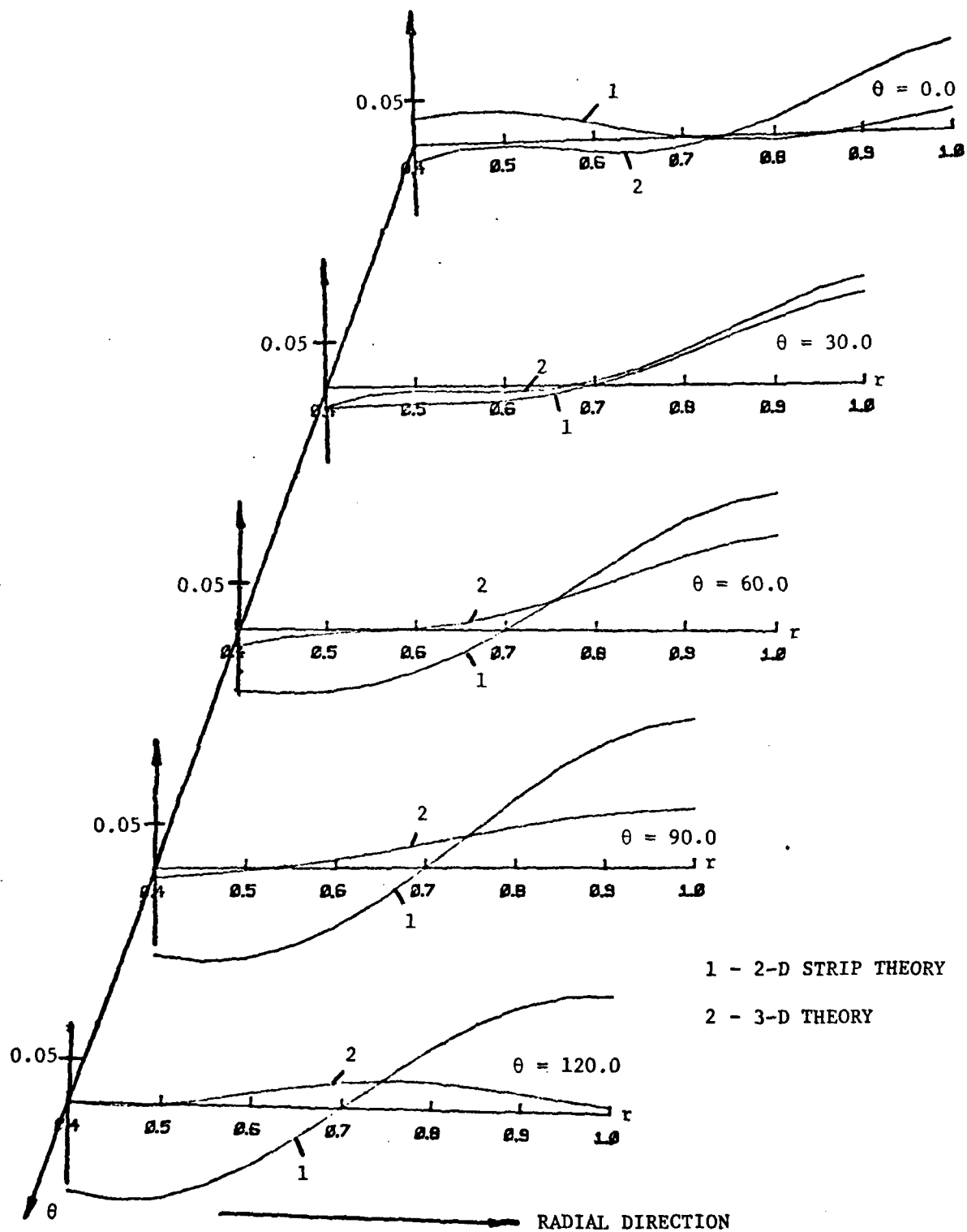
the vorticity field with the mean swirl and are associated with the presence of a persistent static pressure field. In this sense, the static pressure and vorticity disturbances are coupled in a swirling flow. This result is in agreement with that in Refs. 40 and 41. Comparisons have also been made with the available experimental data and good agreement has been seen (Ref. 42).

This initial work established the importance of three-dimensional effects. However, the analysis was restricted to situations in which the circumferential non-uniformity in total pressure was invariant with radius and the flow was incompressible. In view of this, efforts are now being made to relax these two restrictions.

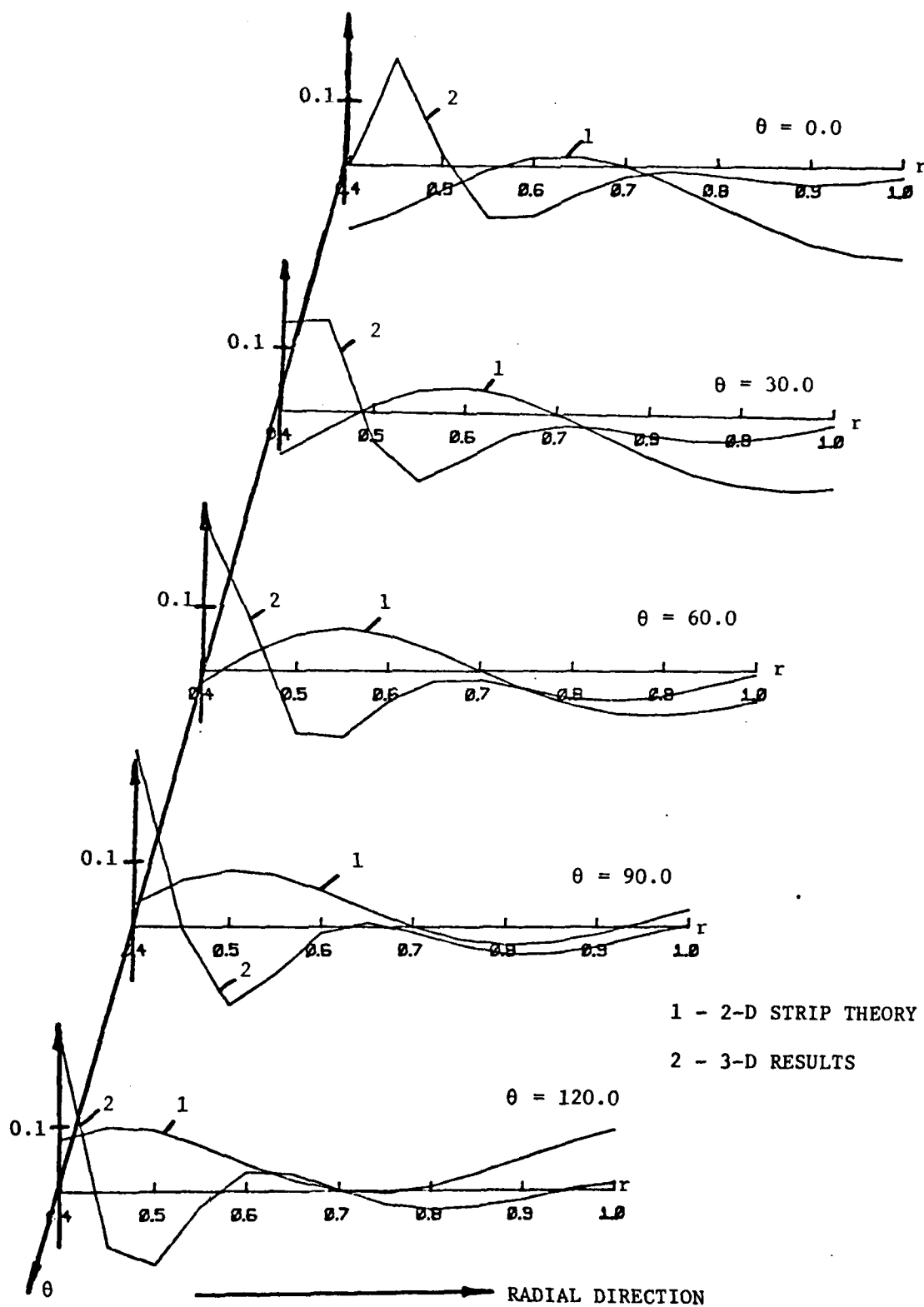
In the period covering 10/79 - 9/80, we have modified the analysis and the computer program to permit the study of a combined radial-circumferential inlet distortion through an annular blade-row. The results of this analysis can be compared with these of a strip theory approach which ignores the aerodynamic interference between different radii along the blading. In other words, the use of strip theory implies that the flow field at each radius can be considered as virtually the same as that through a two-dimensional cascade. The comparisons show that the difference between the two theories can be substantial and that the validity of strip theory for the flows of interest is thus far from universal.

Representative results of the calculations are shown in Figs. 31 and 32. Figure 31 shows the static pressure perturbation (normalized by the incoming average dynamic pressure) at various circumferential positions around the annulus at the location of the actuator disk representing the blade-rows. Figure 32 shows the corresponding axial velocity perturbations (normalized

NORMALISED STATIC PRESSURE

FIG. 31 DOWNSTREAM STATIC PRESSURE PERTURBATION AT $Z = 0.0$ (ROTOR)

NORMALISED AXIAL VELOCITY PERTURBATION

FIG. 32 DOWNSTREAM AXIAL VELOCITY PERTURBATIONS AT $z = 3.0$ (ROTOR)

by the upstream mean axial velocity) at perturbations (normalized by the upstream mean axial velocity) at an axial plane three tip radii downstream from the blade-row. Note that not only there is a substantial difference in magnitude, but also a phase difference in the results as given by the two theories. One point that should be mentioned is that the combined radial-circumferential distortion in total pressure chosen has a vanishing spanwise gradient at the hub and tip. This condition is necessary to ensure uniform convergence in the resulting Fourier-Bessel series for the solution. The solution also indicates that the spanwise gradient in the blade circulation at the hub and tip is zero, however, this is not true if the upstream flow has a non-zero spanwise gradient in total pressure at the hub and tip. The apparent analytical difficulty encountered above can be overcome through the use of a combination of radial polynomials and Fourier-Bessel series as a solution with the coefficients of the polynomials being chosen in such a way that uniform convergence of the Fourier-Bessel series is guaranteed. This extension of the analysis has also been implemented.

The analytical technique (the Clebsch Formulation) used for treating non-uniform incompressible inlet flows can readily be adopted for analyzing the case where compressibility effects can no longer be neglected. This is basically achieved by defining a transformed flow field (or reduced flow field) while maintaining the conservation of momentum, mass and energy. The transformed flow field is related to the actual flow field through

$$\rho_R = \rho e^{s/C_p}, \quad V_R = e^{-s/2C_p} \underline{V} \quad (9)$$

where ρ is the density, s is the entropy, V the velocity, C_p the specific heat at constant pressure and the subscript R refers to transformed flow field. The resulting analysis is valid for an inlet distortion in stagnation pressure and stagnation temperature. Note, however, that for a stationary blade row the presence of an inlet non-uniformity in stagnation temperature alone would not lead to non-convected disturbances, since Munk and Prim's substitution principle, all flows with a different stagnation temperature distribution but the same distribution of stagnation pressure have the same geometrical pattern of streamlines as one with uniform stagnation temperature^{30,43,44}. This is not so for flow through a rotor.

In the current contract period, efforts will be made to develop computer programs so that numerical results can be obtained for (i) the analysis of a combined radial circumferential distortion in total pressure which has a non-zero spanwise gradient at the hub and tip, and (ii) the analysis of compressible flow through a blade-row with an upstream inlet distortion.

TASK IV: INVESTIGATIONS OF THREE-DIMENSIONAL FLOWS IN HIGHLY LOADED
TURBOMACHINES

Abstract

Turbomachine performance depends in part on the skill with which desired and actual flow angles, with given mass flow distribution, can be predicted for engineering purposes. Analysis of flow angle, mass flow, and power density distribution have been undertaken for highly loaded 3-D devices. Inlet flow distortion, as well as lossy wakes, effect the results materially, especially because of the high swirl. Concrete estimates of these effects have now been made available. Further, the natural unsteadiness of turbomachine flow has now been analyzed in the presence of these effects (at light loading but in a three-dimensional example). Application to design requires understanding blade-to-blade effects as well. Progress is being made in this context using variations on wing theory. The basic (reference) axisymmetric flow in blade rows of finite chord and various "leading-edge" conditions is being analyzed to facilitate the understanding and application of the blade-to-blade studies. Comparison between theory and experiment is being carried forward.

- 1) The stated objectives of this part of the contract were:
 - a) to develop a method for predicting and understanding the three-dimensional unsteady flow around a blade row.
 - b) to utilize the analytical solutions to provide boundary conditions for current three-dimensional numerical calculation of flow through transonic rotors.

- c) to calculate the blade-to-blade varying flow (with finite chord) using the actuator duct solutions as the axisymmetric mean flow.
- d) to compare the theoretical results with the available experimental data for flow through highly loaded blade rows.

2) Significant Accomplishments

Analysis of flow in turbomachines is facilitated by distinguishing the effects of various types of vorticity. Flow-aligned (Beltrami) and lossy-wake (basically viscous) vorticity evolve differently, but in rotating flows, have very similar effects on turbomachine blade rows. This is true in terms of both steady and unsteady phenomena.

- a) It has been demonstrated that three-dimensional flow problems are amenable to analysis for both steady and unsteady flow. Axisymmetric calculations are not independent of blade-to-blade results.
- b) Non-uniform inlet flow has been studied in several examples. Circumferential distortions were studied first, showing that the present methods are effective in explaining experimental data where available. Sheared inlet flow has been analyzed for secondary flow effects, showing their importance in latter stage design.
- c) Non-uniform and unsteady flow in a 3D blade row has been analyzed. Possibly significant 3D effects on important stability problems have been noted. Blade row performance, on average, is also affected.

- d) Experimental data on an actual (3D) low speed highly loaded rotor has become available. Theoretical results obtained here have compared favorably with these experimental data. This forms the Master's Thesis of Mr. David Miller (see item 3).
- e) Far upstream and downstream boundary conditions in turbomachine flows are difficult to treat numerically. A combination of analytical and numerical approaches has now been carried out for the upstream boundary of the flow field of a transonic rotor, thus providing a rational approach to this problem.
- f) Axisymmetric flow approximations in turbomachines actually have a very intricate meaning, often difficult to interpret. To investigate this, we have developed a new form of "actuator duct" theory, which is useful for examining both the axisymmetric and blade-to-blade features of the flow.
- g) A formulation of the blade-to-blade problem for 3D flow in highly loaded turbomachines, including especially finite chord effects, has been completed.

Three-Dimensional Flow Through Highly-Loaded Blade Rows

Early analytical studies of three-dimensional flows in turbomachinery were limited to blade-rows of light loading;⁴⁵⁻⁵³ i.e., small swirl and small pressure change across any stage. Such restrictions precluded direct application of these analysis, which showed the significance of three-dimensional phenomena in the transonic region, to turbomachines with highly-loaded blade-rows. The idea then evolved that it was possible to use the

azimuthally-average flow, which can be treated exactly (nonlinearly) with the help of the axisymmetric through flow equations, as a reference. The blade-to-blade flow (i.e., the θ -varying flow) can then be described as a perturbation about this azimuthally-average flow, which permits the description of the large overall turning of the flow (therefore highly-loaded blade-rows).

This idea was applied to the study of three-dimensional induced effects due to trailing vorticity from blades with non-uniform circulation and from the vorticity associated with the non-uniformity in stagnation pressure (or rotary stagnation pressure in the case of a rotor) caused by viscous interaction between the working fluid and blade surfaces. Both incompressible and the compressible flow were considered.⁵⁴⁻⁶⁰ The work (in reference 54 to 60), shows that, in agreement with references 61,62,63 in an environment of highly swirling through flow (typical of flow in turbo-machines), the pressure field and the vorticity field are coupled. This coupling is absent if one assumes that the induced disturbances are convected by the mean flow (see Figs. 33 and 34). In particular, if the swirl is of the non-free vortex type, the induced disturbances can effectively persist indefinitely. However, in the limit of free vortex swirl, the induced disturbances increase in magnitude for distances in the neighborhood of the blade-row before beginning to decrease inversely with the axial distance downstream. In the analysis described in references 54 to 60 the blade-row is modelled by a lifting line model. Consequently, the resulting theory is not able to resolve the detail of the flow field around the blades.

CONVECTED DISTURBANCE

77

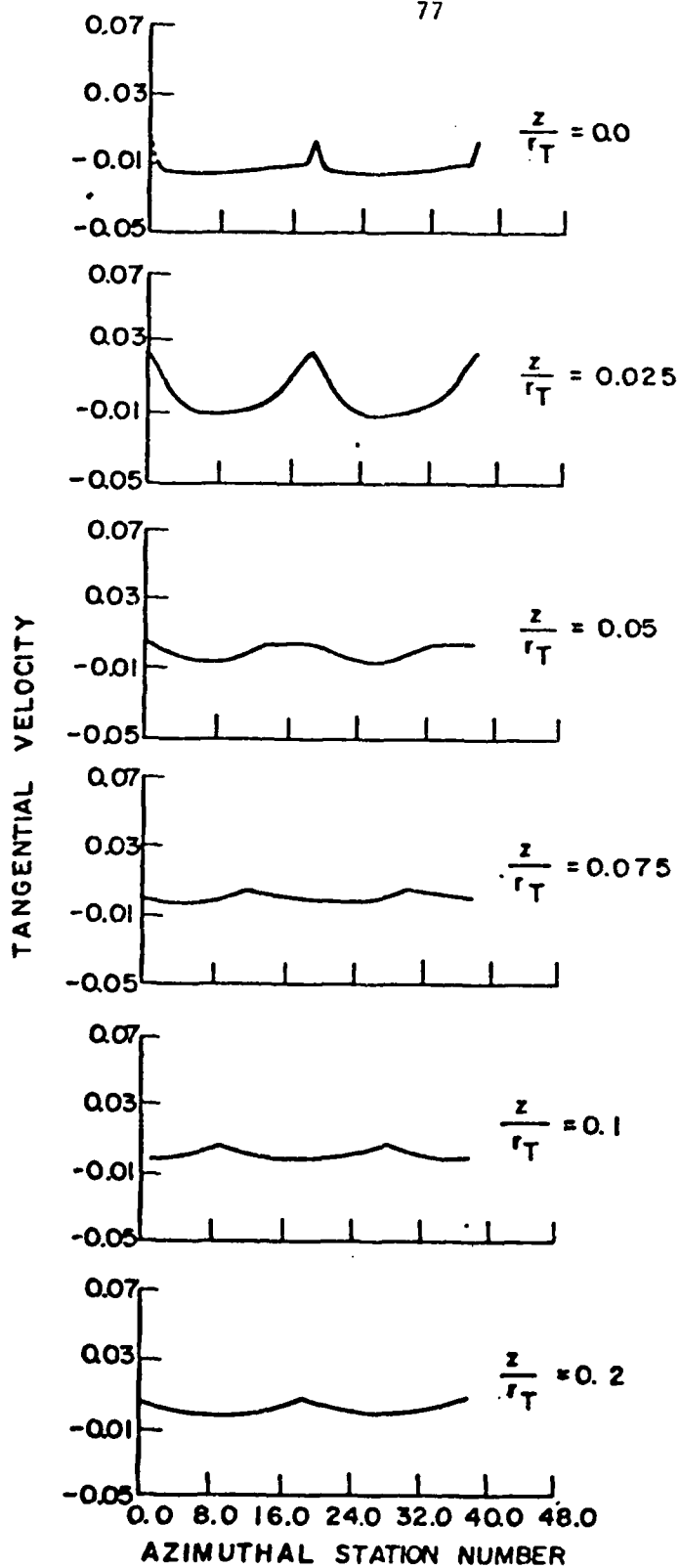


FIGURE 33

NON-CONVECTED DISTURBANCE

78

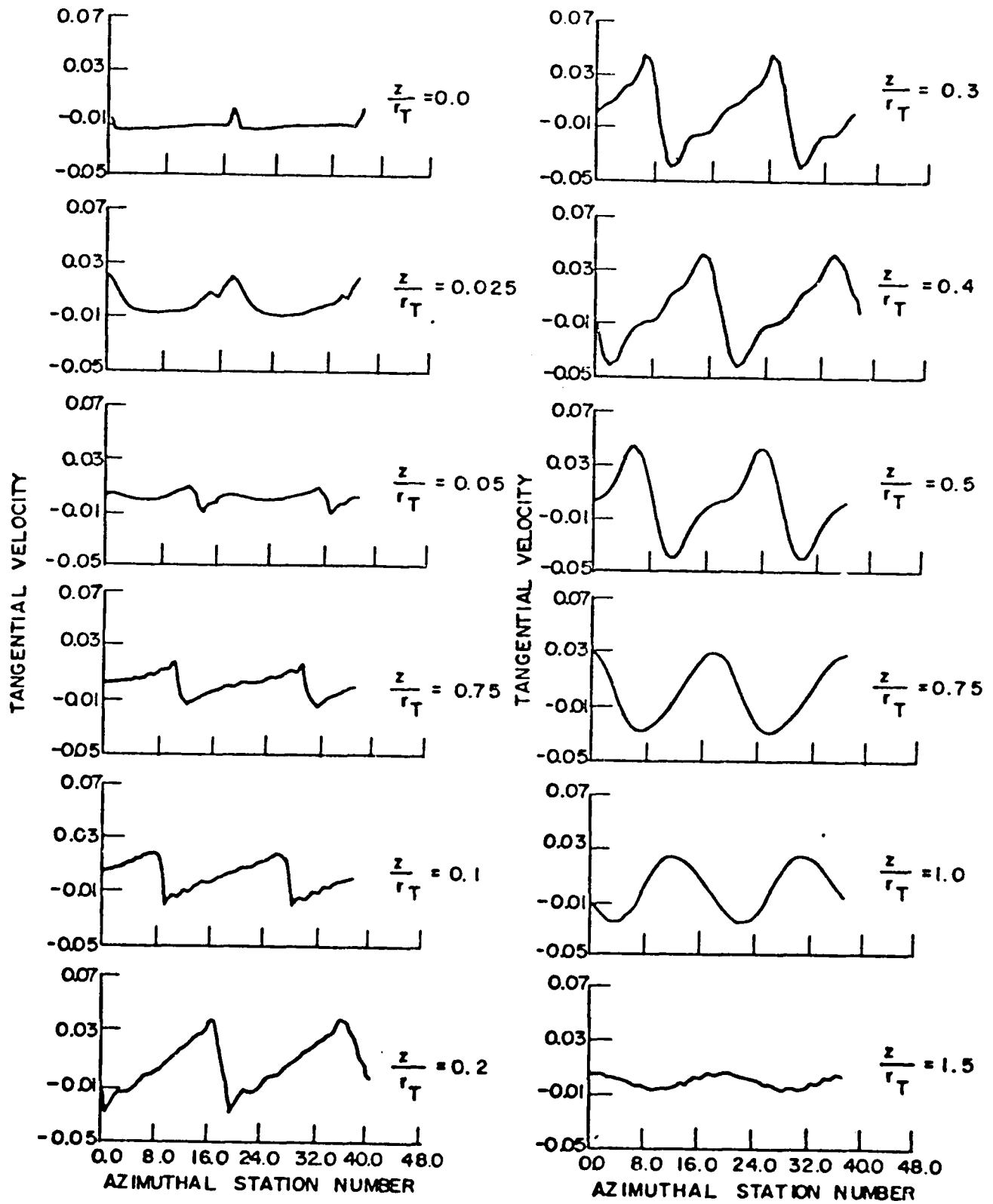


FIGURE 34

Thus, there is a need to extend the analysis to treat flows through an annular blade row with a finite chord length.

Before proceeding to describe the progress we made in the contract period 6/79 to 9/80 on the extension of three-dimensional flow analysis for blade row of finite chord, a description of our attempt to compare the analytical results with the experimental data of Dring⁶⁴ at UTRC is warranted. The results of the three-dimensional theory compared favorably with the experimental data of Dring⁶⁴ (Figure 35 to 38). However, it should be pointed out that some of the features observed in the experimental data are also predicted for the case examined by the two-dimensional strip theory. This may imply that the non-axisymmetric disturbances observed in that experiment are mainly of the convected type. However, this does not preclude the fact that the non-convected type of disturbance, a three-dimensional phenomenon, can at times be dominant. Further work is required for clarification.

Currently, we are working on the extension of the analytical technique (McCune-Tan-Hawthorne) to treat three-dimensional blade-to-blade flow through a high deflection blade-row of finite chord length. The technique will enable one to calculate the actual blade camber associated with a specified (axisymmetric) mean flow, i.e., the departure of the actual stream surfaces from those based on an axisymmetric analysis, due to the three-dimensional effects of discrete blades. As before, an azimuthally-

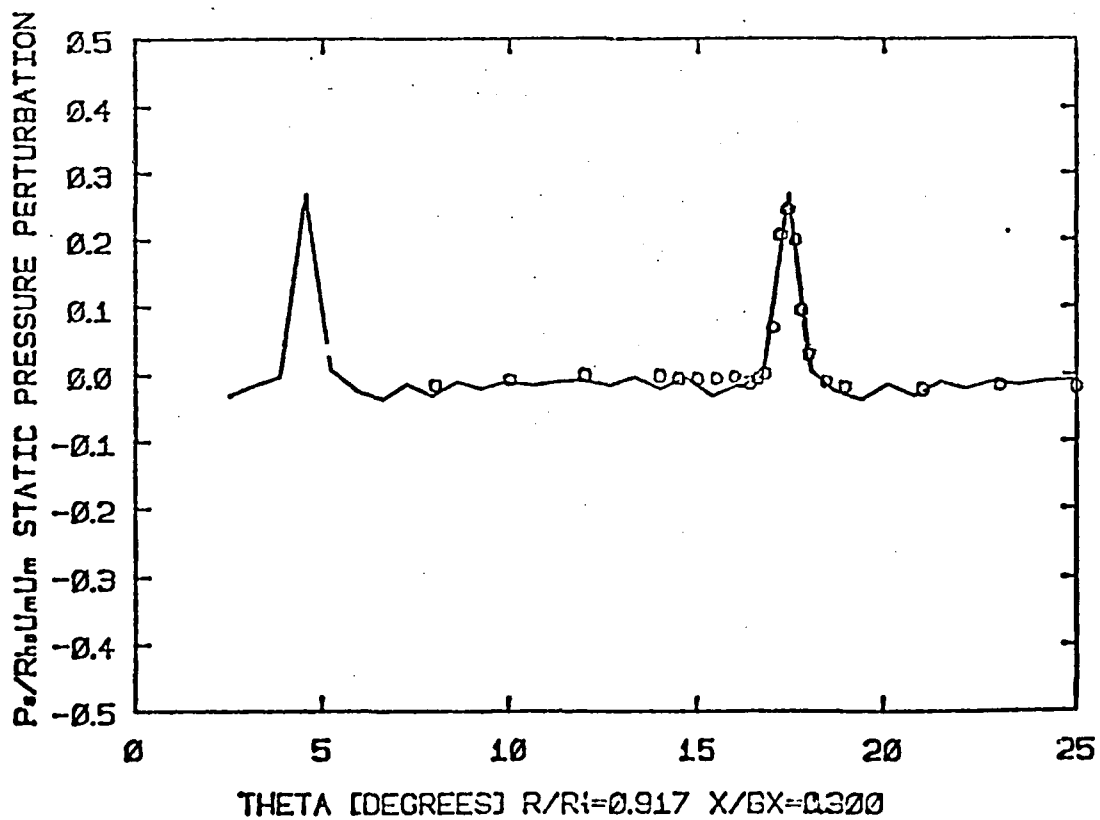
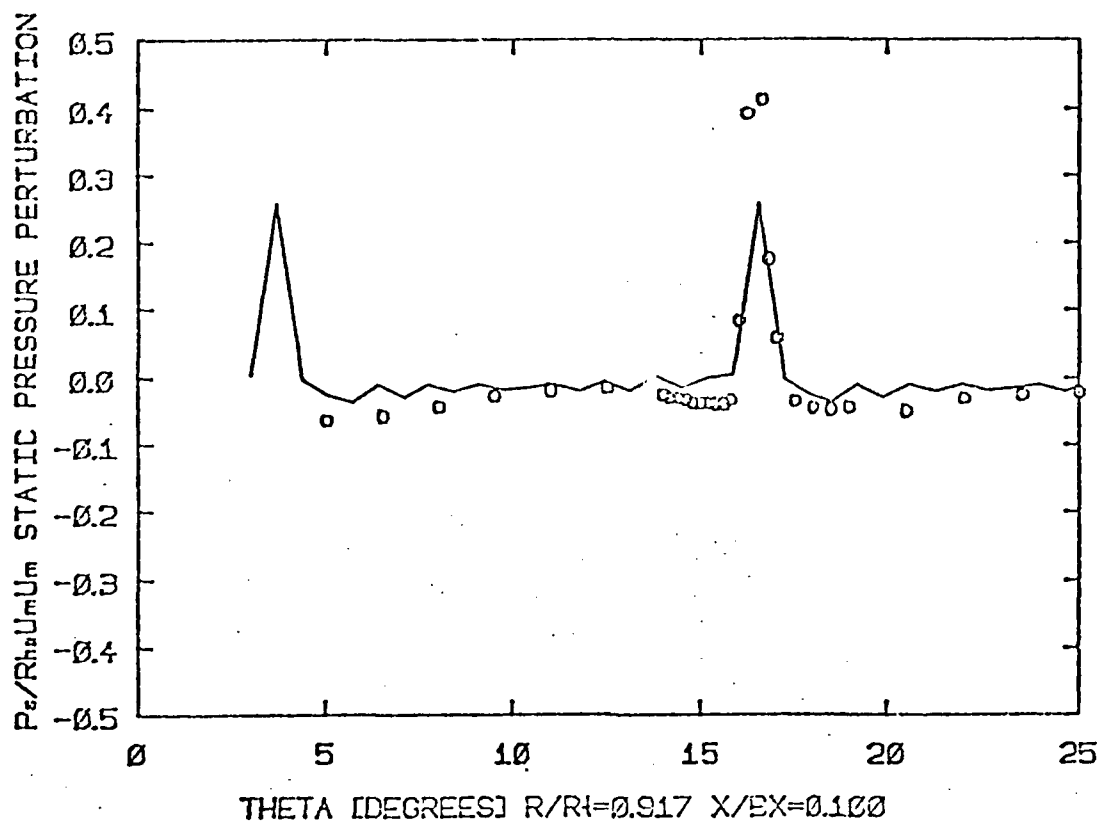


FIGURE 35 Downstream Blade-to-Blade Comparison of the Static Pressure Perturbations at the Off-Design Conditions Near the Mean Radius

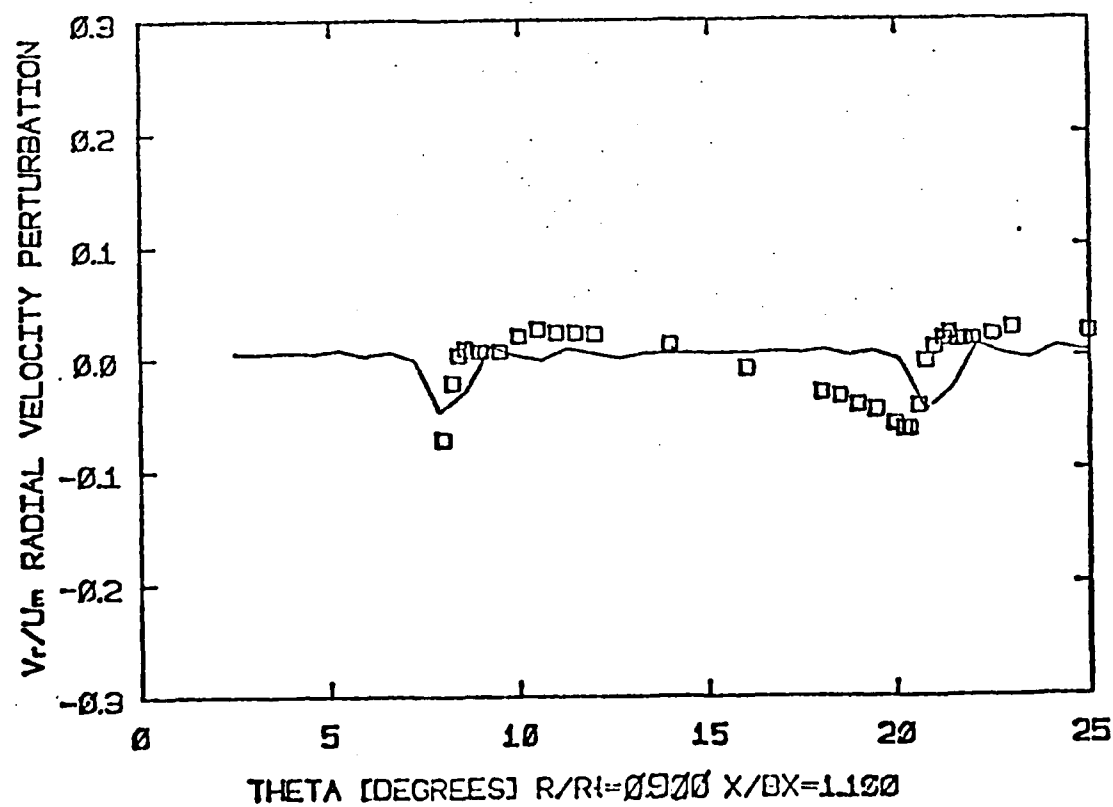
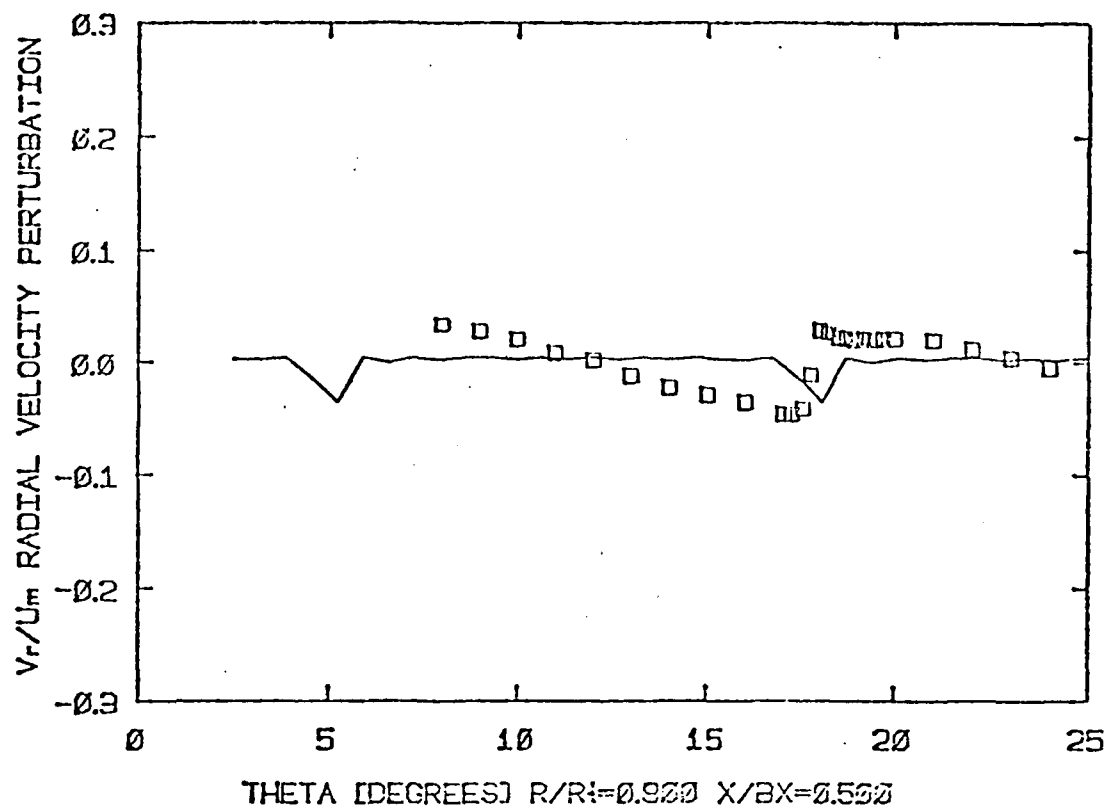


FIGURE 36 Downstream Blade-to-Blade Comparison of the Radial Velocities at the Design Mean Radius

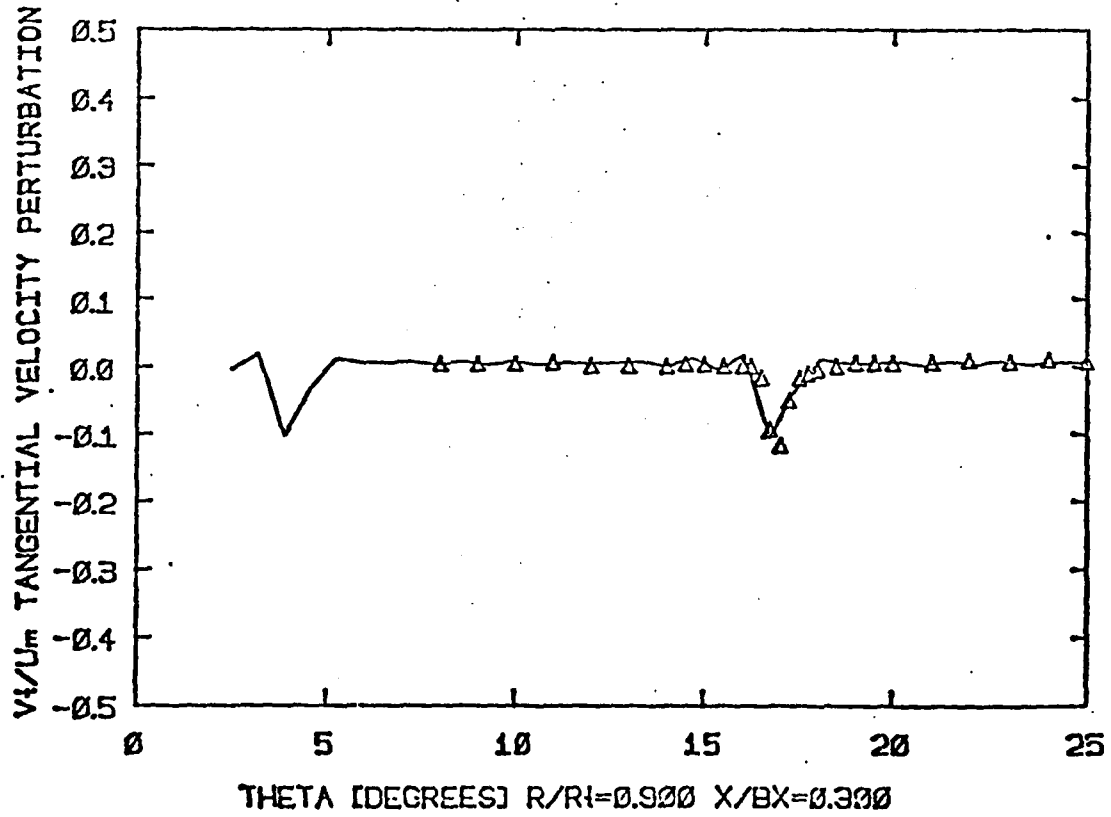
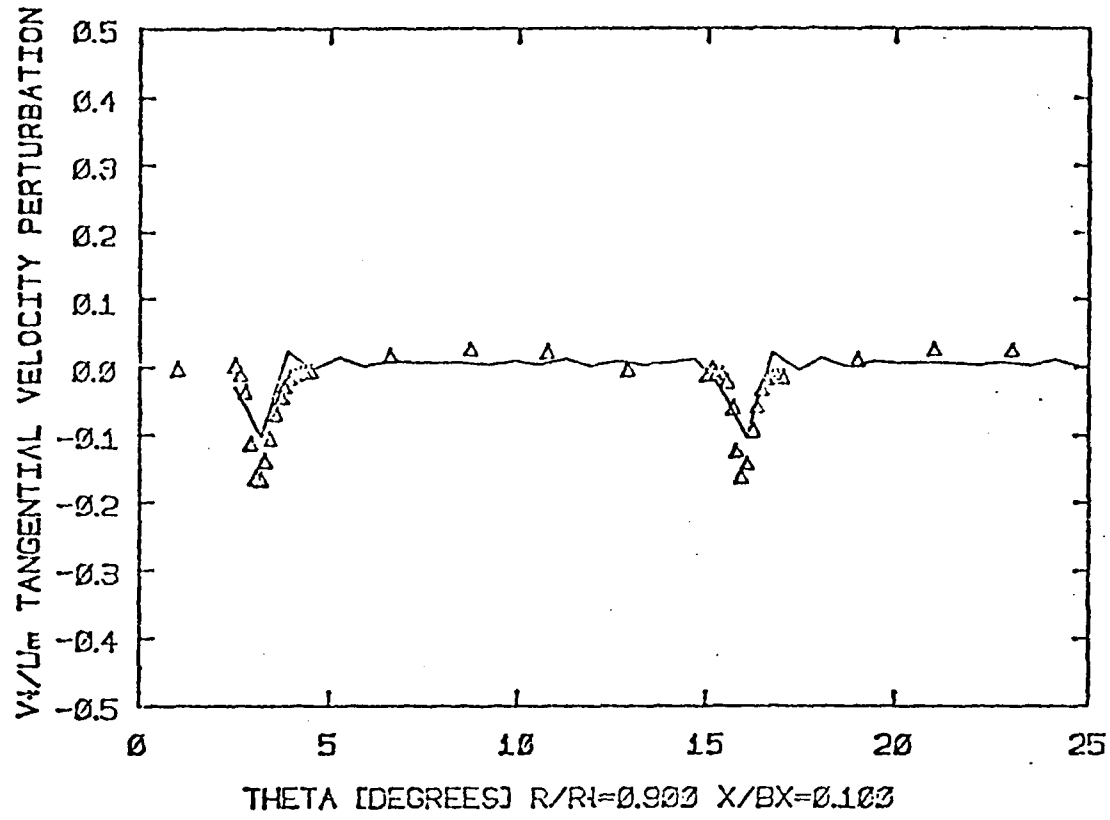


FIGURE 37 Downstream Blade-to-Blade Comparison of the Tangential Velocities at the Design Mean Radius

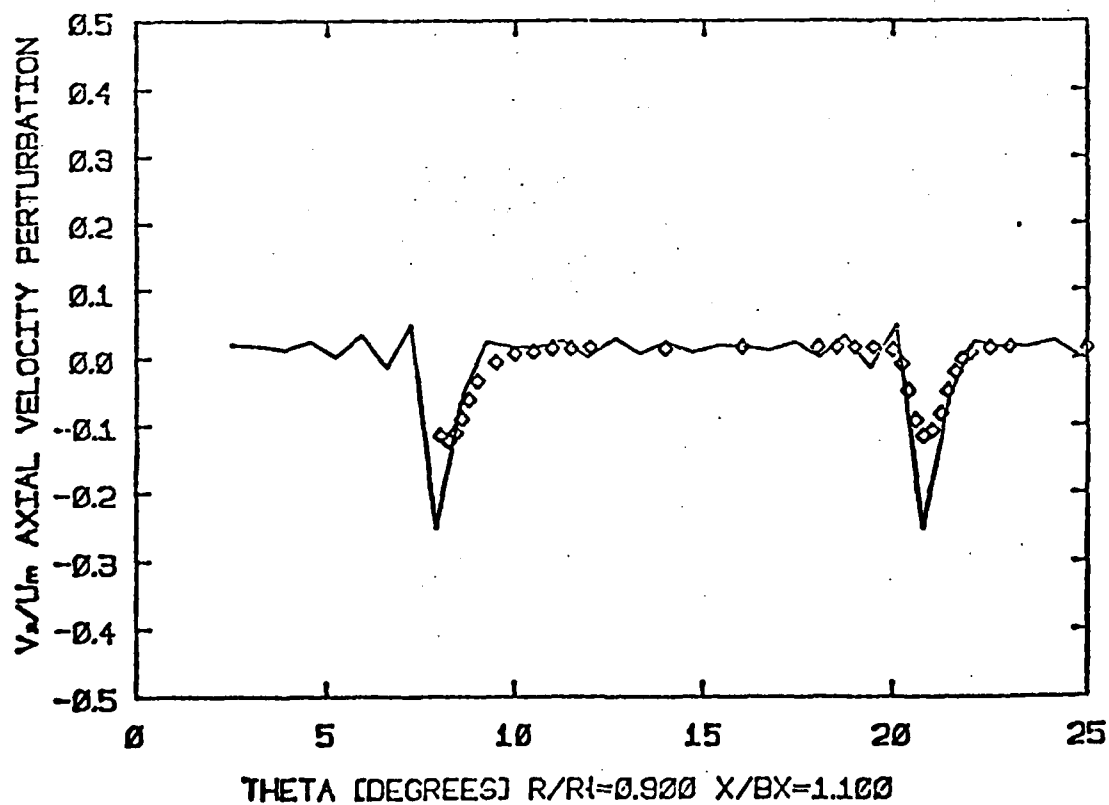
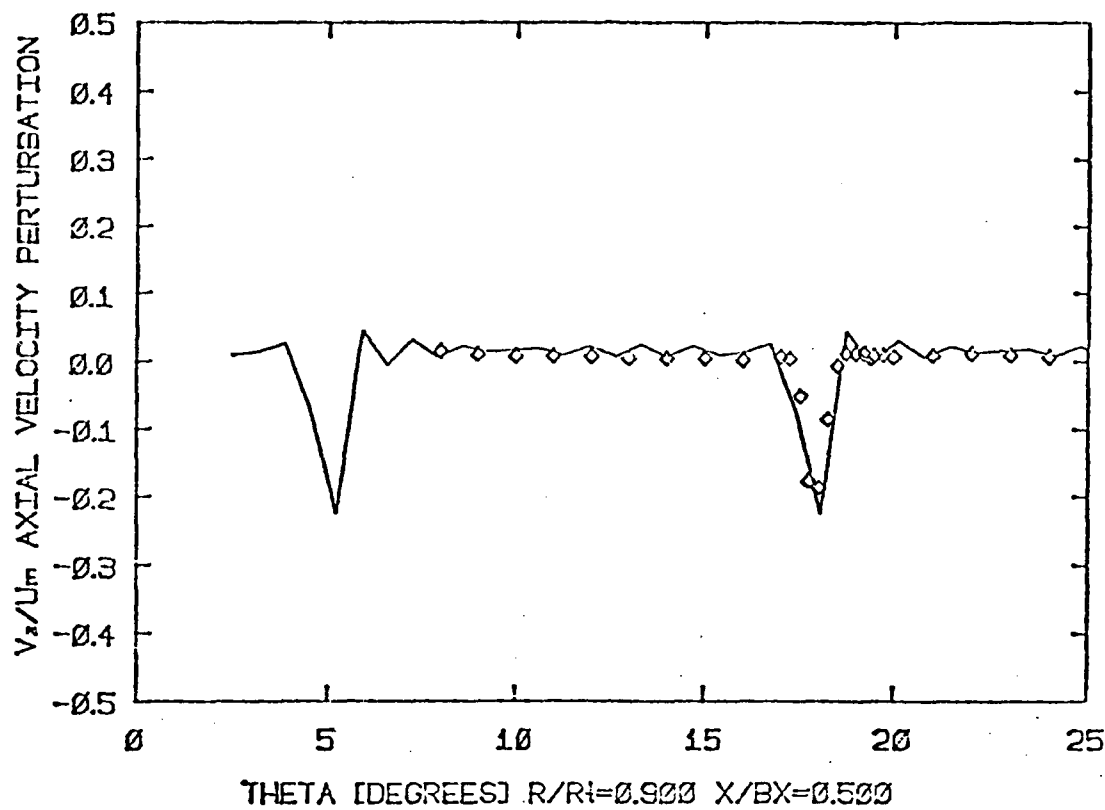


FIGURE 38 Downstream Blade-to-Blade Comparison of the Axial Velocities at the Design Mean Radius

average flow is required so that vorticity can be distributed on the mean stream surface (i.e., the α_0 -surface) so as to create the specified local force. With this knowledge, one can then proceed to calculate the blade-to-blade flow, and hence the actual camber lines relative to the α_0 -surface.

The requirement of the azimuthally average flow leads us to develop an actuator duct theory. We will use these simple actuator duct solutions as the reference flows for formulating the blade-to-blade flows.

A continuous force (and vorticity as well) distribution is employed to represent the blading in actuator duct theory. Consequently, fluid quantities change continuously over finite axial distance rather than discontinuously as in actuator disk analysis. From the axisymmetric through flow equations, we have obtained a class of actuator duct solutions with the torque being proportional to any integral power (positive or negative) of the radius [(i.e., $\frac{rF_\theta}{\rho} = Ar^m$, where r is the radius, F_θ the tangential component of the force, ρ the density, m a positive or negative integer, and A the proportionally constant)]. This class of solutions is applicable to flow through actuator duct with inlet shear as well as uniform inlet conditions. Some preliminary numerical results for the actuator duct solutions are presented in Fig. 39 and 40. The example considered is that of a stator with $\frac{rF_\theta}{\rho} \propto r^2$. It is noted that the shed circulation vanishes at the hub and tip (Fig. 34) as required by the boundary conditions.

For free-vortex blading, the flow is irrotational throughout and the angular momentum introduced is invariant with radius. Thus, one might

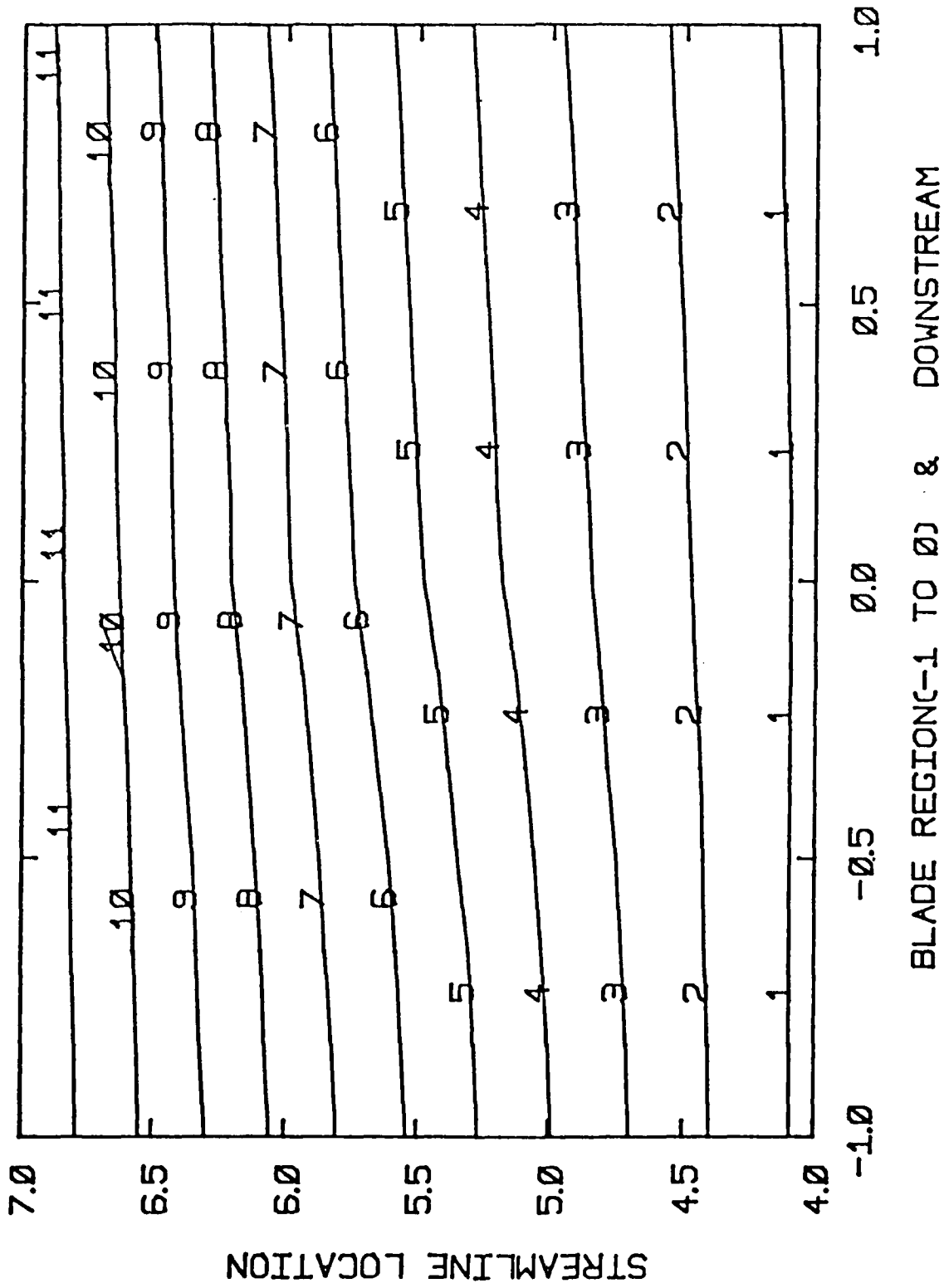


FIGURE 39 STREAMLINE LOCATIONS IN ACTUATOR DUCT.

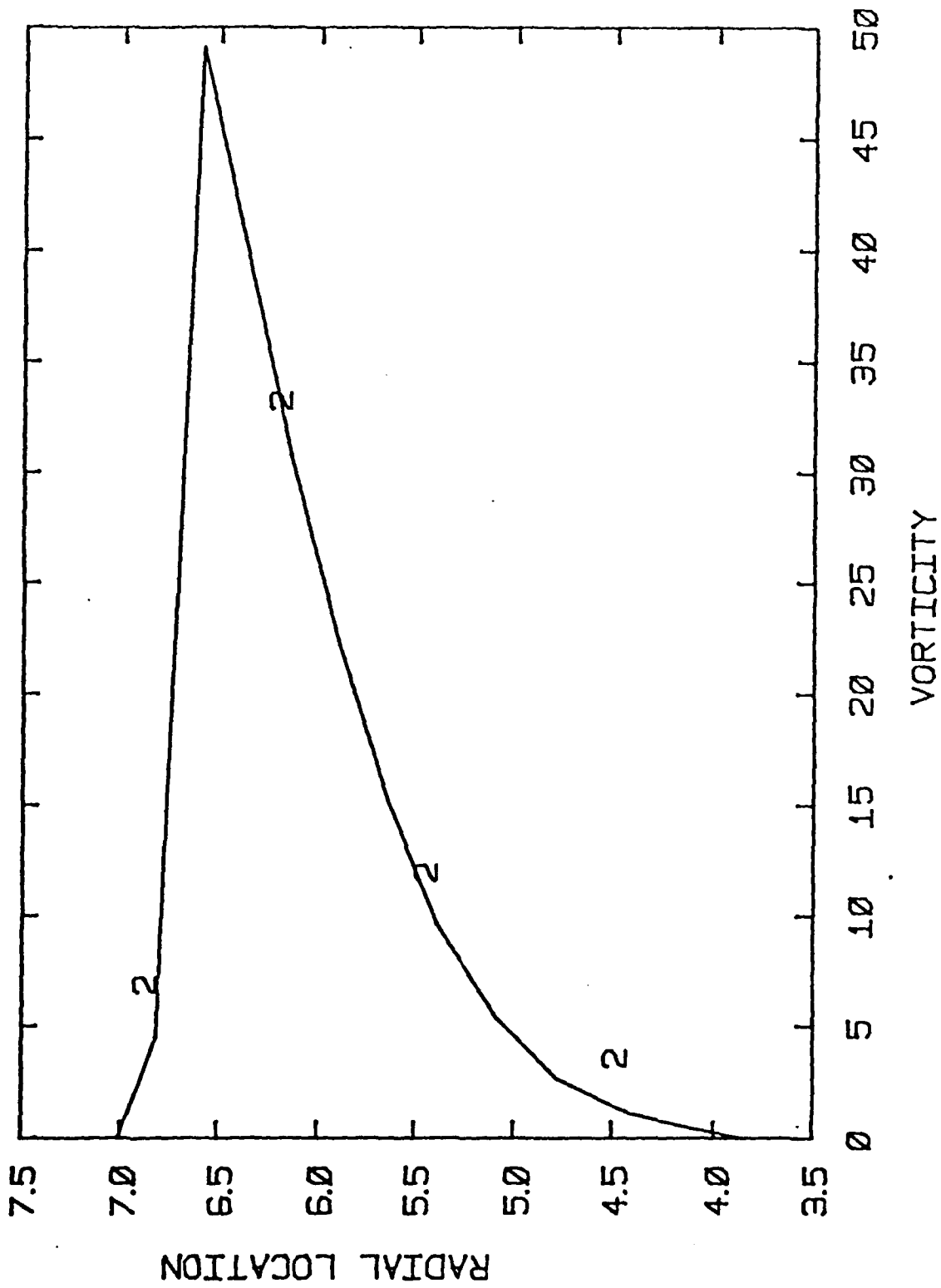


FIGURE 40 TRAILING VORTICITY

anticipate that the angular momentum, $r\bar{V}_\theta$, varies with axial distance z only. This is indeed an actuator duct solution for the case of a free-vortex blading in a stator (Note that $\frac{rF_\theta}{\rho} = \frac{dr\bar{V}_\theta}{dz}$). We have formulated a 3-D blade-to-blade flow analysis with $r\bar{V}_\theta = G_0(Z-Z_{1.e.})$ so that $\frac{rF_\theta}{\rho} = G_0 =$ constant ($Z_{1.e.}$ is the axial location of the blade leading edge). Currently we have also shown that for the case of two-dimensional cascades, the results obtained using our analytical techniques agree with those given by the Biot-Savart Law.

Our effort in the coming year will focus on developing the necessary computer program to obtain numerical results, especially in the case of blade-to-blade flow in addition to the efforts already underway for the actuator duct theory.

3. PUBLICATIONS

Publications in Technical Journals

(Based on work partially or wholly supported by this Contract.)

E. M. Greitzer, "The Stability of Pumping Systems - The 1980 American Society of Mechanical Engineers Freeman Scholar Lecture," presented at ASME Winter Annual Meeting, November 1980. To be published in the ASME Journal of Fluids Engineering (invited review).

W. T. Thompkins, and Siu S. Tong, "Inverse or Design Calculation for Non-Potential Flow in Turbomachinery Blade Passages," to be presented at ASME Gas Turbine Conference, Houston, 1981, and published in Journal for Engineering for Power.

C. S. Tan, "Vorticity Modelling of Blade Wakes Behind Isolated Annular Blade-Rows: Induced Disturbances in Swirling Flows." ASME Paper #80-GT-140 presented at ASME Gas Turbine Conference and Products Show, New Orleans, LA, March 10-13, 1980. To Appear in ASME Journal for Engineering for Power.

Reports

C. S. Tan, "Three-Dimensional Incompressible and Compressible Beltrami Flow Through a Highly-Loaded Isolated Rotor," GT&PDL Report No. 147, October 1979.

C. S. Tan, "Three-Dimensional Vorticity-Induced Flow Effects in Highly-Loaded Axial Compressors," Part I, Ph.D. Thesis, MIT Department of Aeronautics and Astronautics, and GT&PDL Report No. 131, January 1980.

C. S. Tan, "Asymmetric Inlet Flows Through Axial Compressors," Part II, Ph.D. Thesis, MIT Department of Aeronautics and Astronautics, and GT&PDL Report No. 151, January 1980.

Theses

Saeed Farokhi, "Unsteady Three-Dimensional Flow in a Compressor with Inlet Flow Distortions," Ph.D. Thesis, MIT Department of Aeronautics and Astronautics, February 1980.

Mohammad Rahnema, "On Shear Flow Through Highly Loaded Three-Dimensional Cascades," M.S. Thesis, September 1980.

David P. Miller, "The Predictive Study of Flow Phenomena Behind an Axial Turbomachine Rotor," M.S. Thesis, MIT Department of Aeronautics and Astronautics, June 1980.

4. PROGRAM PERSONNEL

Principal Investigators:

Edward M. Greitzer
Associate Professor of Aeronautics & Astronautics

William T. Thompkins, Jr.
Assistant Professor of Aeronautics & Astronautics

James E. McCune
Professor of Aeronautics & Astronautics

Co-Investigators:

Alan H. Epstein
Assistant Professor of Aeronautics & Astronautics
Associate Director of Gas Turbine & Plasma Dynamics Laboratory

Choon S. Tan
Research Associate

Collaborating Investigators:

Jack L. Kerrebrock
Professor of Aeronautics & Astronautics

Sir William R. Hawthorne
Senior Lecturer

Graduate Students:

9/80 - Present	Peter Cheng
9/79 - Present	Francesca DeSiervi
6/79 - 2/80	Saeed Farokhi**
9/79 - Present	Mohan Krishnan
9/80 - Present	Wen Liu
2/80 - Present	Alexander Lifshits
6/79 - 5/80	David Miller*
9/80 - Present	Wing-Fai Ng
9/79 - Present	Mark Prell
9/79 - 8/80	Mohammad Rahnema*
9/79 - Present	Keith Theirrin
9/79 - Present	Siu Shing Tong
6/80 - 11/80	Henri Viguier

* S.M. Thesis Completed

** Ph.D. Thesis Completed

5. INTERACTIONS

Presentations and Lectures

E. M. Greitzer, Lectures on, "Unsteady Flows in Turbomachines," "Inlet Distortion," and "Surge and Rotating Stall," at ASME/ISU Turbomachinery Institute Course on Fluid Dynamics of Turbomachinery, Ames, Iowa, July 1980.

E. M. Greitzer, "Strut Induced Aerodynamic Forcing Functions in Axial Compressors," seminar delivered at NASA Lewis Research Center, Cleveland, Ohio, November 1979.

E. M. Greitzer, Lecturer in ASME Short Course, "Foundations of Axial Turbomachinery Aerodynamics," presented at ASME International Gas Turbine Conference, New Orleans, LA, March 1980.

E. M. Greitzer, Seminars on "Prediction of Compressor Performance in Rotating Stall," and "Asymmetric Swirling Flow in Turbomachine Annuli," Department of Mechanical Engineering, Virginia Polytechnic Institute, Blacksburg, VA, January 1980.

A. H. Epstein, "Computer Aided Data Collection and Reduction in A Blowdown Compressor Facility," presented at AGARD Fluid Dynamics Panel meeting on Integration of Computers and Wind Tunnel Testing, September 24-25, 1980, Chattanooga, TN.

Visits and Technical Discussions

E. M. Greitzer, Visit to Whittle Laboratory, University Engineering Department, Cambridge University, Cambridge, England (Contact: Dr. N. A. Cumpsty).

E. M. Greitzer, Technical Discussions with Mr. A. B. MacKenzie, Head Compressor group, Rolls-Royce, Ltd.

E. M. Greitzer, Technical Discussions with Professor J. H. Horlock, Vice-Chancellor, Salford University, England (A joint paper is being planned on asymmetric flows due to non-uniform tip clearances.)

J. E. McCune, Extended visit (six weeks) to Whittle Laboratory, University Engineering Department, Cambridge University, Cambridge, England.

J. E. McCune, Technical Discussions at Rolls-Royce, Darby, England, June, July, 1978; June, July, August, 1979 - Present. Rational three-dimensional turbomachine design techniques.

J. E. McCune, Technical Discussions at Holset, Huddersfield, England, Discussion of transonic impeller design, high performance turbocharger, August 1978, July 1979, Present.

W. T. Thompkins, Summer spent with Computational Fluid Dynamics group at NASA Ames Research Center, Moffet Field, CA (Contact: Dr. Dean Chapman).

E. M. Greitzer, Visit from Dr. W. H. Hankey, Computational Fluid Dynamics Group, Air Force Flight Dynamics Laboratory, Wright-Patterson Air Force Base.

J. E. McCune and C. S. Tan, Technical Discussions at Calspan, Buffalo, NY, (Contact: Dr. William Rae and Dr. J. Lordi). Exploration of alternative numerical approaches for three-dimensional rotating flows, January 1980, August, 1980, November, 1980, continuing.

J. E. McCune, Technical Discussions at United Technology Research Center, East Hartford, CT, analysis of new data from an actual three-dimensional rotating compressor blade row, Spring 1979, continuing. (Ref: D. P. Miller)

A. H. Epstein and W. T. Thompkins, Technical Discussions with R. Moritz, Rolls-Royce, Inc. on transonic turbine testing.

AD-A093 375

MASSACHUSETTS INST OF TECH CAMBRIDGE GAS TURBINE AND--ETC F/G 20/4
CURRENT PROBLEMS IN TURBOMACHINERY FLUID DYNAMICS.(U)
NOV 80 E M GREITZER, W T THOMPkins F49620-78-C-0084

UNCLASSIFIED

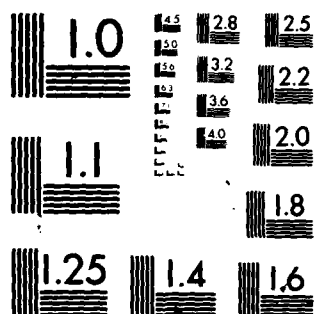
AFOSR-TR-80-1355

NL

AD-A093 375



END
DATE
FILED
2-8-81
DTIC



MICROCOPY RESOLUTION TEST CHART
NATIONAL BUREAU OF STANDARDS-1963-A

J. E. McCune, Session Chairman for Session on Turbomachinery Fluid Mechanics at ASME Gas Turbine Conference and Products Show, New Orleans, LA March 10-13, 1980.

E. M. Greitzer, Vice-Chairman of Session on Turbomachinery Fluid Mechanics at ASME Gas Turbine Conference and Products Show, New Orleans, LA, March 10-13, 1980.

E. M. Greitzer, Consultant to United Technologies Research Center (Pratt & Whitney Aircraft) on compressor stability and unsteady flow in turbomachines.

E. M. Greitzer, Invention evaluator (turbomachinery) for Office of Energy Related Inventions, National Bureau of Standards.

In addition to the above, the Gas Turbine and Plasma Dynamics Laboratory has an active seminar program with several speakers from industry and government per term. During the time period discussed, these were:

Dr. L. H. Smith, Jr., Manager Compressor and Turbine Aerodynamics General Electric Aircraft Engine Group (topic: "Flows in Multistage Compressors.")

Dr. A. M. Pfeffer, Head Turbine Group, Pratt & Whitney Aircraft (topic: "Turbine Cooling.")

Mr. R. S. Mazzaway, Senior Research Engineer, Pratt & Whitney Aircraft (topic: "Stagnation Stall.")

Dr. J. J. Adamczyk, NASA Lewis Research Center, (topic: "Supersonic Stalled Flutter.")

Dr. W. Jansen, Northern Research and Engineering, (topic: "Surge Margin Increase in Centrifugal Compressors due to Casing Treatment.")

Dr. L. E. Snyder, Head, Structures Group, Detroit Diesel Allison, Indianapolis, IN, (topic, Turbomachinery Design to Avoid High Cycle Fatigue.")

6. DISCOVERIES, INVENTIONS AND SCIENTIFIC APPLICATIONS

At this stage in the project no new "devices" have been developed. However several of the methods discussed on the detailed task description section are either new or novel adaptation of existing methods.

7. CONCLUDING REMARKS

The AFOSR multi-investigator program at MIT is proceeding in reasonable accord with schedule. The largest deviation has been in that part of the program involving further measurements on the AFAPL HTF stage. Reasons for these delays are discussed in the task description; one of them being due to the desire to implement the mechanical diaphragm cutter in the Blowdown Facility. However, the renewed participation of A. H. Epstein in the effort should be a positive step toward the completion of this project.

Also, as a result of the last year's activities, we have been able to upgrade and expand the overall capabilities for turbomachinery research at MIT. It is expected that this will continue since one of the products of a successful research program is increased understanding and the consequence of sharper focus on central issues. In addition we are starting to reach a stage where we have developed a "critical mass" of (especially) graduate students, faculty, and support staff who have a common interest in the type of problems addressed by this project and can interact fruitfully. Aside from the technical results, this active effort will result in an output of talented young engineers with a strong interest in high performance turbomachinery.

REFERENCES

1. Bauer, F., Garabedian, P., and Korn, D., "Supercritical Wing Section III", Lecture Notes in Economics and Mathematical Systems, Vol. 150, Springer-Verlag, New York, 1977.
2. Ives, D. C., and Liutermozu, J. L., "Analysis of Transonic Cascade Flow Using Conformal Mapping and Relaxation Technique", AIAA Journal, Vol. 15, May 1977, pp 647-652.
3. Stephens, H. E., "Supercritical Airfoil Technology in Compressor Cascades: Comparison of Theoretical and Experimental Results", AIAA Journal, Vol. 17, June 1979, pp 594-600.
4. Zannetti, L., "Time-Dependent Method to Solve the Inverse Problem for Internal Flows", AIAA Journal, Vol. 18, July 1980, pp 754-758.
5. Haymann-Haber, G., and Thompkins, W. T., "Comparison of Experimental and Computation Shock Structure in a Transonic Compressor Rotor", ASME paper No. 80-GT-81 (To appear in Journal of Eng. for Power).
6. Steger, J. L., "Implicit Finite-Difference Simulation of Flow about Arbitrary Two-Dimensional Geometries", AIAA Journal, Vol. 16, July 1978, pp 679-686.
7. Viviani, H., "Conservative Forms of Gas Dynamic Equations", La Recherche Aerospatiale, No. 1, Jan. - Feb. 1974, pp 65-68.
8. McCormack, R. W., "Computational Efficiency Achieved by Time Splitting of Finite Difference Operators", AIAA Paper 72-154.
9. Beam, R. M., and Warming, R. F., "An Implicit Factor Scheme for the Compressible Navier-Stokes Equation", AIAA Journal, Vol. 16, April 1978, pp 393-402.
10. Gopalakrishnan, S., and Bozzola, R., "Numerical Representation of Inlet and Exit Boundary Conditions in Transient Cascade Flow", ASME Paper No. 73-GT-55, 1973.
11. Kerrebrock, J. L., et al., "The MIT Blowdown Compressor Facility", J. of Eng. for Power, Vol. 46, No. 4, October 1974.
12. Kerrebrock, J. L., Thompkins, W. T., and Epstein, A. H., "A Miniature High Frequency Sphere Probe", ASME Gas Turbine Conference, New Orleans, March 1980.
13. Ng, W. F., "Detailed Time Resolved Measurements and Analysis of Unsteady Flow in a Transonic Compressor", SM Thesis, MIT, August 1980.
14. Titcomb, F. D., "Design of a Diaphragm Cutter for the MIT Blowdown Compressor Facility", SM Thesis, MIT, February 1980.

15. Takata, H., and Tsukuda, Y., "Study on the Mechanism of Stall Margin Improvement of Casing Treatment", ASME Paper 75-GT-13, March 1975.
16. Prince, D. C., Jr., Wisler, D. C., and Hilvers, D. E., "Study of Casing Treatment Stall Margin Improvement Phenomena", NASA CR-134552, March 1974.
17. Osborn, W. M., Lewis, G. W., Jr. and Heidelberg, L. J., "Effect of Several Porous Casing Treatments on Stall Limit and on Overall Performance of an Axial-Flow Compressor Rotor", NASA TN D-6537, Nov. 1971.
18. Moore, R. D., Kovich, G., and Blade, R. J., "Effect of Casing Treatment on Overall and Blade-Element Performance of a Compressor Rotor", NASA TN D-6538, November 1971.
19. Fabri, J., and Reboux, J., "Effect of Outer Casing Treatment on Stall Margin of a Supersonic Rotating Cascade", ASME Paper 75-GT-95, ASME Gas Turbine Conference, Houston, Texas, March 1975.
20. Tesch, W. A., "Evaluation of Range and Distortion Tolerance for High Mach Number Transonic Fan Stages: Task IV Stage Data and Performance Report for Casing Treatment Investigations, Volume I", NASA CR-72862, May 1971.
21. Bailey, E. E., and Voit, C. H., "Some Observations of Effects of Porous Casing on Operating Range of a Single Axial-Flow Compressor Rotor", NASA TM X-2120, October 1970.
22. Bailey, E. E., "Effect of Grooved Casing Treatment on the Flow Range Capability of a Single-Stage Axial Flow Compressor", NASA TM X-2459, January 1972.
23. Horlock, J. H., and Lakhwani, C. M., "Propagating Stall in Compressors with Porous Walls", ASME Paper 75-GT-59, March 1975.
24. Smith, G. D. J., "Casing Treatment in Axial Compressors", Ph.D. Thesis, Cambridge University, 1980.
25. Greitzer, E. M., et al., "A Fundamental Criterion for the Application of Rotor Casing Treatment", ASME J. Fluids Engineering, 101, June 1979, pp 238-243.
26. Jansen, W., et al., "Improvements in Surge Margin for Centrifugal Compressors", presented at AGARD 55th Specialist's Meeting, "Centrifugal Compressors, Flow Phenomena and Performance", May 1980.
27. Motycka, D. L., "Ground Vortex - Limit to Engine/Reverser Operation", ASME paper No. 75-GT-3, March 1975.

28. Colehour, J. L., and Farquhar, B. W., "Inlet Vortex", *Journal of Aircraft*, Vol. 8, No. 1 January 1971, pp 39-43.
29. Motycka, D. L., Walter, W. A., and Muller G. L., "An Analytical and Experimental Study of Inlet Ground Vortices", AIAA paper No. 73-1313, November 1973.
30. Hawthorne, W. R., "On the Theory of Shear Flow", MIT Gas Turbine Laboratory, Report No. 88, 1966.
31. Lighthill, M. J., "Drift", *Journal of Fluid Mechanics*, Vol. 1, 1956, pp 31-53.
32. Hess, J. L., Mack, D., and Stockman, N. O., "An Efficient User-Oriented Method for Calculating Compressible Flow in and about Three-Dimensional Inlets", McDonnell Douglas Report No. MDC J7733, also NASA CR-159578, April 1979.
33. Viguier, H. C., "A Secondary Flow Approach to the Inlet Vortex Flow Field", SM Thesis, Department of Mechanical Engineering, MIT, November 1980.
34. Kotansky, D. R., "Thin Airfoils in Rotational Flow", MIT Gas Turbine Lab Report No. 80, 1965.
35. Rannie, W. D., and Marble, F. E., "Unsteady Flows in Axial Turbomachines", ONERA, Comptes Rendus des Journees Internationales de Sciences Aero-nautiques, Part 2, pp 1-21, Paris, May 27-29, 1957. Also Daniel and Florence Guggenheim Jet Propulsion Centre, Cal. Inst. Tech., USA Report, May 1957.
36. Flourde, G. A., and Stenning, A. H., "Attenuation of Circumferential Inlet Distortion in Multistage Axial Compressors", *Journal of Aircraft*, Vol. 5, No. 3, 1968, pp 236-242.
37. Ehrich, F., "Circumferential Inlet Distortion in Axial Flow Turbomachinery", *J. Aero. Soc.*, 24, 6, 413-17, June 1957.
38. Hsuan Yeh, "An Actuator Disc Analysis of Inlet Distortion and Rotating Stall in Axial Flow Turbomachines", *J. Aero/Space Sci.*, 70, 956-957, October 1966.
39. Callahan, G. M., and Stenning, A. H., "Attenuation of Inlet Flow Distortion Upstream of Axial Flow Compressors", *Journal of Aircraft*, Vol. 8, 1971, pp 227-233.
40. Greitzer, E. M., and Strand, T., "Asymmetric Swirling Flows in Turbomachine Annuli", *J. of Eng. for Power*, 100, 618, 1978.

41. Kerrebrock, J. L., "Small Disturbances in Turbomachine Annuli with Swirl", GTL Report #125, MIT, 1975. Also AIAA J., 15, 6, June 1977.
42. Hawthorne, W. R., McCune, J. E., Mitchell, N. A., and Tan, C. S., "Non-Axisymmetric Flow Through an Annular Actuator Disc; Inlet Distortion Problem", J. of Eng. for Power, 100, 604, 1978.
43. Hawthorne, W. R., "The Applicability of Secondary Flow Analyses to the Solution of Internal Flow Problems", in Fluid Mechanics of Internal Flow, ed. by Sovran.
44. Nemenyi, and R. Prim, "Some Geometric Properties of Plane Gas Flow", J. of Math. & Physics., 27, 1948.
45. Namba, M., "Lifting Surface Theory for a Rotating Subsonic or Transonic Blade Row", Aero. Res. Council, R & M No. 3740.
46. Falcao, A. F., deO., "Three-Dimensional Flow Analysis in Axial Turbomachines", Ph.D. Thesis, Eng. Dept., Cambridge University, 1970.
47. McCune, J. E., "A Three-Dimensional Theory of Axial Compressor Blade Rows--Subsonic, Supersonic and Transonic", Ph.D. Thesis, Cornell Univ., (1958). [See also USAFOSR TN-58-72, J. Aero. Space Sci., 25, 544 and 616 (1958)].
48. Okurounmu, O., and McCune, J. E., "Transonic Lifting Surface Theory for Axial Flow Compressors", United Aircraft Res. Labs., E. Hartford, CT, Report No. K 213580-1 1971.
49. Okurounmu, O., and McCune, J. E., "Lifting Surface Theory of Axial Compressor Blade Rows: Part I--Supersonic Compressor", AIAA J 12, 1363, 1974.
50. Okurounmu, O., and McCune, J. E., "Lifting Surface Theory of Axial Compressor Blade Rows: Part II--Transonic Compressor", AIAA J 12, 1372, 1974.
51. McCune, J. E., and Okurounmu, O., "Three-Dimensional Flow in Transonic Axial Compressor Blade Rows", Proc. Inst. Symp. Fl. Mech., Acoustics and Design of Turbomachinery, Penn State Univ. (Ed. B. Lakshminarayana, W. R. Britisch and W. S. Gearhart) 1970. (See also NASA Sp. Publ. SP-304, Pt 1 (N75-11174), p 155).
52. McCune, J. E., and Dharwadhar, S. P., "Lifting-Line Theory for Subsonic Axial Compressor Rotors", MIT Gas Turbine Lab Report No. 110, July 1972.
53. Homicz, G. F., and Lordi, S. A., "Three-Dimensional Lifting-Surface Theory for an Annular Blade Row", presented at ASME Gas Turbine Conference, March 11-15, 1979.

54. McCune, J. E., and Hawthorne, W. R., "The Effects of Trailing Vorticity on the Flow through Highly-Loaded Cascades", J. Fl. Mech. 1976.
55. Cheng, W. K., "A Three-Dimensional Theory for the Velocity Induced by a Heavily Loaded Annular Cascade of Blades", SM Thesis, Aero & Astro, MIT, June 1975.
56. Cheng, W. K., "Uniform Inlet Three-Dimensional Transonic Beltrami Flow through a Ducted Fan", MIT GTL Report 130, 1977.
57. Adebayo, A. O., "Three-Dimensional Beltrami Flow in Turbomachinery with Strong Arbitrary Swirl", Ph.D. Thesis, MIT, June 1978.
58. Tan, C. S., "Three-Dimensional Vorticity-Induced Flow Effects in Highly-Loaded Axial Compressors", Ph.D. Thesis, MIT, June 1978.
59. Tan, C. S., "Three-Dimensional Incompressible and Compressible Beltrami Flow through a Highly-Loaded Isolated Rotor", MIT GTL Report 147, October 1979.
60. C. S. Tan, "Vorticity Modelling of Blade Walls behind Isolated Annular Blade-Rows: Induced Disturbances in Swirling Flows", to be published as ASME Transaction, 1980.
61. Kerrebrock, J. L., "Small Disturbances in Turbomachine Annuli with Swirl", GTL Report No. 125, MIT, 1975. Also AIAA J 15, 6, June 1977.
62. Greitzer, E. M., and Strand, T., "Asymmetric Swirling Flow in Turbomachine Annuli", J. of Eng. for Power, 100, 618, 1978.
63. Hawthorne, W. R., McCune, J. E., Mitchell, N. A., and Tan, C. S., "Non-Axisymmetric Flow through an Annular Actuator Disc; Inlet Distortion Problem", prep. for ASME mtg, London, April 1978. Published in J. of Eng. for Power, 100, 604, 1978.
64. Dring, R. P., Joslyn, H. D., Hardin, L. W., "Experimental Investigation of Compressor Rotor Wakes", AFAPL Technical Report, AFAPL-TR-79-2107, January 1980.
65. Miller, D. P., "The Predictive Study of Flow Phenomena behind an Axial Turbomachine Rotor", SM Thesis, Dept. Aero/Astro, MIT, June 1980.